Check for updates

Received: 4 January 2022 | Revised: 28 April 2022 | Accepted: 3 May 2022

DOI: 10.1002/er.8103

REVIEW PAPER

INTERNATIONAL JOURNAL OF ENERGY RESEARCH WILEY

Modern practices in electrophoretic deposition to manufacture energy storage electrodes

Barun Kumar Chakrabarti[1] | **Metin Gençten**[2] | **Gerard Bree**[1] | **Anh Ha Dao**[1,3] | **Daniel Mandler**[4] | **Chee Tong John Low**[1]

[1]WMG, Warwick Electrochemical Engineering Group, Energy Innovation Centre, University of Warwick, Coventry, UK

[2]Department of Metallurgy and Materials Engineering, Faculty of Chemistry and Metallurgy, Yildiz Technical University, Istanbul, Turkey

[3]Battery R&D, Umicore Research, Development & Innovation, Umicore SA, Olen, Antwerp, Belgium

[4]Institute of Chemistry, The Hebrew University of Jerusalem, Jerusalem, Israel

Correspondence
Barun Kumar Chakrabarti and Chee Tong John Low, WMG, Warwick Electrochemical Engineering Group, Energy Innovation Centre, University of Warwick Coventry, CV4 7AL, UK.
Email: barun.chakrabarti@warwick.ac.uk (B. K. C.) and c.t.j.low@warwick.ac.uk (C. T. J. L.)

Funding information
Engineering and Physical Sciences Research Council, Grant/Award Numbers: EP/P026818/1, EP/R023034/1; University of Warwick, United Kingdom

Summary

The applications of electrophoretic deposition (EPD) to the development of electrochemical energy storage (EES) devices such as batteries and supercapacitors are reviewed. A discussion on the selection of parameters for optimizing EPD electrode performance, such as light-directed EPD, co-deposition of active materials such as metal oxides and materials manufactured with high porosity and fibrous properties is highlighted. Additionally, means for overcoming obstacles in the improvement of the mechanical properties, conductivity and surface area of EES materials are discussed. The exceptional benefits of EPD such as low cost, small processing time, simple apparatus requirements, homogeneous coatings, binder-free deposits and selective modification associated with thickness and mass loadings leading to effective EES electrode materials are highlighted. Finally, EPD processes have evolved as modern manufacturing tools to produce technologically improved solid electrolytes and separators for lithium-ion and/or sodium-ion batteries, and further research and development programmes are encouraged towards industrialisation.

KEYWORDS

electrode materials, electrophoretic deposition, lithium-ion batteries, sodium-ion batteries, supercapacitors

1 | INTRODUCTION

Electrochemical energy storage (EES) plays a significant role at scales as large as electric grid balancing down to everyday power electronic devices,[1-6] in addition to the extensive application of batteries and supercapacitors in electric vehicle development over the years.[7,8] They are crucial for economies such as the United Kingdom to achieve sustainability and carbon emission reduction.[9] Similarly, the UNFCCC (during the Paris Climate Conference in 2015) has encouraged global leaders from the developing nations to consider reducing greenhouse gas emissions such that global average temperature is allowed to settle at well below 2°C above pre-industrial levels.[10] Therefore, much research work in recent years has focused on developing ground-breaking concepts for membranes and electrode materials for various EES devices.[11] These key components are designed in such

This is an open access article under the terms of the Creative Commons Attribution License, which permits use, distribution and reproduction in any medium, provided the original work is properly cited.
© 2022 The Authors. *International Journal of Energy Research* published by John Wiley & Sons Ltd.

manners that the mechanism of charge storage in batteries and supercapacitors are different; battery materials are aimed towards high energy density applications, whereas supercapacitor materials are designed for high power density use.[12] In all such cases, electrode materials play one of the most important roles in enhancing the performance of EES systems from the viewpoint of long cycling life, high specific capacity and/or high rate capability.[13-16]

Electrodes for energy storage have classically been prepared in various ways in both academia and industry such as slot-die coating or slurry casting.[2] In these methods, electrode materials are dispersed/dissolved in a solvent to form a viscous slurry, and a film is obtained after coating and solvent evaporation. In spite of that, it is not easy to optimize thickness control or film assembly efficiency. Furthermore, conventional techniques suffer from significant drawbacks when it comes to preparing nanostructured energy materials owing to a lack of control in the effective dispersion of the nanoparticles in viscous slurry pastes leading to disadvantageous agglomeration. This is mainly applicable for the cases of chemical and thermal methods, which are susceptible to adulteration of the active materials with unwanted impurities, thereby decreasing electrode performance.[17,18] Alternatively, methods reported for manufacturing microbatteries, which include radio-frequency sputtering, physical and/or chemical vapour deposition (CVD) or pulsed laser deposition, suffer from high processing costs that affect their applicability at scale.[19]

Considering the aforementioned approaches for manufacturing effective electrode materials, it is imperative to find versatile and cost-effective processes that do not compromise EES performance. In this regard, electrophoretic deposition (EPD) has been reported to possess several benefits, including scalability, facile and economical set-up, as well as the ability to prepare electrode materials in relatively small time scales.[20] The mechanism of EPD is summarised in Figure 1.[21] Electrophoresis occurs when charged suspended particles in a suitable solvent migrate towards an oppositely charged surface upon application of an electric field between two electrodes. The charged materials migrate towards the deposition electrode and aggregate into a relatively dense and uniform film (known as deposition). The EPD technique may, therefore, be applicable for any solid material in fine powder form (eg, ranging from micro- to nanostructures) or as a colloidal formulation that may involve polymers, metals, ceramics and glasses.[22]

EPD was discovered in 1808 (see the following section for a historical overview) and was modelled for the first time by Hamaker in 1940. The requirement for stable suspensions to form an adhering sediment due to gravitation when allowed to stand still has since been defined mathematically for the EPD technique.[23] Several authors have explained how the positively charged particles move towards the cathode (negative electrode) in the EPD bath (colloidal solvent formulation), thereby overwriting the coagulation mechanism without increasing electrolyte concentration at the electrode.[24] This follows up with a distortion and a reduction in the diffuse double layer (known as lyosphere) thickness owing to the combined effects of the applied electric field and fluid dynamics leading to coagulation of particles. Figure 1 summarises the main steps in an EPD process.[21] The equation inset in the figure relates to the electrolyte solvent and the resultant particle mobility. The deposition process itself is more complicated, and different theories

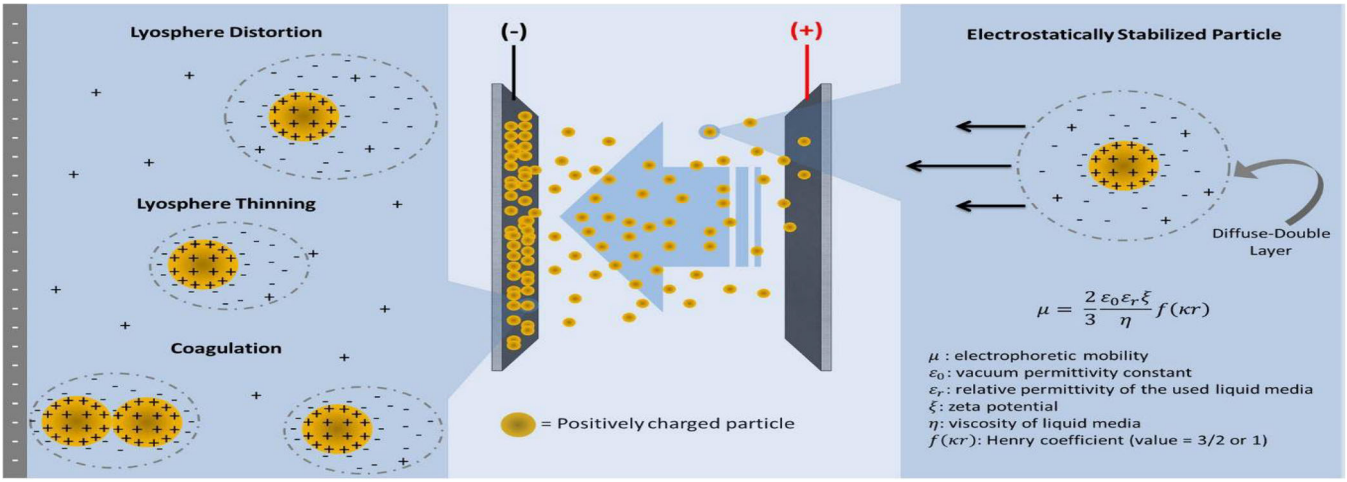

FIGURE 1 Diagram showing the electrical double-layer distortion and thinning mechanism during an EPD process. An important equation is also displayed that summarizes the key parameters that affect EPD performance. Reproduced with permission from Elsevier[21]

have been proposed; the distortion and thinning of the particle double layer, the flocculation by the accumulation of particles, neutralization of the particle charges, and several other postulations that are described elsewhere.[22,25] Since EPD is affected by several parameters that are commonly related to each other (eg, a change of the suspension medium will produce a change of the viscosity, but also a change of the zeta potential of the particles due to a different particle-medium interaction), a correlation of the experimental parameters and deposition results is not straightforward and can suffer from inconsistencies. For this reason, comprehensive investigations of the EPD process are a key factor to produce coatings with preferred features depending on the desired application.

Conventional EPD employs pure water[26] or aqueous-based solutions[27] as suspension media, because the high dielectric constant(s) of these solvents facilitates the development of charge on the dispersed colloidal particles and therefore stabilizes the suspension.[28] For industrial purposes, aqueous suspensions have the advantage of high solid loadings and low environmental impact.[29] However, these solvents may undergo electrochemical reactions, such as the formation of ions as well as hydrogen and oxygen evolution at the electrode surfaces, which interfere with the EPD of the particles.[28] The use of nonpolar media (usually organic) minimizes the interference of electrochemical reactions, for example, water electrolysis, thereby circumventing turbulent flow and other hydrodynamic effects of the solvent. Moreover, nonpolar media provide more control over the film thickness and the roughness of the film surface than aqueous solutions.[30] As a consequence, more and more research investigations involving organic colloidal formulations are gaining popularity within the scientific community.[28]

EPD is strongly dependent on the presence of a stable colloidal formulation.[19] The stability of a suspension, adjustable with surfactants, is correlated with electrostatic repulsive and van der Waals attractive interactions. The stability of suspension/colloid is characterized by zeta potential, the value of which represents the magnitude of repulsive interaction while the sign represents the migratory direction of particles. Factors that influence zeta potential include electrolyte pH, temperature and surfactant type. Other factors that affect particle migration in the EPD solvent such as the voltage field or deposition time (also dependent on electrolyte viscosity) are discussed in Section 3.[31] A typical EPD system includes a power supply, a conductive substrate and a counter-electrode. As the voltage is applied, active material particles in the liquid suspension are deposited on the substrate. Electrolyte sedimentation may be prevented by adding dispersing agents,[32] while conductive additives like Super P (carbon black) or acetylene black are often added to achieve deposits with good electrical conductivity.[19]

The utilization of EPD for preparing EES devices relies on the direct deposition of active particles on the current collector.[19] Employing conductive substrates is a prerequisite for both EES devices and the EPD process. Combining EPD in electrode fabrication for EES applications also reduces the interfacial resistance and increases the mechanical flexibility of the electrodes.[31] In addition, EPD of binder-free films for rechargeable batteries[33] or supercapacitors[34] has been reported, demonstrating a promising possibility to increase the energy density of such EES materials.[19] The cycling performance or conversion efficiency can also be improved due to the densely packed EPD coatings.[35] Furthermore, controllable nanostructures can be realized using EPD and such electrodes usually exhibit improved performances when applied as micro-energy storage devices.[19]

Although research on electrode materials is fast developing, the fundamental mechanistic understanding regarding how the design of EPD and properties of nano- and/or micro-structured electrodes prepared by EPD can improve electrochemical reaction efficiencies is still not fully understood. To the best of our knowledge, this is the first review article that explains in-depth the advantages of applying the versatile EPD process for specifically making and applying energy storage electrodes with relevance for both academia and industry. This is likely to be so because a general search of the literature on EPD processes for energy storage and conversion results in the identification of two review papers published in the recent past focussing mainly on academic studies,[19,36] while this paper focuses more stringently on EES devices and how they can be of benefit for industrial type applications. The most recently published review paper on EPD focuses on the progress and challenges of carbon nanotubes (CNTs),[20] which once again confirms the timely impetus of our work presented below.

To systematically illustrate the production convenience, versatility and high performance of EES electrode materials produced by EPD, studies involving lithium-ion batteries (LiBs), supercapacitors, redox flow batteries (RFBs) and regenerative fuel cells (RFCs) are highlighted in this paper. The basic comparison of these EES devices is discussed in some depth. Also, a relevant perspective is drawn for the potential application of EPD in other emerging EES technologies such as sodium-ion capacitors, magnesium-/aluminium-ion batteries and battery-supercapacitor hybrids. Finally, the opportunities and

challenges associated with scaling-up the EPD technique for the production of industrially viable electrode materials for EES devices are detailed. This review paper also shows early evidence of the evolution of EPD processes and manufacturing tools to produce technologically improved solid electrolytes and separators for LiBs, and further research and development programmes are expected to support their industrialisation.

This review is divided into eight sections. Section 1 introduces this work and Section 2 describes a brief history of the EPD process along with a useful timeline up to the point where EPD was first reported to produce an energy storage electrode. Section 3 discusses the key principles behind the application of EPD to prepare surface coatings. Section 4 covers some industrial studies on EPD. Section 5 provides an overview underlying the successful use of EPD for producing an energy storage electrode. Section 6 discusses various in-depth applications of energy storage electrodes produced by means of EPD with relevant examples of LiBs, RFBs and supercapacitors. Section 7 discusses the remaining challenges of EPD for producing energy storage electrodes with some applications for sodium and magnesium ion batteries. Section 8 concludes this review and provides a short perspective.

2 | BRIEF HISTORY OF EPD

The electrophoresis phenomenon was originally reported by Reuss in 1808 who observed the electrical migration of suspended clay particles in water.[24] Since then, the first quantification of the phenomenon for thin double-layer electrophoresis was reported by Smoluchowski.[37] Smoluchowski's equation was further improved by Henry by means of a fitting parameter as a function of Debye length and particle size for taking into account changes in double-layer thicknesses.[38] More complicated mathematical formulations were developed since then by various scientists. For instance, Overbeek modelled the electrophoretic motion of a spherical particle in his PhD thesis in 1941.[39] Other researchers like Booth developed mathematical relationships describing how the initial application of an electric field on a colloidal liquid suspension affects the electrophoretic retardation force and relaxation effect (see Figure 2A for a historical timeline on electrophoresis).[40,41] This was followed by independent studies by White as well as Ohshima and O'Brien, who enhanced the theories for regimes to account for higher concentrations of particle and larger zeta potentials in electrolyte suspensions.[42-44] Deposition mechanisms were also proposed in the 1940s and beyond, such as EPD yield quantification by Hamaker followed by the effect of deposition substrate and consequently the electrode materials (eg, planar, 2D fibre mats and/or 3D porous materials) on deposited films.[38]

Despite such progress, the literature lacks a converging viewpoint on the actual mechanism for the EPD process. In general, the scientifically accepted consensus banks on the Derjaguin-Landau-Verwey-Overbeek (DLVO) theory that attempts to quantify colloidal stability by accounting for the interaction potentials between particles and the consequent influence of the applied electric field on the electric double layer.[38] In particular, DVLO accounts for the opposing influences of van der Waals attractions and electrostatic repulsions on particle deposition.[39] Three factors play a significant role as explained by the DLVO theory and these include the Hamaker constant (a function of van der Waals forces), particle surface potential (a function of electrostatic forces), and electrolyte concentration (accounting for electrostatic effects upon Debye length).[37] A successful EPD is postulated to be influenced by the electric field applied that disrupts the electrolyte balance close to the electrode materials—this occurs by means of an increase in concentrations of counter-ions along with a corresponding decrease in co-ions concentrations around the electrode surfaces. Therefore, the double layer associated with the colloidal particle as well as the Debye screening length changes significantly enough to cause colloidal destabilization and deposition. The accumulation of particles due to a flocculation phenomenon is also considered to be a significant theory reported in several EPD-based literature.[23] In particular, this postulation accounts for the fact that van der Waals forces between particles apply a considerable influence on the particles when they are within a certain critical range, resulting in flocculation of the particles and consequently deposition on a charged surface (see Figure 1). However, to bring the particles within the aforementioned van der Waals range, the particles need to be pressurized by means of electrostatic forces of attraction to overpower opposing repulsive electrostatic forces and compel them to move within the critical range for deposition to occur.

EPD has been successfully used in the past for various ceramics-based applications,[45,46] but has recently been employed for a range of different exciting applications (see Figure 2). Examples include porous electrodes and membranes for batteries, capacitors, and fuel cells[47-49] (see Figure 2B that illustrates the rapid growth in the publication of EPD for making energy storage electrodes up to 2020). For instance, Wang et al[50] have applied EPD for fabricating structural composites like diamond and/or

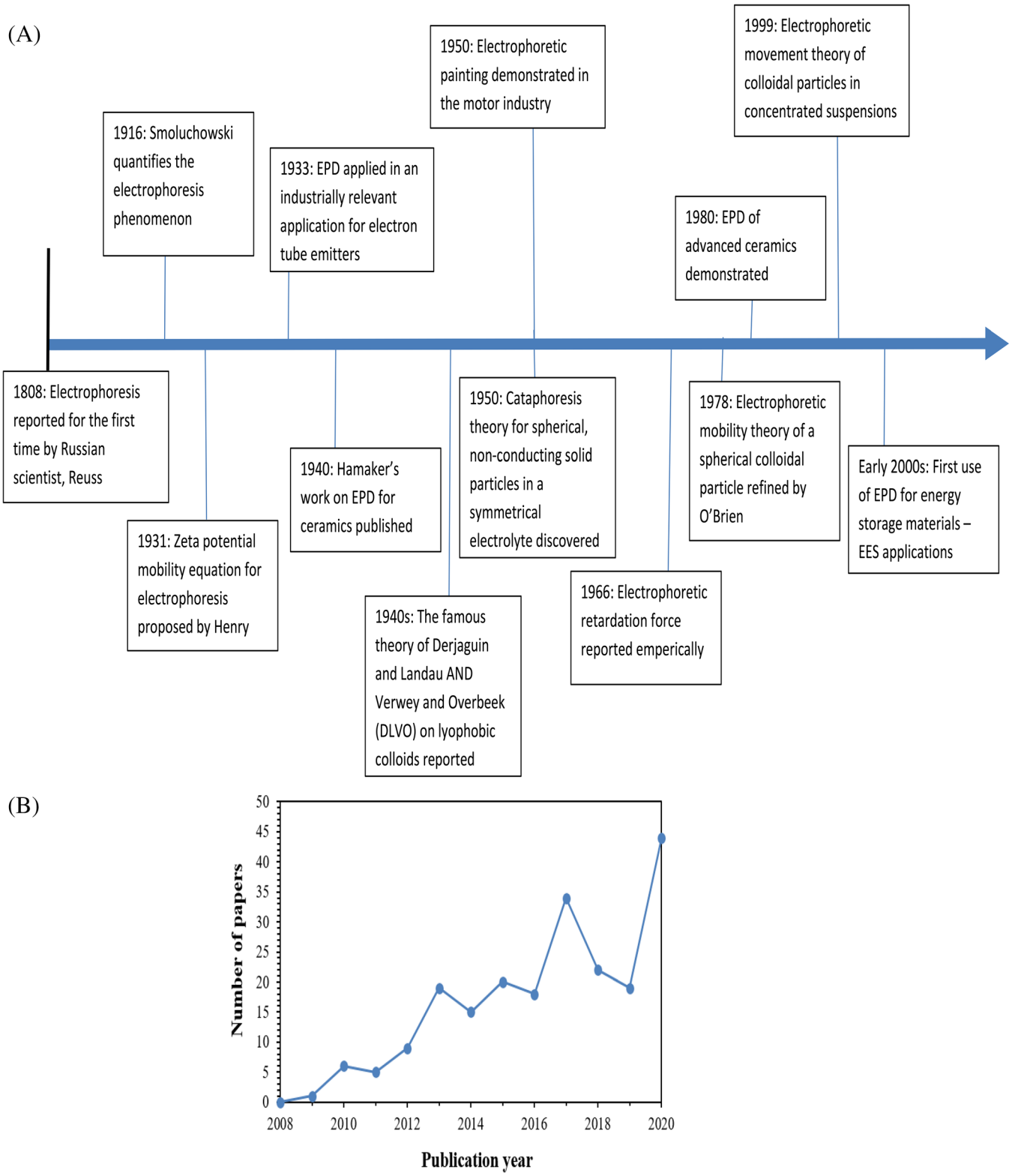

FIGURE 2 (A) Historical timeline on the development of EPD from its discovery to the early 2000s when it became significant for the manufacture of EES materials. (B) Graph showing the rapid growth in applying (from 2008 to December 2020) EPD for energy storage electrodes (data obtained from Web of Science)

borosilicates. Such examples cover a small spectrum of applications describing the significant versatility of EPD for functional materials deposition and further elaborations are reported in consequent sections of this review, focussing particularly on design and application of advanced electrodes for EES devices.

3 | PRINCIPLE OF ELECTROPHORETIC DEPOSITION (EPD) TO PRODUCE SURFACE COATINGS

In most metal-based applications, coatings are an essential part of the protection of the material's surface from wear and corrosion. Coating methods may be divided into two according to the phase from which the active material is deposited onto the respective material surface. Such coating processes are ubiquitous owing to the big diversity of applications. These processes contain various online/offline parameters that are functions of material microstructure, process effectiveness and other relevant factors.[51] A small selection of deposition techniques to produce surface coatings is summarised in Figure 3A. Some examples of gaseous phase depositions involve physical vapour deposition (PVD), plasma spraying and CVD, while a few examples of liquid phase deposition include thermal spraying, dip coating and electrochemical methods.[54] Among liquid phase surface coating processes, electrochemical deposition and EPD (Figure 3B) ensure cost-effective and controlled material films (≈25-100 nm) at high deposition rates (≈240 μm thickness in 1 hour). The fact that EPD can be performed successfully to prepare highly functional materials on a range of different deposition substrates at room temperature and pressure displays its excellent features.[55,56] Therefore, in recent years, these deposition processes, using hard particle dispersion in the metallic matrix, have attained widespread importance in chemical, mechanical and electrical applications.[54]

In other words, EPD as a suspension-based colloidal manufacturing process meets the criteria for inexpensive mass production of surface coatings and objects for additive manufacturing.[28] This technique offers a number of advantages including high efficiency, convenience and cost-effectiveness, and allows for versatile manipulation of micro/nanoparticles in a colloidal solution.[19] Surface coating thickness, particle size and inter structure of surface coatings produced by means of EPD are controllable by adjusting the suspension/process parameters.[57] Efficient production of surface coatings typically requires a good substrate.[19] With excellent conductivity and surface

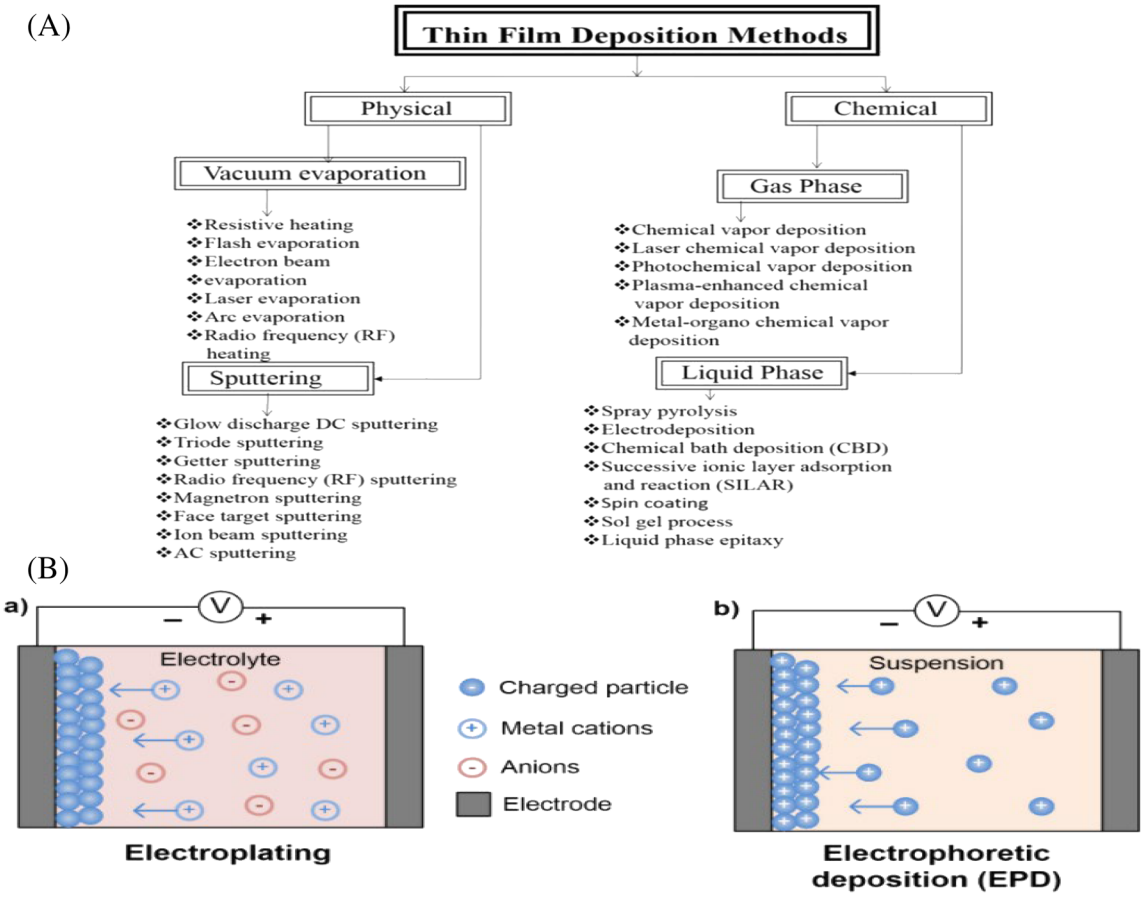

FIGURE 3 (A) Flow chart showing some fabrication methods for thin-film surface coatings. With permission from InTech Open.[52] (B) Simplified diagrams of two types of cathodic electrodeposition processes: (A) electroplating and (B) electrophoretic deposition (EPD). Reproduced with permission from InTech Open[53]

evenness, indium tin oxides (ITOs), metal layers and graphite sheets are commonly used as substrates. In addition, the standard of the deposited films correlates closely with the dimensions and therefore the surface features of EPD precursors.[58]

Owing to the fact that EPD is a low-cost non-line-of-sight coating process, it is very likely to produce coatings of uniform dimensions on complex substrates with uneven morphology. In addition, high-quality film coatings with tailored morphology specific to the required application may be designed by means of EPD—the versatility of the process is highlighted by the fact that film thicknesses can vary from nano- to millimetre-scale that has a direct effect on the mass loadings.[59] Thus, this versatile process is capable of manufacturing polymer coatings for a wide range of applications, one example being the biomedical industry.[60] This is drawn from the simplicity of EPD to operate in mild aqueous/organic environments at low temperatures and pressures,[61] with excellent efficiency,[62] and short processing times[63] that facilitate a facile scale-up towards commercial production.[64]

Despite the aforementioned exceptional features, EPD faces such drawbacks as poor film/coating adhesion, challenges in morphology control, and rates of deposition that are far from linear.[28] This is particularly influenced by the time dependency of crucial EPD processing parameters that include colloidal concentration, composition, electric field effects, pH, electrophoretic mobility, etc., which, in turn, severely impact the deposited surface films/coatings quality.[25] Besides these parameters that significantly impact upon the quality of surface coatings, there are several fundamental factors that need particular attention and are reviewed in detail in other relevant papers.[19,21,25,36]

4 | CURRENT DEVELOPMENT IN EPD INDUSTRIAL ACTIVITIES

EPD technology is industrially scalable and involves simple processing methodologies to manufacture at scale. This technology has been employed for industrial electrophoretic painting purposes from 1970 onwards (Figure 2A). The low levels of pollution, ease of digital automation, and the ability of EPD to produce homogeneous functional coatings are advantages that have enabled its widespread adoption in painting car bodies on an industrial scale.[65] It continues to excel in depositing films with controllable microstructures as a function of the processing conditions. Thus, there is great potential to apply this highly versatile technology for large-scale processes despite a lack of a holistic understanding of the interaction of complex factors that influence EPD. This suggests an exciting opportunity for EPD technology to manufacture an uncountable number of electrode designs, for tailored energy storage performances that will be reviewed later.

There is a growing interest in using EPD as a manufacturing method because of its compatibility with a vast material set including metals,[66] ceramics,[24,67] biomaterials,[68] polymers,[69] semiconductors[70] and composites,[71] and its speed, with depositions, typically lasting from seconds to minutes that can yield composite functional materials with several centimetres of thicknesses.[72] It has been successfully used in a wide variety of applications such as solid-state lighting,[73] reactive materials,[74] energy storage,[75] drug delivery,[76] and photovoltaics.[77] Figure 4 highlights some of these applications, which are discussed in depth in a recent book chapter.[78]

EPD can be extensively applied for industrial coatings onto conductive substrates,[79] such as for UV curable coatings.[65] EPD coatings on relevant substrates provide enhanced chemical shielding, thereby preventing corrosion and discoloration unlike what is noted for their anodic counterparts.[80]

During the use of EPD for painting automobiles, entire car bodies or their assemblies are dipped into a liquid vessel in order to prevent the coated substrate from future corrosion.[81] However, there are several overhanging problems that need attention. For instance, the effect of trapped air bubbles during the dipping process may cause non-uniform coating owing to poor coverage of the EPD solvent on the charged body surface. Additionally, liquids that remain entrapped after completing the aforementioned process are likely to cause corrosion in follow-up processing steps. Moreover, automotive parts containing rubber, plastics and other components are deformed easily when subjected to high-temperature baking, which itself increases the manufacturing cost due to energy and resource wastage. As a consequence, new methods of drying such as UV curing have been applied successfully in several industrial EPD activities in the last decade.[65] UV curing has some unique advantages such as high-curing speed, solvent-free formulations (reduced emissions of volatile organic carbon), and low-temperature processing with minimal energy consumption.[82-84]

Some investigators applied EPD electrodes with special features such as the ability to change position during EPD and/or the ability to be reconfigured in order to form free-standing films or turbulent gradients that is normally not attainable under standard conditions.[67] Of particular note, Anné et al applied a series of four counter-electrodes to prepare a functionally graded net-shaped femoral ball head.[85] Nold and co-workers were

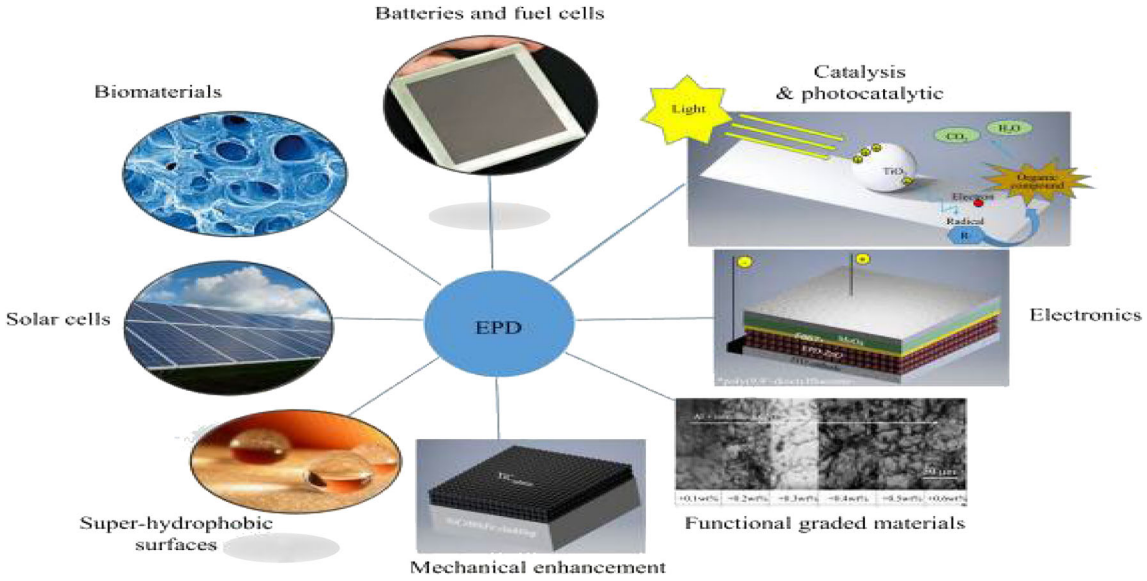

FIGURE 4 Some of the scalable applications of EPD for potential industrial use. Reproduced with permission from Elsevier[78]

the first to explore the reconfigurable electrode concept when they reported the use of both a movable coaxial cable electrode set-up as well as an addressable electrode array to localize deposits onto a surface to create an EPD computer-aided manufacturing system.[86] Pascall and co-workers demonstrated the formation of composites with gradients both in-plane and along the deposition direction using light-directed EPD,[87] as discussed in the following paragraph.

As mentioned above, EPD is well-suited for multi-material deposition and has been proven at industrial scale, but patterning of fine features and voids generally has not been possible.[67] Pascall and co-workers previously demonstrated a new additive manufacturing technique called 'Light-Directed EPD', which involves the use of photoconductive electrodes, laser-cut photomasks and UV light to locally control the electric field.[87,88] The use of laser-cut photomasks, while reconfigurable, limits the scalability, the ability to be automated, and the resolution of the technique to 100 seconds of μm.[67] A more recent work expands on that of Pascall and co-workers' by moving to a projection-based system that not only removes the need to produce physical masks, but additionally enables an adaptable depositing pattern to form as a function of processing parameters. This opens the door to rapid fabrication of complex structures over large build areas. Therefore, a free-standing bridge structure produced via EPD was demonstrated recently.[67]

In another example of the industrial application of EPD, a jet engine used up about 1.8 tonnes of nickel alloys, which made it possible for the plane to complete nearly 20 000 flight hours without significant maintenance, a considerable achievement for EPD in the aerospace industry.[89] Besides the numerous applications of Ni, the destruction of these appliances (aircrafts, electromagnetic devices, supercapacitors, sensors, etc.) by wear, corrosion and fatigue is of a major concern.[54] Since the protection of these crucial components is critical, electrophoretically deposited Ni-carbonaceous coatings have presented glowing properties, which make them a reliable coating variant that can protect bare Ni during everyday use as well as in corrosive environments.[54]

Another popular industrial application of EPD involves physical synthesis techniques for combining biochar with graphene for potential applications in supercapacitors.[90] For instance, for manufacturing graphene-coated biochar, the charged particles migrate under an electric field and deposit onto the electrode of the opposite charge. However, graphene is electrically neutral. Therefore, graphene oxide (GO) is used instead because it contains charged functional groups, mostly negatively charged. After the GO is electrophoretically deposited on the biochar, it is subjected to chemical or electrochemical reduction to obtain rGO, since GO is electrically insulating. In previous studies, GO has been electrophoretically deposited on CNTs and carbon fibres.[91,92] A more recent study aimed to improve the electrical conductivity of pinewood-derived biochar via EPD of GO followed by electrochemical reduction.[90] The loading amount of rGO was affected by the concentration of the GO suspension, while the electrochemical reduction voltage was varied to control the reduction degree. The electrode conductivity was influenced by rGO content as well as the quality of its reduced state. A specific capacitance of 167 F g^{-1} is reported after depositing rGO in comparison to 39 F g^{-1} for a supercapacitor using biochar electrodes in the

absence of rGO (>4 times higher capacitance in the presence of rGO). Furthermore, the supercapacitor can undergo 10 000 charge/discharge cycles without displaying capacitance fade at a relatively high current density of 5 A g^{-1}.

The next section reviews the application of EPD for energy storage systems. Following onwards, detailed aspects of three exemplary EES devices are considered including RFBs, lithium-ion technologies and supercapacitors.

5 | OVERVIEW OF EPD TO MANUFACTURE EES DEVICES

Classical electrode fabrication in any research area mainly relies on various deposition techniques such as spray deposition, sputtering (eg, radio-frequency sputtering), electrochemical deposition, CVD, EPD, atomic layer deposition, pulsed laser deposition, sol-gel, layer-by-layer deposition and spin-coating.[93] These physicochemical deposition methods result in simple and versatile means for manufacturing EES electrodes. Despite that, such deposition methods face several limitations such as complicated material handling procedures, and challenging thickness and uniformity control of thin films when used for on-chip integration and large-scale manufacturing applications.[94] Industrial EES devices are manufactured in general by means of high-speed roll-to-roll processing, which commences with chemicals deposition, rolling of electrodes, roll slicing and then proceeds into the construction of the EES cell by combining the electrodes with a separator. The follow-up processes involve electrolyte addition and soaking of electrodes and separator, and ultimately packaging along with relevant incisions based upon commercial standards.[93] This elaborate process, which was originally adopted in the 1980s and 1990s from Japanese magnetic tape factories, requires significant amounts of times to manufacture an electrode and faces obstacles in scaling-up processes, including costly expansion of production lines. Automatic and sophisticated industrial production steps can significantly reduce the upfront investment and manufacturing time.[95]

In other words, conventional electrode manufacturing steps such as blade-coating (whereby a slurry suspension is prepared by physically mixing the active material with binder and conductive agent, for application over a current collector surface) face limitations related to film assembly efficiency and thickness control.[96] Unfortunately, the EES device usually has lower energy and tap densities in addition to high interfacial resistance as a consequence of the presence of non-active substances.[19] Such disadvantages could easily be circumvented by manufacturing high-performance binder-free electrodes by means of EPD (with its unique advantage of ensuring decent control of surface coating thickness and mass loadings).[96] In fact, the need of using binders in the electrode production process adds an extra cost to the process.[97]

Additionally, the drying process of the widely used solvent N-methyl pyrrolidone (NMP) is time-consuming and expensive, especially at large scale. Drying can take a long time for some electrodes and can vary between 12 and 24 hours at 120°C or 60°C under vacuum.[84,98-100] In the EES manufacturing industry, recycling and recovery of the NMP solvent from the drying step is essential because the substance is not only dangerous to handle but also a potential threat to the environment (due to its toxicity).[101,102] High capital investments are also needed to introduce NMP recovery systems, which offset any economic benefits arising from recycling and re-use of NMP.[103] Such an extensive drying step is less important for electrodes made via EPD, especially if applying low boiling point organic solvents as the colloidal media.

One inferred disadvantage of EPD could be the increasing electrical resistance of the deposits that could ultimately stop the EPD process. This 'thickness limiting' effect is ideal for depositing onto the surface of an irregular 3D structure.[104] If the deposits were a film of porous layer (which is the case in battery and supercapacitor electrodes), the voltage drop across the layer will remain very low because of the presence of conductance pathways available throughout the accessible porous film.[105] If a sufficiently conductive electrolyte is used, the layer's electrical resistance will not limit its growth. This suggests the possibility of an unlimited layer thickness. Biest and co-workers have confirmed that porous deposits (10%-60% porosity usually) with thicknesses reaching several millimetres can be achieved with relative ease.[106] This suggests the manufacture of 100 mm thick electrodes for practical energy storage is encouragingly possible using EPD technology.[107-109] The process also offers improved electronic and physical connectivity to the current collector surface by creating an electrochemical bond unlike a physical one as in standard slurry cast-based coating.[110,111]

In conclusion to this section, it is noted that EPD for producing energy storage electrodes is a widely researched topic with some recent reviews.[20,112,113] Most of these academic assessments have tended to remain rather general, with a specific focus on the combination of both energy conversion and EES devices. The specific details related to improving the EPD parameters for energy storage electrodes have not been evaluated in much depth. Therefore, this elegant area of research is

anticipated to undergo further investigations. The following section expands upon the various applications of EPD in specific EES devices.

6 | RESEARCH, DISCOVERY AND INNOVATION ACTIVITIES ON EPD FOR EES DEVICES

Since the 1990s, significant research studies on EES devices have been conducted with a special focus on advanced electrodes design.[114,115] The use of EPD for such purposes is gaining momentum in recent times due to good control of the electrode uniformity and thickness, resulting in highly structured porous electrodes with complex 3D geometry.[116,117] Furthermore, EPD can easily be scaled-up for meeting demands for large electrode sizes and volumes by effectively controlling the colloidal processes that influence the deposition process (see Section 3 for more details).[21,73]

In recent times, studies for the design of advanced electrodes for EES devices have increased significantly because of the excellent processing techniques used in the manufacturing activities to enable high performance (see Figure 2B showing a rising trend in the number of publications in this field of research).[118] Therefore, there is a general scientific consensus that additional research on EES devices is necessary.[25] Needless to say that in this regard, EPD has produced promising results for EES devices.[19] Presently, such devices have been dynamically engaged for electric vehicle (EV) purposes, but EVs nonetheless need low-cost and robust energy sources and/or storage means to reduce operating costs. The development of the EES technology for diverse uses is a means to minimize such issues and EPD can play a major role in this regard. The following subsections discuss some of the advances made in the EPD of electrodes for some key applications.

6.1 | Lithium-ion batteries (LiBs)

LiBs are important energy storage devices for vehicle electrification and portable electronics.[119] Today's LiB electrodes are manufactured by a standard slurry casting process (also known as doctor blade method). The process involves mixing electrochemically active materials, electrically conductive carbon particles and binders in a liquid media, which are then physically cast as a slurry onto metal foils, such as Cu, stainless steel and Al, followed by drying and compression. Despite its significant application, it has been optimized by trial and error, which limits the quality of the manufactured electrodes. For instance, they face drawbacks such as occlusion of the surface of active materials that result in an unwanted drop in the material conductivity and also reduce the gravimetric capacity.[120] As a commonly used binding material, polyvinylidene fluoride (PVDF) is not amenable and thus is unable to sustain wear and tear due to expansion and contraction processes as a consequence of LiB charge and discharge, resulting in a weakening of bonds between the conductive carbon material, active cathode material and the current collector. This, in turn, affects long-term performance such as capacity fade upon cycling. Furthermore, NMP solvent, which dissolves PVDF effectively, is costly, poisonous and may affect pregnant women adversely.[120] Additionally, binders like PVDF have been reported to catalyse thermal runaway reactions in LiBs.[121] Likewise, battery manufacturing costs require further reduction—therefore replacing NMP-based slurry casting techniques is an essential requirement. Especially, binder-free immobilization of the active materials on the electrode surface has great importance in reducing cost and the effects of impurities.[122]

In standard studies involving flexible LiBs, the doctor blade technique, CVD, physical vapour deposition and nanofabrication, among others, are usually harnessed for preparing flexible electrodes.[123] These processes work well for lab-scale prototypes, but are found significantly lacking and also expensive when applied for industrial-scale mass production of flexible electrode materials (that also need to be sufficiently adhesive to current collectors).[124,125] CVD is an expensive technique because thermal curing of the substrate during the course of deposition or annealing of the obtained coating is crucial for enhanced battery performance.[124] Among other solution-based electrode processing techniques, EPD is currently gaining much attention for formulating LiB electrodes mainly due to its simplicity of operation and relatively low cost in comparison to aforementioned manufacturing techniques.[124,126] Additionally, EPD ensures great flexibility in manufacturing different classes of materials, while preserving structure and particle size of the commencing powders in the deposited surface coatings.[126] Mass loadings and film thicknesses of EPD electrode materials may be simply controlled by means of adjusting the interaction between applied current or voltage, composition of electrolyte (and/or colloid) as well as the time of deposition.[124]

Recent research has demonstrated that new manufacturing methods, which include EPD, can produce improved electrodes with more capacity and greater power, which could enable vehicles to travel longer distances and result in higher performances.[127,128] This section will report on the latest findings from the

literature regarding the manufacturing research of electrochemical engineering approaches to produce improved electrodes by means of EPD. For the EPD process, formulation of the colloidal electrolytes can be formed according to the solvents. Three kinds of solvents (aqueous, organic polar and nonpolar) can be used to obtain a colloidal electrolyte. Although nonpolar solvent enables more homogenous depositions, it needs elevated applied potentials. On the other hand, aqueous solutions can result in hydrogen and oxygen evolution side reactions beyond certain potentials. Therefore, the choice of solvents mainly depends on the formulation of the film which will be formed on the electrode surface.

The EPD process can directly allow a controlled placement of different shapes, sizes and types of materials at different positions to produce non-monolithic electrodes.[19] This can be easily achieved by controlling the properties of charged materials and their electric fields. The ability to deploy dilute colloidal electrolytes (eg, using <10 g dm^{-3} of materials), as opposed to the viscous slurry casting technique, drastically increases the technological applicability of EPD to produce electrodes with a higher fraction of materials density. This is because typically <1 wt% of inactive materials (ie, charging agent and polymer binder) are required to provide surface charge on the materials and adhesion property to the current collector surface, respectively. Putting this in the context of LiBs means higher density of active material electrodes can be readily deposited because only relatively tiny quantities of inactive materials are required for processing, as opposed to at least 5 to 30 wt% of inactive materials, which are needed for slurry casting techniques.[2]

Very recently, Lalau and Low (WMG)[2] reported that EPD of $LiN_{1/3}Mn_{1/3}Co_{1/3}O_2$ (NMC111) was carried out at 80 V constant voltage applied for 5 minutes using an NMP-based colloidal coating medium. Industrial-level mass loadings of above 30 mg cm^{-2} and film thicknesses exceeding 150 μm were deposited successfully on 3D Al mesh, which was found to be twice the mass loading and film thickness in comparison to that on 2D Al foil current collector. The LiBs with EPD electrodes distinctively exhibited high capacitance retention, albeit for short-cycling, which was a decent step towards future scale-up studies, especially with electrodes possessing high materials mass loadings and density (90 wt%), as well as thick surface coatings that met industrial standards (as shown in Figure 5). In a separate investigation, Seo and co-workers produced CNT/graphene nanosheet composites by means of EPD, applying 300 mA of a constant current (DC) for 1 hours, and used it successfully as a negative electrode in a LiB.[129]

Uceda and co-workers performed EPD with lithium titanate oxide (LTO) nanoparticles that were carbon-coated to prepare highly conductive but thick LTO electrodes with very good rate capability when compared with their traditionally fabricated LTO counterparts.[130] Other researchers[125] prepared electrodes with LTO coatings of 3.3 μm thickness for micro-battery applications by means of EPD employing a 95/5 vol% ethanol/water mixture, a charging agent comprising entirely of magnesium chloride, and a throbbing potential.[130] The Mg^{2+} cations (generated by means of cathodic hydrolysis were reported by Benehkohal and co-workers in a separate work and for a different cation)[131] were co-deposited as magnesium hydroxide (this acted as a binding agent to improve the LTO conductivity) along with the LTO. The film, however, became non-uniform with extended time resulting in an effective thickness limited to 6.5 μm.[130]

A recent publication was reported on an EPD process that is capable of producing strongly adherent, and highly conductive LTO-Carbon (Acetylene Black) composite electrodes by applying C-coated LTO nanoparticles.[130] This accomplishment was realised by

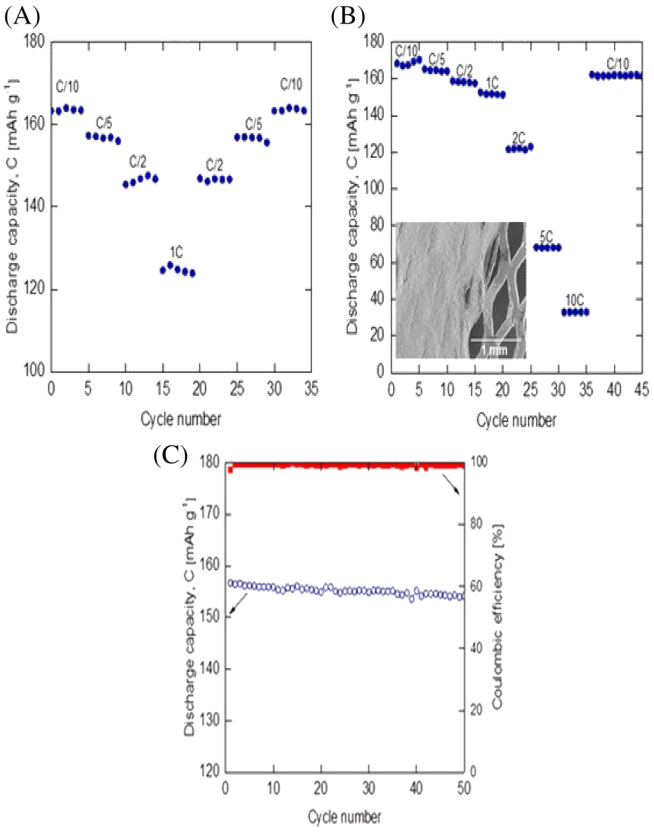

FIGURE 5 Galvanostatic charge/discharge cycling of a LiB whose electrode materials were produced by means of EPD at WMG. C-rate evaluation of EPD NMC111 electrodes deposited on (A) Al 2D foil and (B) 3D Al mesh current collectors. Charging occurred at a constant C/10 rate, while discharging was performed at a range of different C-rates as displayed. (C) NMC's successive cycling performance parameters at C/5. Reproduced with permission from Wiley[2]

employing a water soluble binder, namely styrene butadiene rubber (SBR), which is already well established in the commercial battery manufacturing sector. SBR acts as both a binder for the electrode assembly as well as a stabilizing agent for the nano-C-coated LTO-Carbon formulation. However, applying a common solvent to disperse LTO and carbon (two non-similar materials) is challenging, especially when it comes to preparing a stable suspension. After a thorough evaluation of solvents Uceda et al settled for a 10 wt% water diluted acetonitrile medium for the purposes.[130] The addition of SBR enhanced the kinetics of deposition of LTO/carbon material on the current collector, producing high-quality electrodes for LiB applications. For instance, the conductivity, as determined by electrochemical impedance spectroscopy (EIS), of the compressed EPD electrodes was 15 times better when compared with their counterparts prepared using traditional slurry cast methods employing PVDF binding materials.[2] In addition, rate capability studies showed higher capacitances for electrodes prepared by means of EPD.[130] This, therefore, paves a way forward for EPD to apply standard industrially relevant materials to produce high-value EES electrodes for commercial LiB applications.

A number of studies concentrated on EPD of LFP for manufacturing LiB electrodes, besides the thesis referred above.[120,132,133] Even though successful results were reported from such investigations, the authors highlighted some useful areas for enhanced research and development on the EPD technique. Some complications were highlighted due to the development of uniformly charged colloidal formulations during EPD of LFP with conductive additives, which negatively affected the adsorption of dispersants and binders on the particles, thereby inhibiting the formation of adherent surface coatings.[134] Some authors overcame most of these issues by using aqueous-based polyelectrolytes successfully such as poly[1-[4-(3-carboxy-4-hydroxyphenylazo)benzenesulfonamido]-1,2-ethanediyl, sodium salt] (PAZO-Na) and carboxymethyl cellulose sodium salt (CMC-Na) for the EPD of a range of different substances, like CNTs, oxides, polymers and hydroxides.[135,136] In a more recent study, the EPD LFP electrode, displayed a capacity of 146.7 mA h g^{-1} at a C-rate of C/10 along with steady long-term charge/discharge successive cycling performance.[134] Similarly, Cohen and co-workers prepared a membrane-electrode-architecture by coating Celgard separators with LFP (positive electrode) and LTO (negative electrode) by means of a concurrent EPD method.[124] The LiB with this three-layered electrochemical assembly delivered capacities ranging from 125 to 140 mA h g^{-1} at various C-rates, as shown in Figure 6.

Yilmaz and co-workers recently prepared a highly conductive three-dimensional cathode having an array of micropatterned vertically aligned CNTs on Al foil by means of EPD.[120] The 3D structure's practical usefulness was shown by processing commercially available LFP powder with two different methods—EPD and vibration-assisted drip-coating. EPD cathodes displayed a high specific capacity of 143 mAh g^{-1} at a C-rate of C/20 at a cell voltage of 3.4 V, which was better than those fabricated by means of vibration-assisted drip-coating. This was postulated due to a more uniform particle coating, and stronger particle attachment to the CNTs, leading to better electrochemical performance for EPD electrodes.[120] In summary, such investigations involving the EPD technique to apply LFP as a successful battery material for LiBs as well as microbatteries are given in Table 1.[132] It is also noted that some studies reported on binder-free EPD LiB electrodes, which is a decent step forward in terms of reducing operational costs.[137]

Oltean et al[140] coated TiO_2 on alumina pillars via EPD and employed the rods as current collectors. Moreover, Pascall and co-workers[87] applied photoconductive electrodes with an EPD method to arbitrarily produce micropatterned LiBs. The conductive part on the electrode surface was patterned with the as-deposited multiple materials.[19] In particular, the surface resistance changed with illumination variations. Similar to these examples, traditional methods of fabricating 3D structures also provide insights into the efficient EPD of 3D micro-LiBs.[141]

In another work, positive electrode architectures were effectively fabricated by means of the EPD of a functional coating comprising lithium iron phosphate (LFP)/carbon black/PVDF materials onto carbon fibre assemblies.[133] The electrochemical investigation on the EPD-coated carbon architectures exhibited that they operate nicely as positive electrodes, with a specific capacity ranging within 60 to 110 mAh g^{-1}, and 99.8% coulombic efficiency. Das and co-workers also recently showed the successful application of binder-free EPD of SbNP/rGO (antimony nanoparticles embedded in reduced GO) on Cu foil for enhanced LiB and Na-ion battery (SiB) performances at high C-rates for long cycles (as shown in Figure 7A).[138] This was a significant achievement because traditional doctor-blade slurry coating cannot prevent Sb delamination on Cu foil, whereas EPD was proven to be a viable technique to fabricate relatively rapid binder-free electrodes in about 3 minutes while also hindering Sb delamination.[142] Majumdar's group also prepared EPD anodes (bismuth iron oxide) that displayed exceptional performance in both LiBs and SiBs (Figure 7B), thereby showing significant promise for advanced battery technologies.[143] Based upon such progress, it is, therefore, important to summarize the key contribution of EPD on LiB electrode fabrication in comparison to some standard electrode manufacturing

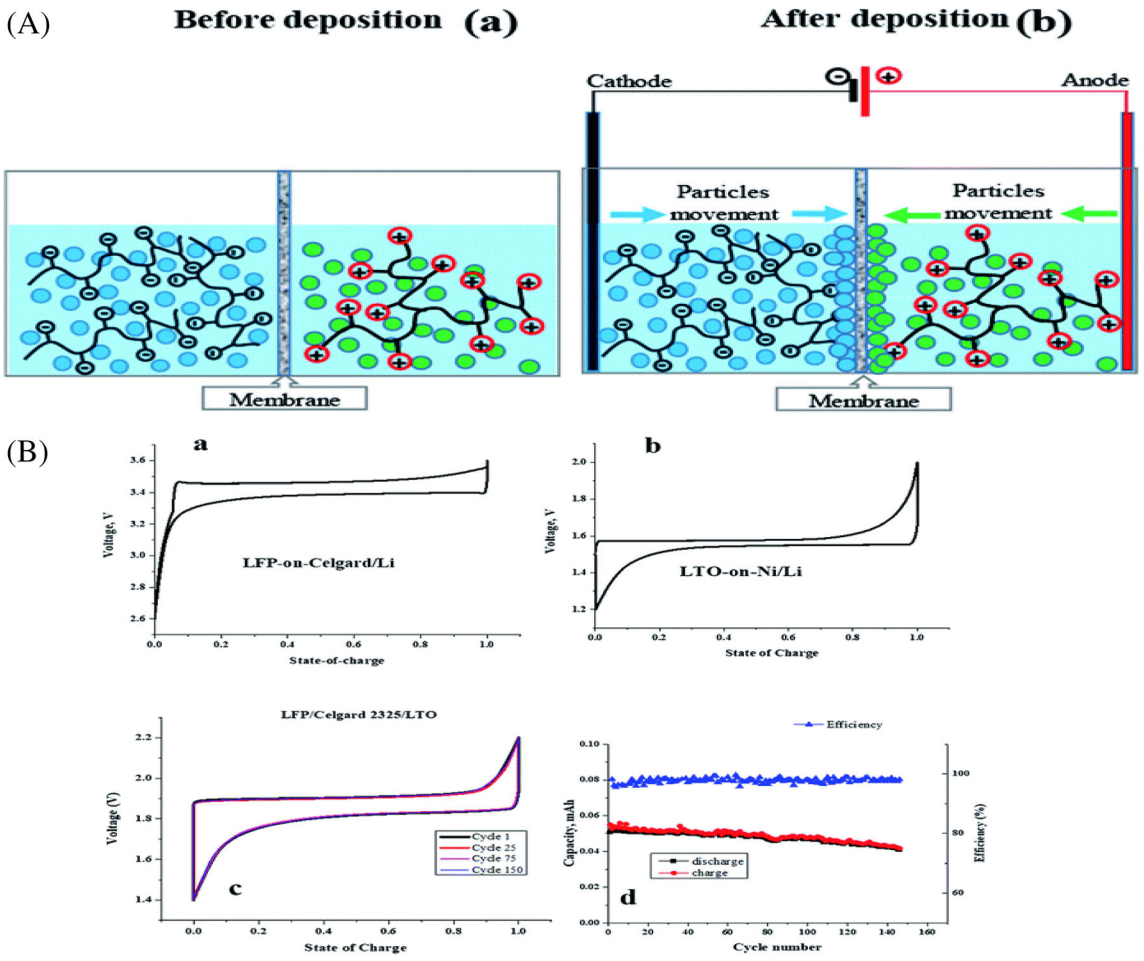

FIGURE 6 (A) Cartoon showing the EPD process for preparing membrane-electrode-assembly for LiBs. (B) Charge/discharge voltage profiles (a-c) of the flexible cells with EPD membrane electrodes (electrodes deposited on the Celgard 2325 separator) and cycle life (d) of the LFP/Celgard/LTO membrane-electrode battery assembly, consisting of $LiPF_6$ EC: DEC electrolyte. Reproduced with permission from RSC[124]

processes (mentioned briefly in Section 3) and this is given in Table 2 to complete this important sub-section.

It is also worth mentioning that one of the latest publications on conversion-type anodes for lithium half-cell application[147] mentions about the drawbacks of such systems involving transition metal oxides. In particular, capacity fading is a serious issue suffered from nickel ferrite anode materials and therefore various approaches have been tried and tested in the literature to circumvent this, for example, encapsulation by means of carbonaceous substances in addition to applying a range of binders.[153] However, the complexity and expenses associated with scaling-up is not a practical solution for industrial applications. In contrast, EPD is a facile method that can be scaled-up on demand and can produce uniform deposition of LiB electrode materials with good porosity networks as reviewed very recently.[154] High porosity enables a decent buffering of volume changes in nickel ferrite anodic materials upon cycling, thereby enabling the maintenance of good performances. Similar to the above example, the porosity control advantage offered by EPD enables optimization for particular active materials, that is, allowing for expansion of high capacity materials like silicon, or chemical changes as for conversion-type cathodes such as those being used for lithium/sulphur chemistries.[155,156]

Besides the above discussions on the application of EPD for LiBs, the importance of modifying electrode functional properties by means of nanomaterials, nanoarchitectures or nanocrystals is elaborated in the consequent sub-section. Additionally, EPD for manufacturing micro-LiBs is briefly touched upon to conclude this section, as this is a growing area of research.

6.1.1 | Nanocrystals

In order to exploit the functional properties of nanomaterials in practical devices, nanocrystals (NCs) are commonly assembled into dense and yet larger

superstructures.[157] A bottom-up method is used to prepare such compact structures and has the following advantages: (a) significant cost reduction in comparison to classical 'top-down' tactics such as CVD, and (b) unique properties that are yet to be explored in-depth.[158] Furthermore, the nature of the assembly (eg, ordered arrays, chains) can be effectively controlled by modulation of NC shape and ligand environment.[159]

EPD can be used to form NC films with advantageous properties such as high conductivity, and easily controllable thickness.[160,161] EPD offers several advantages over other methods of coating formation. Firstly, it is scalable; electrode size can vary from nanoscale to automotive-sized.[162] Secondly, the deposited coating properties (thickness, density, and morphology) can be tweaked in a facile manner by changing essential EPD parameters that are discussed in Section 3 (such as deposition voltage, inter-electrode distance, deposition time, etc.). Finally, the formation of configured deposits is possible by means of electrode templates. As a consequence, thin films of NCs,[161,163,164] CNTs[160,165] and rGO[116] have been demonstrated. Robinson's group also revealed a significant enhancement in conductivity when comparing a film of $Cu_{2-x}S$ NCs deposited by means of EPD with one deposited by means of spin-coating (Figure 8A).[161] The same group demonstrated in a later publication that they could successfully prepare robust LiB electrodes from copper sulphide, manganese sulphide and germanium nanoparticles by means of binder-free EPD techniques in addition to negating the use of conductivity enhancing agents (detailed in Figure 8B).[166] Furthermore, Ha and co-workers demonstrated an enhancement of mechanical adhesion of EPD films compared with the more conventional slurry or drop-cast-based deposition methods.[167]

A further advantage of EPD is demonstrated in the case of deposition of nanorods (NRs). Here, the in-built dipole causes the NRs to orientate and deposit along the electric field lines, causing dense, uniform and aligned films of easily controllable thickness to be deposited successfully.[168] These coatings exhibit improved charge transfer when compared with spherical NCs.[169] This work, therefore, demonstrates an economical combination of the EPD and nano-synthesis processes.

When chalcogenide-based NCs are dispersed in any kind of non-polar solvents, an electric field (direct current or DC) corresponding to several hundred volts per centimetre is usually needed to ensure quick deposition.[161,170] In a recent publication by Bree and co-workers, a programmable dip coater in combination with a high voltage source was used to conduct EPD with stringent control over electrode spacing, electric field and deposition time.[171] Two copper electrodes were used to apply 300 V to a freshly prepared colloidal formulation of

TABLE 1 Important processing parameters and obtained electrode characteristics in selected reports involving the EPD of LFP for LiB applications

Material and content	Bath	Carbon additive	Binder	Charging agent	Other	Substrate	Voltage	Time	Thickness, mass loading	Ref.
LFP	Acetone	CNT	-	-	3D CNT array	Aluminium foil	1.9 kV/m	-	0.4 mg	120
LFP	Acetone	C45, C65	LiPAA	Polyethylene imine	X-100	3D printed conducting polymer	50-100 V	1-2 minutes	2 μm	132
LFP 86-92%	Acetone 300 mL	CB (Super P) 4-8%	PVDF 4-8%	Iodine	X-100	Carbon Fibres	61-65 V	5 minutes	Very thin	133
LFP—0.45 g/L	25% water 75% EtOH	CB - 0.5 g/L	CMC-Na	PAZO-Na	N/A	Aluminium foil	10-50 V	3-10 minutes	4.3 mg cm^{-2}	134
LFP—2.5 g/L	IPA	GO - 0.5 g/L	Binder free	$Mg(NO_3)_2$-0.5 g/L	No additives	Carbon cloth	90 V	Not given	Not given	137
LFP—91%	Acetone	Black Pearl—4%	PVDF—5%	None	X-100 surfactant (0.8% v/v)	Nickel Disc	60-100 V	-	10 μm, 6 mg cm^{-2}	138
LFP—89%	EtOH	Super C45-9%	XG	-	2 cm IED, Al foil counter	Fibrous carbon cloth	100 V	10 minutes	2, 10, 20 mg cm^{-2}	139

Abbreviations: EtOH, ethanol; IED, inter-electrode distance; IPA, isopropyl alcohol; X-100, Triton non-ionic surfactant; XG, xanthan gum.

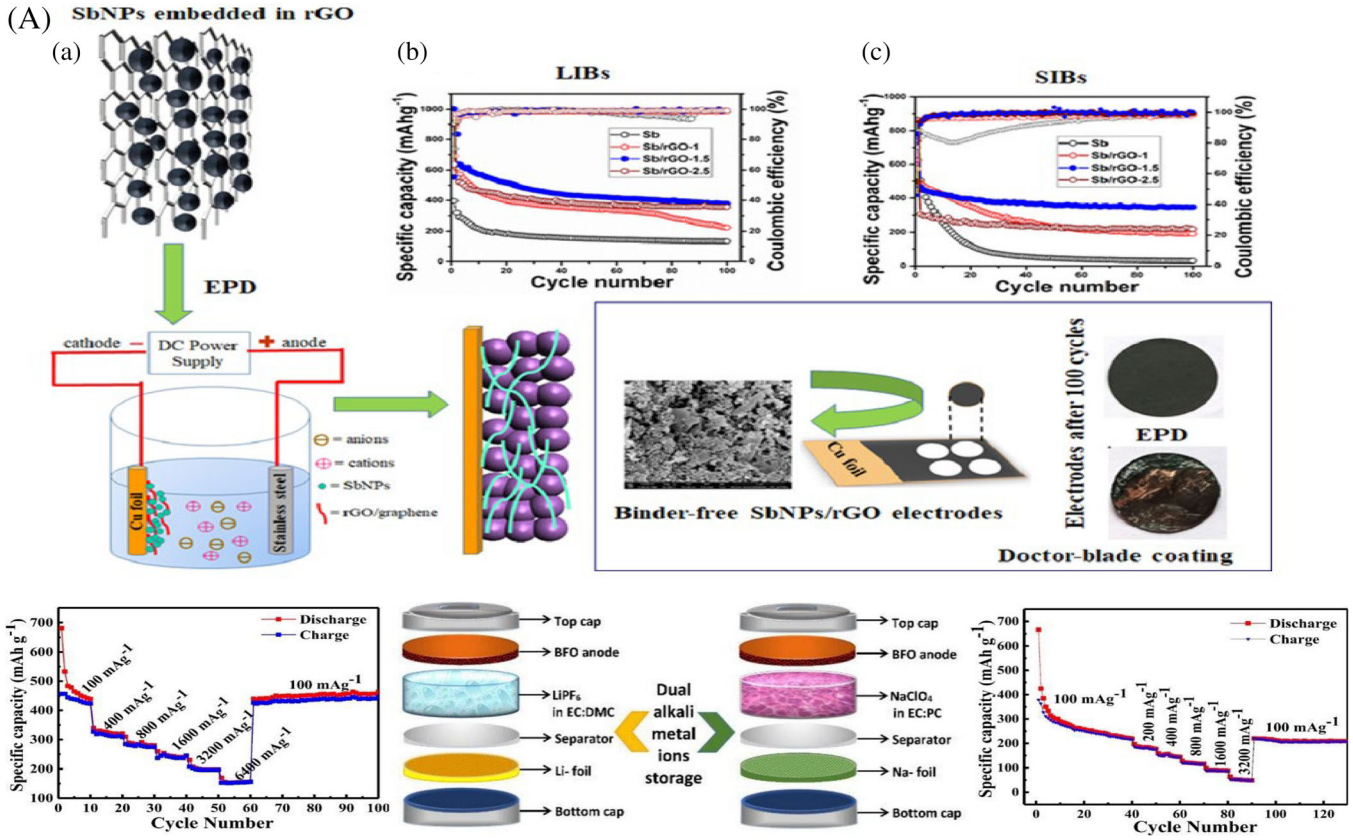

FIGURE 7 (A) Hydrothermal material synthesis and binder-free SbNPs/rGO electrodes fabricated on copper foil by EPD (a); galvanostatic discharge-charge cycling for SbNPs, SbNPs/rGO-1, SbNPs/rGO-1.5, and SbNPs/rGO-2.5 electrodes tested in LiBs (b); and galvanostatic discharge-charge cycling for SbNPs, SbNPs/rGO-1, SbNPs/rGO-1.5, and SbNPs/rGO-2.5 electrodes tested in SiBs. Numbers 1, 1.5 and 2.5 refer to the original concentration of GO (mg mL^{-1}) in the reaction mixture for preparing the EPD electrodes (c). Image reproduction approved by Elsevier.[138,142] (B) Majumdar's group successfully prepared anodes via EPD that gave excellent rate performance (~465 and 151 mAh g^{-1} at current density of 0.1 and 6.4 A g^{-1}, respectively) and cyclability during lithium storage while giving highly reversible, stable discharge capacity of ~223 mAh g^{-1}, maintained beyond 100 cycles with a constant coulombic efficiency of 98% during SiB applications. Reproduced with permission from Elsevier[143]

NCs (toluene was used as a solvent in the case of tin sulphide (SnS) and anhydrous hexane for Cu_2ZnSnS_4 (CZTS)), as illustrated in Figure 9A.[171] Deposition was allowed to occur for 5 minutes, during which the liquid colour changed, and became colourless when all the NCs were deposited. For both materials reported by Ryan et al, the NCs were deposited on the positive electrodes alone (Figure 9B).[171] The deposited electrode microstructure is shown in the cross-sectional SEM image in Figure 9C.[170,172,173]

In another study by Bree et al, SnS nanocubes were used as LiB anodes.[171] The nanocubes were deposited as compact, lean conductive surface coatings with elevated gravimetric capacity by means of a binder-free EPD process. A discharge capacity of 552 mAh g^{-1} was obtained with a minimal loss of around 0.08% per cycle for over 400 charge/discharge cycles. Finally, as demonstrated in similar investigations for LiBs,[2] the application of 3D current collectors enabled higher mass loadings of SnS nanocubes in the EPD electrodes.[171]

6.1.2 | 3D micro-LiBs

In a micropatterned EES device (battery or capacitor), large contact area is obtained by forming an interdigitated structure,[174,175] and such a structure improves the rate capability of LiBs and lithium-ion capacitors (LiCs).[19] In addition, studies also reported a 3D LiB configuration consisting of a number of micro-LiBs.[125] In such a battery, micro-LiBs made via EPD are connected in parallel onto a substrate. The entire micro-LiB possesses a sizeable electrochemical surface area owing to the fact that each of its electrode has decent electrolyte exposure. Therefore, the 3D micro-LiBs supply a large current and a decent-power density. In addition, brilliant rate capability and successive cycling operation are displayed by such 3D LiBs.[176] In EPD, a 3D arrangement may be obtained by shaping a conductive layer onto a resistive surface, and the process may be likened to integrated circuit plate designing. Mazor and co-workers performed EPD of a lithiated-graphite anode layer along with $LiFePO_4$ on a perforated-

TABLE 2 EPD parameters for preparing LiB electrodes and key results reported in recent literature and compared against a few electrodes prepared via industrially approved processes

Electrode Material	Binder	Time (minutes)	EPD voltage (V)	EPD Solvent/Charging agent	Electrode thickness (μm)	Electrode mass loadings (mg cm^{-2})	Specific capacity (mAh g^{-1}), cycle number and C-rate for charge/discharge	Coulombic efficiency (%)	Ref.
LFP on C fibres + ErGO	PDDA	5	70	DMF with PDDA in EtOH + CB	1-5	1	91 at 1C that drops to 84 in 500 cycles	99.9	144
LTO + rGO	None	5	35	EtOH +2D Li titanate hydrate + GO	15-20	1.67	175 at 1C that drops to 147 in 150 cycles	99.9	145
Bismuth iron oxide	None	3	100	IPA + CB + poly-acrylic acid and nickel nitrate hexahydrate	7	Not given	Drops from 680 to 420 in 60 cycles at 100 mA g^{-1}	> 90	143
LFP and CNT	None	Not given	1900/m	Acetone	6-15	0.4	89 at 1C	Not given	120
LFP and LTO on Celgard	Poly (acrylic acid)	5	50 or 100	Polyethyleneimine in acetone	Not given	0.5-12	Drops from 140 to 125 in 150 cycles (C-rate not given)	> 90	120
LFP	Xantham gum	10	100	EtOH	Not given	2-20	67 at 1C with about 15% drop in 300 cycles	<100	139
TiN on Cu foam	None	20	40	EtOH + magnesium nitrate	Not given	2-5	141 at 2C in 700 cycles	98	146
MOF-NFO	Poly acrylic acid	3	100	IPA + CB + nickel (II) nitrate	89	Not given	275 at 8 A g^{-1}	99	147
LFP Graphene Composite	PVDF	N/A	N/A	N/A	Not given	1.3	168 at 0.1C	Not given	148
LFP Carbon Composite	PVDF	N/A	N/A	N/A	Not given	8.9	162 at 0.1C	Not given	149
LTO	PVDF	N/A	N/A	N/A	90	16	157 at 0.1C	Not given	150
LTO	PVDF	N/A	N/A	N/A	60	7.3	170 at 0.1C	Not given	151
LFP	PVDF	N/A	N/A	N/A	70	7.3	170 at 0.1C	Not given	152

Abbreviations: EtOH, ethanol; MOF, metal-organic-framework; NFO, nickel ferrite; TiN, titanium nitride.

silicon surface to function as the cathode.[177] Furthermore, a patterned gold-coated substrate was connected to 10 000 micro-LiB units per cm^2 to create a 3D design.[19] At 100% depth of discharge (DoD), the micro-LiB configuration exhibited a stable operation over 200 cycles.

6.2 | Lithium-ion capacitors (LiCs)

LiCs bridge the gap between LiBs and supercapacitors by employing an LiB anode with one supercapacitor cathode in the presence of a lithium-ion enriched electrolyte.[178] The electrolyte commonly used involves the dissolution of the lithium-based salt in an organic solvent like propylene carbonate due to a larger potential window than that of aqueous electrolytes, thus providing a higher energy density.[96] Since the capacity of the LiC electrode is much lower than that of the LiB electrode, the cathode is the key to improving the energy performance of LiCs.

Activated carbon (AC) is a conventionally employed cathodic substance for LiCs as a consequence of its prominent specific surface area, decent electrical conductivity and modest price.[66] However, AC possesses relatively minimal specific capacity.[179] Therefore, to cultivate LiCs as a contesting candidate for EES applications, it is imperative to fabricate unconventional cathodic substances with decent specific capacities and excellent rate capabilities. Thus, Mandler et al recently used a combination of electrodeposition and EPD for assembling porous electrodeposited rGO (ErGO) as an LiC cathode and assessed its operation in both symmetric capacitors and lithium half-cells resulting in improved capacitance by compositing with V_2O_5 nanomaterials.[96] This compositing process improved the capacitance of the LiC significantly. In particular, the ErGO/V_2O_5 LiC displayed capacitance values as high as 168 F g^{-1} at 0.1 A g^{-1}, as illustrated in Figure 10.[96]

Wu and co-workers initially synthesized 1D nitrogen-doped carbon nanoparticle chains (CNCs) by means of thermal pyrolysis of a 3D polymer precursor in the form of zinc hexacyanoferrate without using any additional nitrogen, carbon and catalyst sources.[180] The CNC film was then deposited on a stainless steel (SS, 1 cm × 1 cm) sheet by means of EPD. Then they compared the performance of the CNC electrodes with commercially sourced multiwalled CNT (MWCNT) electrodes. They found that the MWCNT electrodes stored Li^+ ions mainly by means of intercalation, whereas the CNC electrode accumulated Li^+ ions owing to a combination of the adsorption and intercalation phenomena. From these results, the authors

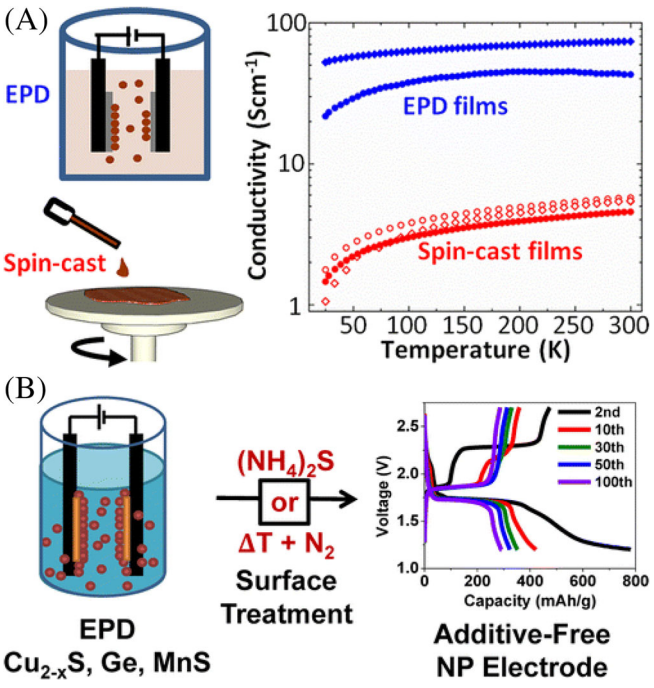

FIGURE 8 (A) EPD results in an order of magnitude enhancement in film conductivity (~75 S·cm^{-1}) over conventional spin-casting.[161] (B) EPD of nanoparticles (NPs) followed by two post-processing treatments ($[NH_4]_2S$ and inert atmosphere heating) can form LiB electrodes that can be cycled successfully with ~30% enhancement in specific capacity due to absence of colloidal additives. Reproduced with permission from ACS[166]

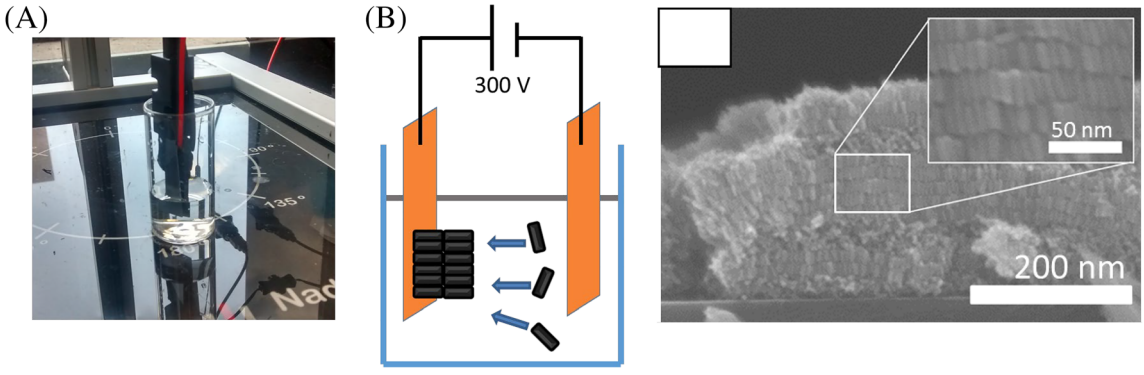

FIGURE 9 (A) Photo of electrodes immersed in solution during EPD using a programmable dip coater. (B) Diagram showing the EPD of CZTS NRs. (C) FIBSEM cross-sectional image of an EPD CdS NR aligned film[170]

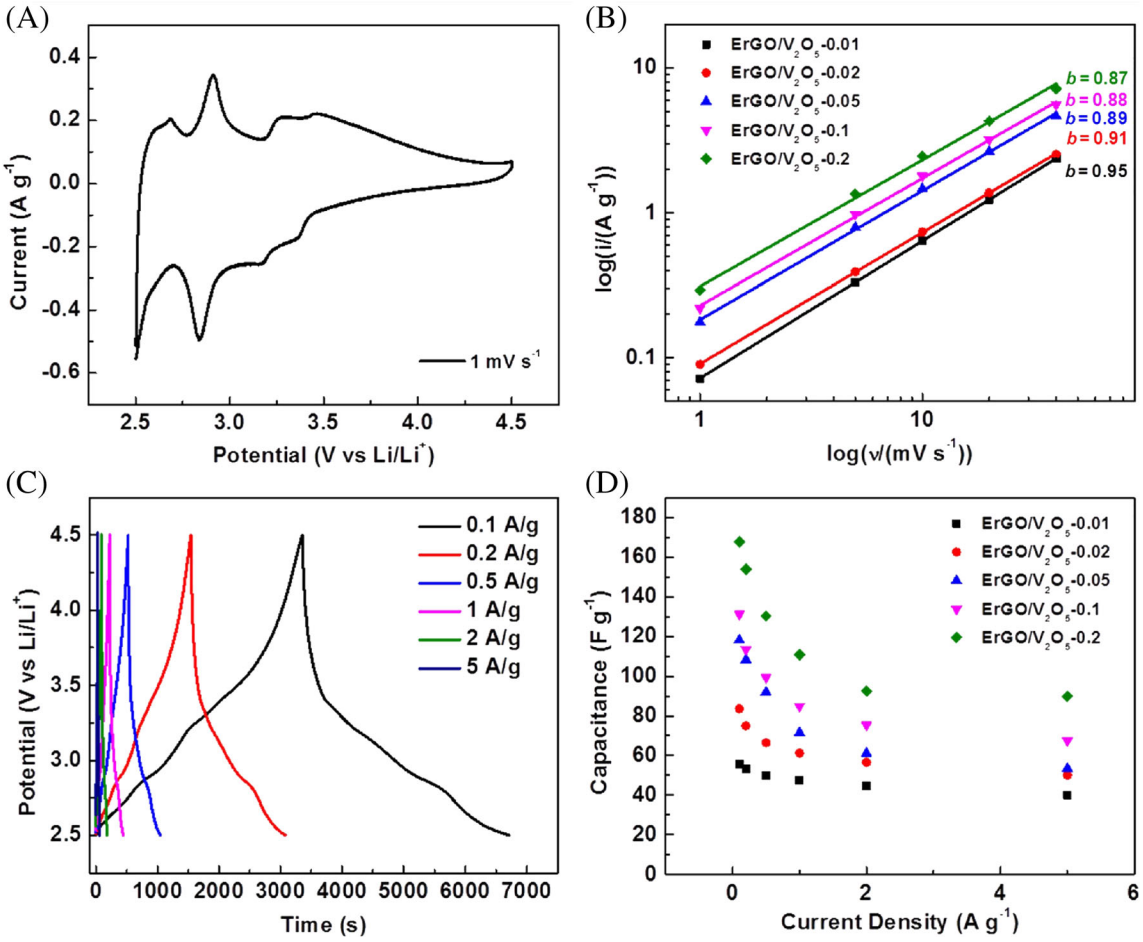

FIGURE 10 (A) Cyclic voltammogram (CV) of ErGO/V_2O_5-0.2 (ErGO rinsed in 0.2 M solution of VOC_2O_4 followed by annealing) at 1 mV s^{-1}; (B) the anodic peak currents of ErGO/V_2O_5-0.2 plotted against the logarithm of the CV scan rate; (C) the charge-discharge profiles of ErGO/V_2O_5-0.2 at various current densities; and (D) the derived capacitances of various ErGO/V_2O_5 composites evaluated. Reproduced with permission from Elsevier[96]

concluded that the CNC electrode had better super capacitive performance than the commercially sourced MWCNT electrode, mainly due to a lower internal resistance of the former. Specifically, the CNC electrode displayed a high capacitance of 680 F g^{-1} at 1 A g^{-1} at a working potential range of 0.01 to 3.50 V vs Li/Li^+, in comparison to that of the MWCNT counterpart that had approximately three times less capacitance of 252 F g^{-1}.[180]

6.3 | Lithium-sulphur (Li-S) systems

The lithium-sulphur battery chemistry, which utilises a sulphur cathode and lithium metal anode, has excellent potential to replace lithium-ion as the standard high energy density EES. The gravimetric capacity of the sulphur cathode (1675 mAh g^{-1}) and lithium anode (4200 mAh g^{-1}) far exceeds that of current generation electrodes. EPD has been successfully utilised in the manufacture of sulphur-based cathodes, largely through the preparation of suitable conductive films, which act as host materials for sulphur. For example, Chung and co-workers successfully used the EPD process without binding agents to decorate a carbon fibre paper (CFP) with carbonaceous nanomaterials to prepare cathodes for Li-S battery applications.[181] The S cathode modified with EPD of CNT on CFP (EPD:CFP/CNT) provided a capacity of around 2.2 times higher (upon completing 50 cycles) than that supplied by its counterpart without the EPD-CNT coating (CFP/S cell) at 0.1 C. Also, the CFP/S electrode's rate capability could be elevated by means of a combination of the EPD-CNT/carbon black and EPD-CNT electrode materials on the CFP surface. As such, the EPD of CNT and Pt nanoparticles resulted in an EES device that displayed a specific capacity of about 730 mAh g^{-1} at 1 C.[181] Finally, the EPD manufactured cathodes outperformed their counterparts prepared by means of the classical slot-die casting process, especially with regards

to successive charge/discharge cycles, polarization and internal resistance. This was as expected and confirmed by other investigations for EPD to prepare high-quality LiB electrodes in comparison to those made by standard slot-die casting of slurry pastes.[2] In particular, the slot-die casting results in the formation of heterogeneous microstructures in the CNT film with blocked porous architectures therefore causing meagre interfacial connection between the CNT clusters. As a consequence, the slurry cast CNT film ended up hindering a uniform sulfide/sulphur deposition during cycling, which resulted in poorer performance when compared with the excellent output from EPD electrodes.

Similarly, some researchers utilised EPD to fabricate a high-quality, conformal nanostructured carbon film, which was then loaded with sulphur through vapour-phase sulfurization.[139,156] When tested as cathodes in Li-S batteries, these electrodes exhibited high capacities in excess of 1200 mAh/g^{-1}.

The major challenge to be overcome to commericialise lithium-sulphur battery is that known as 'polysulfide shuttling', whereby ions such as Li2S4 migrate to, and poison, the anode, leading to rapid capacity loss.[182] A unique application of EPD has been demonstrated to overcome this challenge. Blanga et al reported the formation of a polysulfide barrier through EPD.[183] A $Li_{10}SnP_2S_{12}$ (LSPS)/polyethylene oxide (PEO) film was deposited from acetone solution, and demonstrated high ionic conductivity. When coated on the surface of sulphur and lithium sulfide cathodes, the film enhanced electrode capacity and faradaic efficiency, while effectively mitigating the effect of polysulfide shuttling.

EPD has also shown promise in overcoming another challenge with Li-S batteries, specifically that of lithium dendrite formation at the anode. Zhang et al carried out the EPD of $Ti_3C_2T_x$ nanoflakes onto Cu foam.[184] The 3D structured current collectors demonstrated excellent Li plating/stripping efficiency with reduced overpotential, maintaining a uniform and dendrite-free Li film. The authors attribute this to both the 3D nature of the EPD electrode, which increased the effective surface area and the lithiophilic nature of the nanoflakes. Wang et al reported a similar effect from the EPD of black phosphorus (BP) onto Cu foam, whereby initial lithium nucleation was confined to the BP sites and thus controlled.[185] This effect brought about a significant increase in the plating/stripping efficiency and cycling stability.

Such exceptional results for the EPD electrodes, resulting in high capacities, could therefore transform into high energy densities of Li-S batteries, opening up the scope for scaling-up the EPD technique to commercial Li-S applications in future.[181]

6.4 | Electrodes for flow batteries

Redox flow batteries (RFBs) have many advantages such as high-energy efficiencies (up to 80%), simple control and monitoring systems, long cycling lifetimes, relatively low maintenance costs, flexible design and an environmentally friendly structure.[14] From the environmental point of view, Fernandez-Marchante and co-workers showed the lowest environmental impact from 12 midpoint impact categories, including water footprint, and photochemical oxidation, with a longer lifetime for RFBs considering the re-use of vanadium electrolytes in comparison to conventional LiBs.[186] Although primary studies were done by Thaller in the early 1970s,[187] major improvements were obtained by Skyllas-Kazacos in the 1980s.[14,188-190] This type of battery consists of inert electrodes, flowing electrolytes and membranes as its main structure.[191-195] Cycling life and the performance of the battery are also mainly related to the type of electrodes employed.[14,196-199] Although graphite-based electrodes have been used for positive and negative electrode components, modification of this material by metal oxides and other carbon-based compounds has great importance.[14,197,200-202] In this regard, the preparation of high-performance electrode materials for RFBs can be conducted by means of EPD and its associated advantages are discussed in this review. This is of utmost significance at this time because the application of RFBs for grid-scale load levelling as well as efficient and green storage of renewable energy is expected to increase in the near future. EPD, therefore, has an important role to play in terms of the electrode and, in the future, membrane modification or (even) manufacturing processes. In hindsight, the reported applications of EPD for RFB applications are low (as discussed briefly in the following paragraphs), and this review is expected to advocate its interesting properties for the scientific community to explore.

rGO was deposited electrophoretically on carbon paper (using a horizontal EPD set-up in contrast to the standard vertical means) for use as a positive all-vanadium RFB (VRFB) electrode.[203] An increase in the surface area by 24% was reported due to the deposition of rGO. A decrease in charge transfer resistance (R_{ct}) was also correlated to an increase in electrochemical surface area (ECSA). This investigation was followed up with a study on hydrogen/vanadium regenerative fuel cell (RHVFC) electrodes,[3] as well as on VRFB electrodes,[200] which were modified with rGO in both studies. The investigation on RHVFCs showed enhanced performance due to EPD of rGO on the carbon paper electrodes, especially for ones that were subjected to thermal treatment beforehand (Figure 11),[3] signifying the promise of this

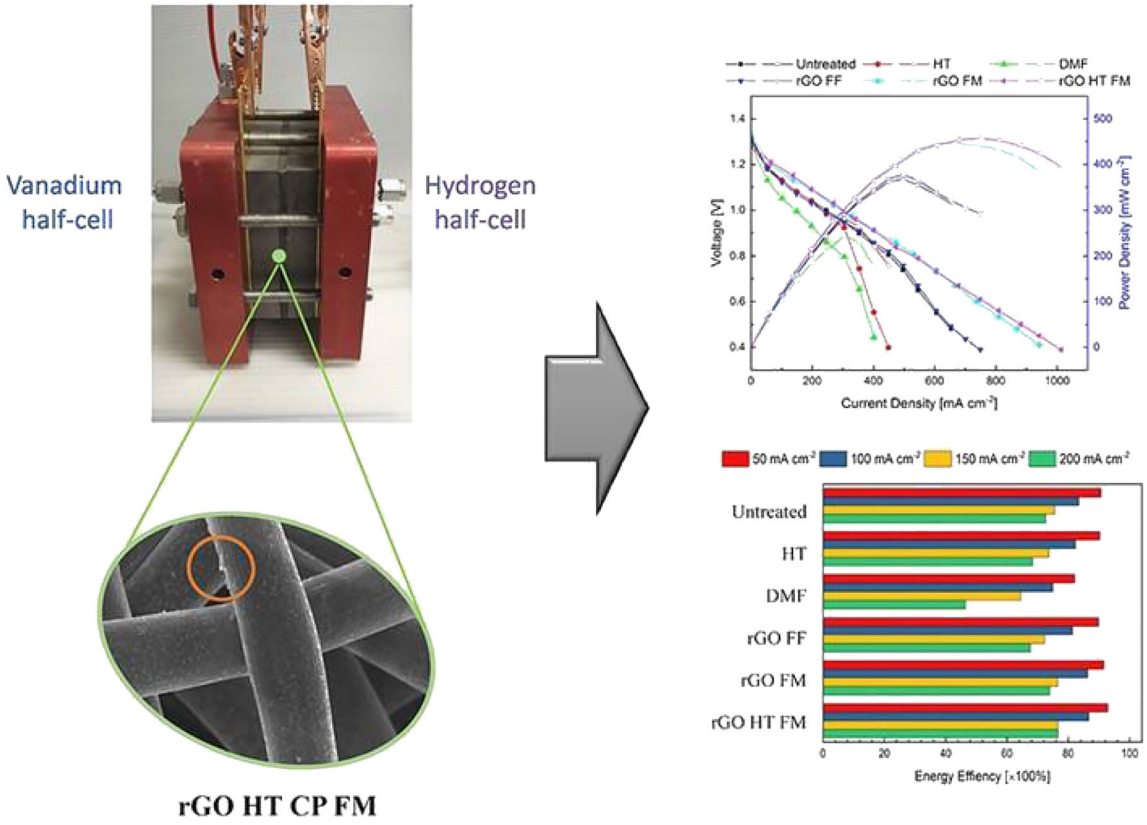

FIGURE 11 Application of rGO modified Freudenberg carbon paper (commercially available) as RHVFC positive electrodes to result in high peak power densities and energy efficiencies when the rGO modified side faced the membrane (rGO FM). The heat-treated CP that underwent EPD with rGO delivered the best performance (rGO HT FM). EPD was conducted with DMF as the solvent. HT, heat treated electrode; DMF, EPD performed with only DMF solvent without rGO dispersed in it; rGO FF, rGO deposited carbon paper electrode facing the flow fields of the RFB. Reproduced with permission from Elsevier[3]

modification technology for flow battery scale-up applications.[204]

Gonzalez and co-workers applied EPD on a graphene oxide (GO) suspension in water to coat graphite felt substrates.[204] From SEM and XPS evaluation of the GO decorated graphite felts, the establishment of a hybrid architecture possessing more oxygen-containing functional groups than standard felts was reported to enhance electrolyte wettability and consequently ECSA. More evidence of this effect was only confirmed by a higher capacitive current from cyclic voltammetric investigations in the same work.[205] The presumption was that graphene-like sheets of rGO (due to partial reduction of GO during heat treatment) may have improved electronic conductance, which was confirmed by separate studies.[99,206-208]

Recently, the EPD of nitrogen-doped graphene (N-G) on carbon paper electrodes (CP) has been reported by WMG to enhance the performance of non-aqueous VRFBs applying deep eutectic solvents (DESs)[113] as well as three different RFCs employing either highly acidic or alkaline electrolytes (Figure 12A).[209] In the first investigation, the DES-based VRFB was subjected to about 20 cycles to evaluate its temporal fluctuation of efficiencies and utilization.[113] Figure 12B, which was reconstructed from x-ray tomographic scans, clearly shows the N-G occupying the porous CP electrode, which was considered responsible for the enhanced improvement of the N-G/CP electrode in comparison to the pristine CP electrodes in the DES-based VRFB. In this respect, Figure 12C displays the cycling curves that show a noticeable energy efficiency and electrolyte capacity utilization enhancement when using N-G/CP electrodes for the DES-based non-aqueous VRFB in a similar manner to aqueous-based RFCs.[209]

The EPD method was mainly applied to carbon-based materials such as rGO and N-G in the literature.[113,206] In this respect, Table 3 displays a range of carbon-based electrode modifications reported in the literature for applications in selected RFB systems.[14,219] As can be noted in Table 3, EPD of carbonaceous materials has provided many benefits in comparison to standard electrode treatment methods such as thermal or chemical. However, this method can also be used for the deposition of other types of materials to improve the electrode

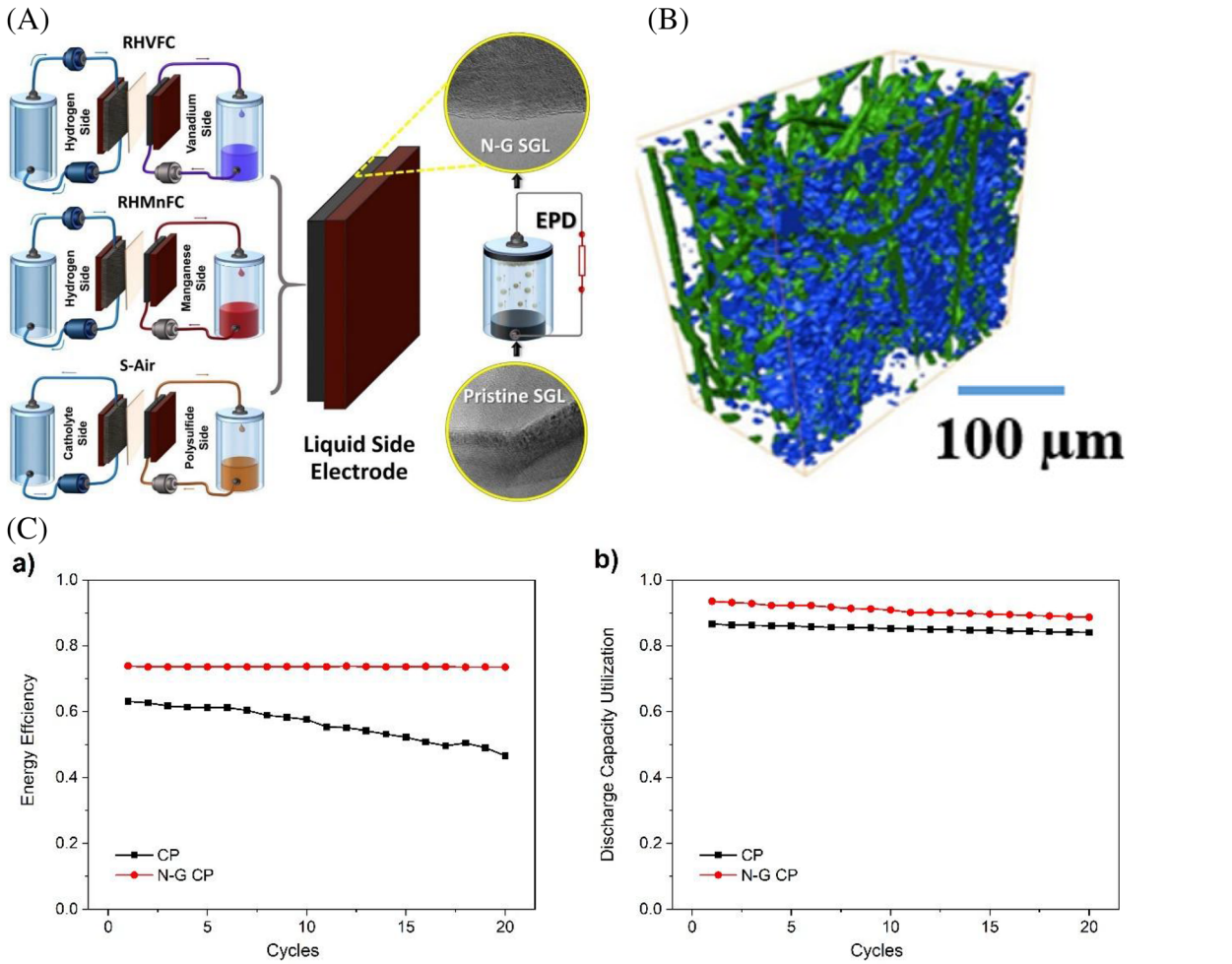

FIGURE 12 (A) Cartoon showing a horizontal EPD method for decorating commercially sourced CP electrodes with nitrogen-doped graphene (N-G). These modified electrodes are successfully employed in three types of RFCs, namely hydrogen/vanadium (RHVFC), hydrogen/manganese (RHMnFC) and polysulfide/air (S-Air). Reproduced with permission from ACS.[209] (B) Reconstructed X-ray computed tomography (XCT) image of the N-G/CP (N-G doped CP) manufactured via EPD. Allowance to reproduce the images obtained from MDPI[113] and Wiley.[203] (C) Performance evaluation studies of 0.1 M vanadium acetylacetonate with 0.5 M tetraethylammonium tetrafluoroborate in a deep eutectic solvent via cycling at 10 mA cm^{-2} charge/discharge current density at 45°C highlighting (a) energy efficiencies and (b) discharge capacity utilization in a non-aqueous VRFB. Reproduced with permission from MDPI[113]

performance of the RFBs. Especially, metal-based materials such as TiO_2, TiN, TiC, MnO_2, etc. or metal-organic frameworks can be used as effective modifiers to the surface of the carbonaceous materials for both positive and negative electrodes.[211] Increased active sites due to the modification of RFB electrodes with such kind of materials via the EPD method can increase the electrocatalytic selectivity of the electrode materials for redox reactions associated with the flow battery type. Indeed, enhanced properties such as high discharge capacity, high energy and columbic efficiencies in battery properties can also be obtained by this modification process.[14] This, therefore, advocates a strong case to perform more extensive investigations on EPD for enhancing the electrodes and/or membranes of RFBs in future studies, with a particular emphasis towards advocating the widespread commercial adoption of this EES device.[220]

6.5 | Electrodes for supercapacitors

Supercapacitors represent a critical class of EES devices with vital advantages such as elevated power response and exceptional cycling stability owing to their lofty power density, rapid charge/discharge rate, and high coulombic efficiencies.[221] Supercapacitors are conventionally classified into two types that owe their distinction to contrasting energy storage features.[222] One such classification is known as the electrical double-layer capacitor (EDLC) that owes its performance uniqueness to ion

TABLE 3 Some representative electrode modifications using carbonaceous additives for vanadium-based RFBs and hybrid RFCs sampled from the literature

Carbon electrode	Modification procedure(s)	RFB type	Efficiency increase (%)[a]	Cycles	Current Density (mA/cm^2)	Ref.
Carbon Paper (CP)	**EPD of rGO from DMF on thermally treated CP**	**RHVFC**	**24**	**10**	**50**	3
CP	**EPD of N-G**	**DES-based organic VRFB**	**80**	**20**	**10**	113
GF	**EPD of GO from water suspensions**	**VRFB**	**15**	**20**	**25**	204
CP	**EPD of N-G**	**RHVFC**	**20**	**150**	**100**	209
		RHMnFC	**50**	**50**	**100**	
CF	**EPD of functionalized CNTs or GO**	**VRFB**	**10[b]**	**Not evaluated in a RFB**		210
GF	Solvothermal insertion of CoS_2/CoS heterojunction nanoparticles	S-I RFB	50	60	20	211
Graphite felt (GF)	Thermal activation under NH_3/O_2 (1:1) for PAN modified GF	VRFB	79	30	20	212
Carbon felt (CF)	Electrostatic LbL of GN nanoplatelets	VRFB	5	4	30	213
GF	Catalytic chemical etching and thermal treatment	VRFB	21	50	300	214
CF	Electrochemical deposition of ErGO	VRFB	50	20	60	215
PAN-based GF	N-doped CNT doped via thermal treatment with Fe	VRFB	30	30	100	216
PAN-coated GF heat	N-doping with thermal oxidation	VRFB	10	100	100	217
Carbon-metal fabric (CMF)	Electrospun deposition of Fe + carbonisation	RHVFC	15	500	200	218

Note: Electrodes modified by means of EPD are highlighted in bold. For more information the reader is referred to a good review on the topic.[14]
Abbreviations: DES, deep eutectic solvent; DMF, *N′N′*-dimethylformamde; ErGO, electrochemically reduced graphene oxide; GN, graphene; LbL, layer by layer deposition; N-G, nitrogen-doped graphene; PAN, polyacrylonitrile; RHMnFC, hydrogen/manganese hybrid flow battery; RHVFC, hydrogen/vanadium hybrid flow battery; S-I RFB, polysulfide/iodide redox flow battery.
[a]**Energy efficiency** increase due to the electrode modification process.
[b]Estimated from cyclic voltammetry data at a scan rate of 25 mV s^{-1}.

desorption and adsorption. This is a function of the accessible electrode surface to ions from the electrolytic solvent. Indeed, heteroatoms formed, including functional groups, on the electrode materials significantly affect the performance of EDLCs.[212,223-226] Arvas et al explained this phenomenon with the use of sulphur doped graphene electrodes prepared by means of Yucel's one-step method.[223]

The other classification is known as a pseudo-capacitor whose mechanism is dependent upon a rapid and reproducible faradaic process that occur as a consequence of electroactive species.[227,228] Similar to batteries, supercapacitors comprise of a couple of electrodes, a separator and an ionic solvent/electrolyte.[229] Symmetrical supercapacitors tend to consist of two duplicated electrodes fabricated from identical materials, whereas asymmetrical supercapacitors consist of two dissimilar electrodes prepared from varying capacitive and faradaic materials. The industrially approved standard method for manufacturing electrodes involves paste-coating that can cause binding agents (commonly employed) to cover the electrode surface or block the open porosity network.

Additionally, a crucial issue for a packed supercapacitor is the need to account for the complete system mass, which comprises electrode films, current collectors, binder, separators, electrolyte, connectors and packing materials.[230] This is also true for supercapacitors meeting the minimum industrially approved active material mass

loading standard of 10 mg cm^{-2}. In these cases, the active electrode mass is around 30% of the total device weight.[231] For such circumstances, the operation of the supercapacitor estimated from the electrode material has to be divided by 3 or 4.[232] The divisor is elevated to 30 if a slender electrode having a 1 mg cm^{-2} mass loading is used.[230] Therefore, adequate electrode mass loading is essential to diminish overheads due to inactive materials, which can effect a decent electrochemical supercapacitor output. Currently, EPD has been considered appealing for manufacturing electrodes owing to its ability to produce surface coatings without employing binders while ensuring quality control over the active material film thickness as well as mass loadings. The consequent paragraphs deliver a sufficient impression of current scientific and technological advances in EPD electrodes manufacturing and performances.[36]

Rashti et al described a scalable, rapid and cost-effective EPD method for manufacturing nickel cobaltite composite electrodes for supercapacitor applications.[233] The composite EPD electrode ($NiCo_2O_4$/PANI/rGO) with rGO and polyaniline (PANI) was post-treated thermally under a reducing nitrogen atmosphere to carbonize the PANI component. $NiCo_2O_4$ platelets, dispensed on carbonized PANI–rGO architectures, were involved in charge storage with decent capacitance, exceptional rate performance (1235 F g^{-1} at 60 A g^{-1}), and 3000 charge/discharge cycles at 10 A g^{-1}.[233] The composite electrode in combination with AC in a symmetrical capacitor displayed a capacitance retention of 78% after 3500 cycles at an enhanced functioning potential of 1.5 V at a practical current density 1 A g^{-1}. This study indicated the significance of the EPD composite construction method that, in turn, influenced the aggregate microstructure.[233]

Binder-free Ti_3C_2 MXene (MXenes are 2D transition metal carbides, carbonitrides and nitrides)/CNTs (Ti_3C_2/CNTs) coatings were effectively decorated on a graphite paper substrate by means of EPD and applied as electrodes for a supercapacitor (Figure 13).[234] The manufactured Ti_3C_2/CNTs electrode displayed elevated specific capacitance, about 1.5 and 2.6 times than that of immaculate CNTs and Ti_3C_2 coatings, respectively. Ti_3C_2/CNTs electrodes impressively gave excellent capacitance retention over 10 000 cycles owing to an effective hindrance to MXene restacking as a consequence of incorporating CNTs into MXene by means of the practical and effective EPD technique.[234]

Graphene quantum dots (GQDs) are comparatively a contemporary genre of carbonaceous nanomaterials with various attractive properties such as photoluminescence and decent surface area.[235] Owing to its large surface area to volume ratio, GQD is an admirable intrant material for application in supercapacitors.[236] Tjandra et al showed an effective means of preparing GQDs by means of a hydrogen peroxide-assisted hydrothermal reaction and then applied it with carbon cloth to manufacture a flexible supercapacitor electrode possessing high rate capabilities and a relatively high areal capacitance of 70 mF cm^{-2}.[237] The authors also prepared full cell flexible supercapacitors using two EPD GQD electrodes (Figure 14 shows the supercapacitor performance with an areal capacitance of 24 mF cm^{-2}).[237]

Wang et al successfully combined a polymer electrolyte based on poly(vinyl alcohol)-H_3PO_4 (PVA-H_3PO_4)

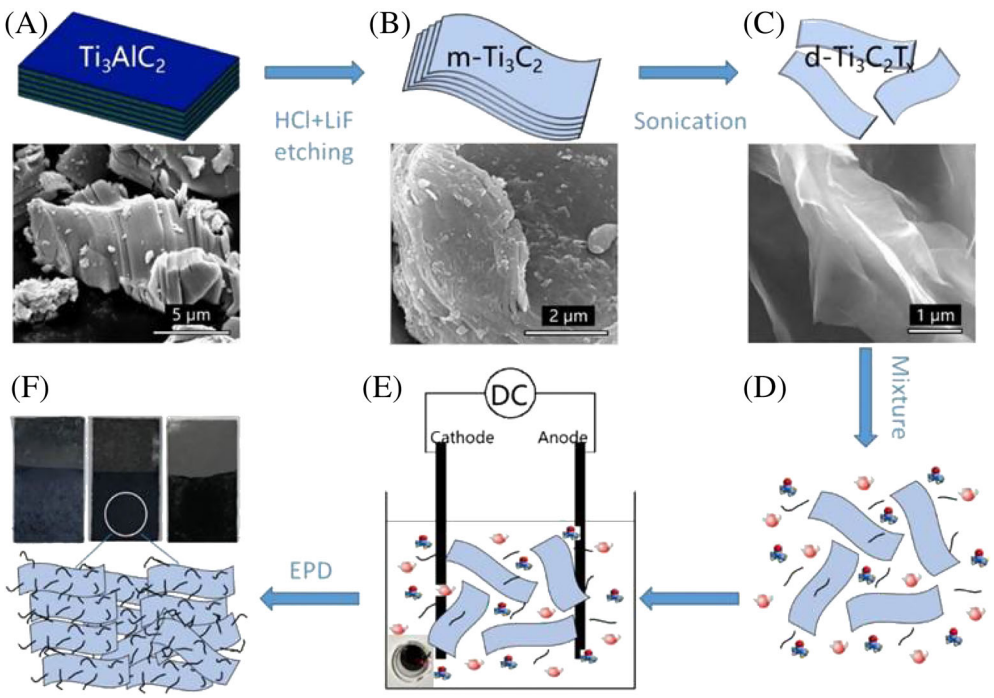

FIGURE 13 Cartoon highlighting the preparation route of electrode films by the EPD method: Drawing and morphology of (A) Ti_3AlC_2; (B) m-Ti_3C_2; (C) d-Ti_3C_2; (D) a solution mixture of deionized water and acetone with d-Ti_3C_2 and CNTs; (E) cartoon showing the EPD process; (F) drawing and photo of d-Ti_3C_2 coating, Ti_3C_2/CNTs coating and CNTs coating. Reproduced with permission from Elsevier[234]

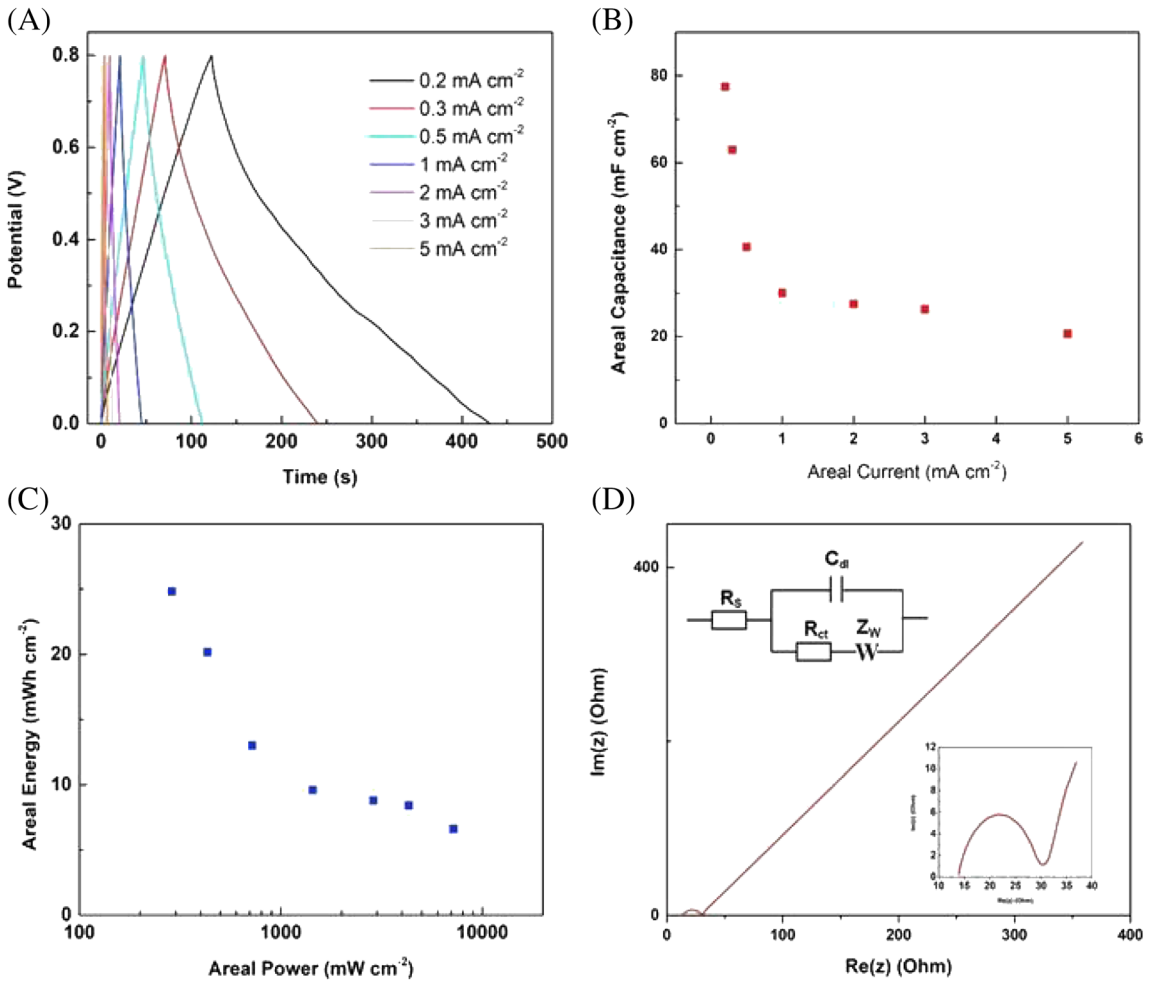

FIGURE 14 (A) Galvanostatic charge and discharge curves of a symmetric supercapacitor at different areal currents; (B) Spatial capacitance of the supercapacitor against the spatial discharge current; (C) Ragone plot of the spatial energy and spatial power of the supercapacitor; and (D) Impedance graph along with an equivalent circuit layout and an inset figure magnifying the supercapacitor impedance in the high-frequency territory. Reproduced with permission from Elsevier[237]

with an rGO membrane-electrode-assembly manufactured by means of EPD to fabricate an all-solid-state supercapacitor.[228] The all-solid-state rGO supercapacitor demonstrates a volumetric capacitance of 108 F cm^{-3} in addition to an energy density of 7.5 Wh cm^{-3} at a power density of 2.9 W cm^{-3}. Furthermore, the supercapacitor is able to sustain 335 000 cycles successfully, which compares well with industrial-level EES devices.[228]

Other workers fabricated micrometre-sized supercapacitors based on onion-like carbon (OLC) particles using EPD on interdigitated gold current collectors.[238] The as-prepared micro-supercapacitors had electrode thicknesses ranging into several micrometres. Additionally, this supercapacitor is capable of delivering over 10 000 stable cycles at 200 V s^{-1} with four orders of magnitude higher capacitance than standard electrolytic capacitors.[19] Additionally, their rates of discharge are about three orders of magnitude greater when assessed against standard supercapacitors.[239]

Liu and co-workers applied an EPD method to fabricate GQDs-based micro-supercapacitors.[236] Both symmetric supercapacitor (with the GQDs as both the cathode and anode) and asymmetric supercapacitor (with GQDs as the anode and MnO_2 as the cathode) were made. These symmetric micro-supercapacitors gave excellent electrochemical performance such as high power response with a small time constant ($\tau_0 = 53.8$ μs in ionic liquid electrolyte and $\tau_0 = 103.6$ μs in aqueous electrolyte) and decent cycling stability.[239] The asymmetric supercapacitor exhibits two times higher specific capacitance and energy density than the symmetric micro-supercapacitor. Other researchers fabricated an MWCNT-based supercapacitor electrode by means of EPD.[240] These supercapacitors exhibit small equivalent series resistance yet high specific power density in addition to very good knee frequency reaction.[239] Niu et al combined photolithography with EPD to build micropatterned rGO interdigitated electrodes coated by gel electrolytes for an

all-solid-state micro-supercapacitor application.[241] Compared with conventional capacitors, these micro-supercapacitors exhibit a combination of enhanced specific capacitance, columbic efficiency and knee frequency due to effective utilization of the electrochemical surface area of rGO layers.[239]

Table 4 shows the important processing parameters and obtained film characteristics in selected reports involving (mainly) binder-free EPD of different electrode materials for supercapacitors. Application of EPD for the production of the electrode materials has important advantages such as relatively quick processing times, as displayed in Table 3. Argüello and co-workers used EPD to obtain manganese oxide and graphene nanoplatelets (GNP) on graphite paper as electrode materials for supercapacitors.[242] They completed the deposition process in only 2 minutes. GNP + MnO_2 based electrode had relatively high specific capacitance of 422 F g^{-1} between 0 and 0.8 V potential range at 0.1 A g^{-1} charge/discharge current density.[242] Nguyen and co-workers also reported on the efficient application of EPD to produce MOF (metal-organic-framework)/$Ni_3(HITP)_2$ based binder-free electrodes for supercapacitor applications.[243] Although the EPD process was completed in a relatively low potential of 0.5 V and in 10 minutes, the system maintained 15.69 mF cm^{-2} capacitance between 0 V and 1.0 V at a charge/discharge current density of 0.10 mA cm^{-2}.[243] Another example of a binder-free electrode fabrication process was achieved by Nguyen et al with the deposition of HRGO (holey reduced graphene oxide)-RuO_2 in 500 seconds at 4.0 V. The flexible electrodes manufactured, when applied in a functional supercapacitor showed 418 F g^{-1} specific capacitance in PVA/H_2SO_4 electrolyte at an operational voltage of 0 to 1.0 V at 1.0 A g^{-1} current density. As can be noted from Table 4, the EPD method for the fabrication of electrodes using many different types of substances such as graphene, rGO, metal oxides and other materials has a significant potential for industrially scalable applications due to its easy, low cost and relatively rapid processing steps.

Table 5 shows a comparison of several AC-based supercapacitors reported in the literature. One of the publications was reporting on commercial type supercapacitor electrode performances, but these were made by slurry casting.[252] In general, EPD of AC on metal substrates has not performed well for supercapacitor electrodes until Shreshta and co-workers managed to isolate a good recipe using IPA and ethyl cellulose (EC) to obtain a supercapacitor with a good gravimetric capacitance of 153 F g^{-1}.[247] According to the authors, this was the first time that an EPD-based AC electrode gave such a high capacitance. Additionally, in comparison to other reports on industrial type supercapacitors (made via slot-die casting),[230] the results presented by Shreshta et al are similar, as highlighted in Table 6.

It is interesting to note from Table 5 that most of the representative electrodes presented in the literature do not meet the commercial standards for deposition thickness and mass loading for supercapacitors.[230] To provide consistent electrochemical performance, a supercapacitor electrode is required to maintain a thickness and active mass loading analogous to electrodes meeting industrial standards, that is, 50 to 200 μm and 8 to 10 mg cm^{-2}, respectively.[171] Also, a good number of publications do not even mention the thickness of the active material (AC and carbon black usually) on the current collector. As a consequence, a comparison of these two important criteria for supercapacitor electrodes (by means of EPD only) reported in the literature is shown in Table 6. From several representative supercapacitors reported in the literature, average mass loadings of around 1 mg cm^{-2} or less (rarely higher) and deposited film thickness of around 1 to 10 μm (rarely 20 μm or above as shown in Table 6) is common. In comparison, a recent work by WMG provides much better mass loadings and film thicknesses, as can be gleaned from Tables 5 and 6.[246] Therefore, a versatile EPD method has been established in WMG for preparing high-performance supercapacitors that meet the industrial standards for good mass loadings and film thicknesses as shown in Figure 15.[248] The EPD conditions used for the study in question were very similar for producing high mass loadings (and decent coating thicknesses) for SiO_2 separators for LiB applications (shown as an example only in Table 6).[254]

In a recently published work, a binder-free EPD procedure was used for preparing TiN nanocoatings with a rapid time constant of 10 ms (determined via impedance spectroscopy).[260] These nanocoatings were then sintered and resulted in high-performance supercapacitor electrodes with a capacitance of 120 F g^{-1} at a high current density of 2 A g^{-1}. The authors successfully compared the theoretical EPD kinetics, determined via Sarkar and Nicholson's method (Equations [1] and [2]),[24] with the actual kinetics and found the latter to have higher values, as shown in Figure 16.[260] They attributed this slight discrepancy to the fact that the model was not comprehensive enough to account for the full phenomena occurring at the solid/liquid interface or at the surroundings near the EPD electrode due to suspension flocculation.

$$\frac{m}{m_0 = \left(1 - e^{\frac{-t}{\tau}}\right)}, \tag{1}$$

$$\tau = \frac{V}{f u_e S E}, \tag{2}$$

TABLE 4 Important processing parameters and obtained film characteristics in selected reports involving the EPD of (mainly) binder-free electrodes for supercapacitors

Material	Binder	Time	EPD voltage	EPD solvent/ charging agent	Electrolyte in charge-discharge	Charge-discharge potential range	Charge/discharge current density or scan rate	Capacitance	Ref.
$Ti_3C_2T_x$ MXene	Free	10-40 s	30 V	Acetone/iodine	1.0 M KOH	−0.75 V-(−0.25) V	5 mV s^{-1}	140 F g^{-1}	34
Nickel Cobaltite/ Polyaniline/ rGO	Free	15 s	30 V	Acetone/iodine	6.0 M KOH	0 V to 0.5 V	60 A g^{-1}	1235 F g^{-1}	233
MXene/CNTs	Free	10 minutes	8 V	50:50 deionized water: acetone/ none	6.0 M KOH	−0.9 V to (−0.4) V	1 A g^{-1}	134 F g^{-1}	234
Graphene Quantum Dots (GQD)	Free	30 seconds to 3 hours	10 V	deionized water and 30% H_2O_2/ none	1.0 M H_2SO_4	0 V-0.8 V	50 mV s^{-1}	70.7 mF cm^{-2}	237
GNP + MnO_2	Acrylic ester and styrene	1 + 1 minutes	-	Deionized water/ none	1.0 M Na_2SO_4	0 V-0.8 V	0.1 A g^{-1}	422 F g^{-1}	242
MOF/ $Ni_3(HITP)_2$	Free	10 minutes	0.5 V	50:50 deionized water: isopropanol/ none	0.5 M Na_2SO_4	0 V-1.0 V	0.10 mA cm^{-2}	170.36 F $g-^{1}$/15.69 mF cm^{-2}	243
NF/NCO-KB	Free	5 minutes	50 V	Isopropanol/Ni $(NO_3)_2{\cdot}6H_2O$ solution	6.0 M KOH	0 V-0.5 V	1 A g^{-1}	460 C g^{-1}	244
HRGO-RuO_2	Free	500 s	4.0 V	Deionized water/ none	PVA/H_2SO_4	0 V-1.0 V	1.0 A g^{-1}	418 F g^{-1}	245

TABLE 5 Recently obtained results[246] are compared with other AC-based supercapacitor electrodes in the literature prepared either via conventional slot-die casting or by means of EPD

Material and means for manufacturing electrodes	Coating thickness (μm)	Mass loading (mg cm^{-2})	Capacitance (F g^{-1})	Voltage range (V) and electrolyte	Ref.
83% AC: 17% PTFE [0.4 mM $Ni(NO_3)_2$] using **EPD** on SS (in IPA)	N/A	N/A	140	0-0.45 in 0.5 M KOH	66
90% AC: 10% AB (10 wt% EC) using **EPD** on Ni foil (in IPA)	200	7.07	153	0-1.00 in 6 M KOH	247
90% AC: 10% CB (10 wt% iodine) using **EPD** on Al foil (in acetone)	155	9.48	154	0-2.70 in 1 M $TEABF_4$ + ACN	248
80% AC: 10% AB: 10% PVDF using NMP-based **slurry casting** on Al foil	N/A	1.50-3.00	190[a]	0-2.00 in 1 M $TEABF_4$ + ACN	249
85% AC: 10% CB: 5% PVDF using **slurry casting** on Ni foam	N/A	N/A	140	0-2.00 in 1 M $TEABF_4$ + ACN	250,251
85% AC: 10% CB: 5% PTFE using **slurry casting** on Ni foam	N/A	6.00	216	0-0.80 in 6 M KOH	251
85% AC: 10% CB: 5% PVDF using **slurry casting** on Al foil	150	8.00-10.00	128[b]	0-3.00 in 1 M $TEABF_4$ + ACN	251,252
8:1:1 AC: EC: AB using **EPD** on ITO (in IPA)	100	N/A	60	−0.20 to 0.80 in 0.5 M K_2SO_4	253

Abbreviations: AB, acetylene black; EC, ethyl cellulose; ITO, indium tin oxide; SS, stainless steel.
[a]Estimated from a value given in the literature of 178 F g^{-1} at a current density of 0.5 A g^{-1}.
[b]Estimated from a value given in the literature of 124 F g^{-1} at a current density of 0.5 A g^{-1}.

TABLE 6 A comparison of mass loadings and film thicknesses for different supercapacitor electrodes prepared by means of EPD as reported in the literature (representative sample) and compared with recent work in WMG[246]

Active material	EPD parameters	Mass loading (mg cm^{-2})	EPD film thickness (μm)	Ref.
$Ti_3C_2T_x$ MXene on Ni foam	30 V, 10 mm IED, 1 minutes, acetone (50 mL)	2.13	90	34
$Ni_3(HITP)_2$ on Ni foam	0.5 V, 10 mm IED, 10 minutes, IPA and water	0.21	10	243
$NiCo_2O_4$ + KB on Ni foam	50 V, 10 mm IED, 5 minutes, IPA (10 mL)	1.50	7	244
AC:CB on Al foil	70 V, 10 mm IED, 20 minutes, acetone (80 mL)	9.48	155	248
SiO_2 on $LiNi_{0.8}Co_{0.15}Al_{0.05}O_2$ film (for lithium-ion batteries)	50 V cm^{-1}, 20 minutes, acetone	13	180	254
PBH-MnO_2-MWCNTs on SS, Pt or Si	10 V, 15 mm IED, 10 minutes, water	0.85	2	255
Co_3O_4/CNT on Ni foil	50 V, 10 mm IED, 2 minutes, IPA (40 mL)	0.03	0.01	256
Hydrous ruthenium oxide/PTFE on Ti plate	50 V cm^{-1} (IED), 10 minutes, ethanol and water (0.7 mL)	4.3	20	257,258
MnO_2/ERGO/SS	4 V, 10 mm IED, 5 minutes, water	0.13	1	259

Note: Capacitances were not compared as electrodes and electrolytes used for each case were different.
Abbreviations: ERGO, electrochemically reduced graphene oxide; IED, inter-electrode distance for EPD; KB, Ketjen Black; MWCNT, multi-walled carbon nanotube; $Ni_3(HITP)_2$, Nickel-2,3,6,7,10,11-hexaaminotriphenylene metal-organic-framework; PBH, 1-pyrenebutyric acid; SS, stainless steel.

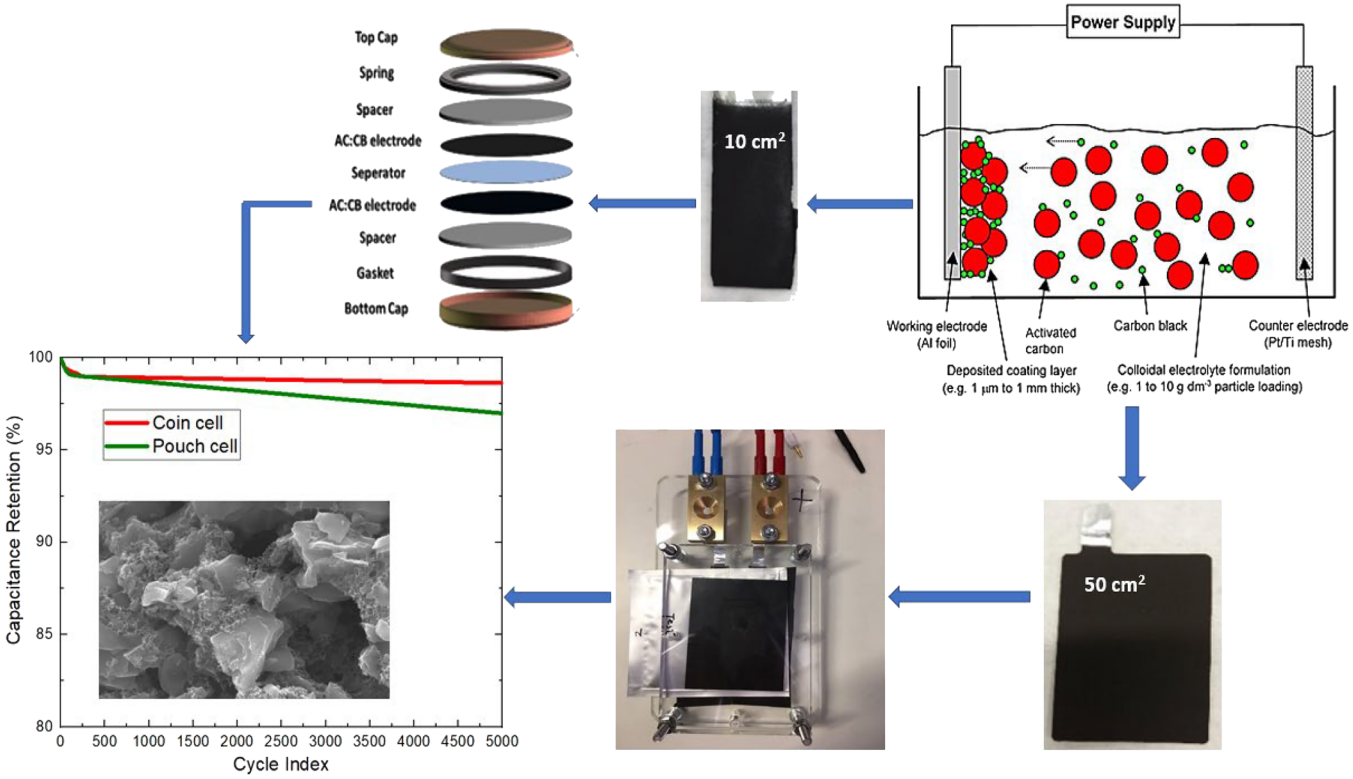

FIGURE 15 An effective EPD technique was developed at WMG to deposit activated carbon on aluminium foil current collectors at industrial-scale mass loadings and film thicknesses. These electrodes were tested in both coin cell and A7 pouch cell supercapacitors and gave very good performance—excellent capacitance retention is noted for both cells at 0.1 A g^{-1} current density. Reproduced with permission from RSC[248]

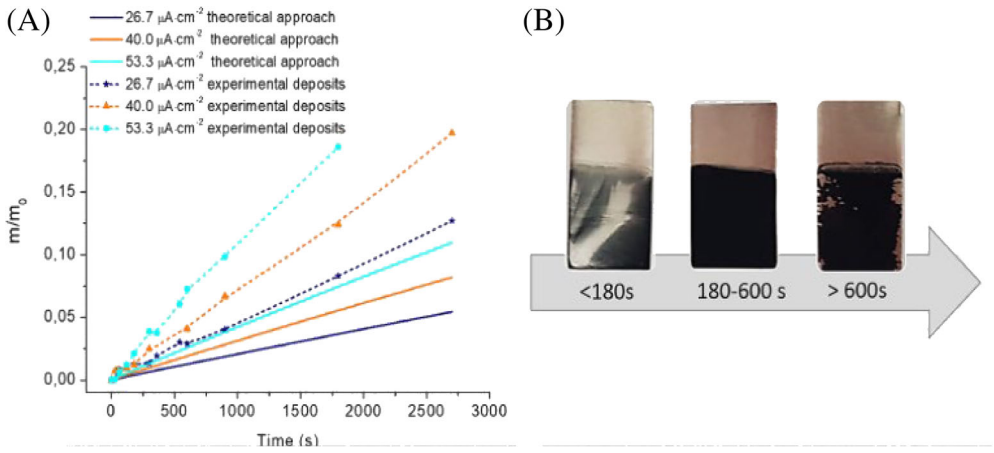

FIGURE 16 (A) Theoretical approximation and experimental values of the EPD kinetics for TiN suspensions deposited on Ni foil at 26.7, 40.0 and 53.3 μA cm^{-2}. Solid lines represent theoretically calculated values from Equations (1) and (2) while dotted lines are practically measured values. (B) Photos of TiN coatings shaped on Ni foil at 53.3 μA cm^{-2} at different deposition times. Reproduced with permission from Elsevier[260]

where m is the mass of deposits (g), m_0 the total suspension mass (g), t is deposition time (s), V is the suspension volume (mL), f is a theoretical factor used by Sarkar and Nicholson,[24] μ_e is the electrophoretic mobility ($cm^2\ V^{-1}\ s^{-1}$), S is the EPD surface (cm^2) and E is the applied electric field (V cm^{-1}).

Finally, hybrid electrodes, which are assembled from a chemical (battery-related) compound and a physical

(electrical double layer) storage material, have exhibited significant capabilities in battery-supercapacitor hybrid (BSH) compilations. In a current investigation by Mandler et al, an EPD-based approach is followed for assembling a binder-free, high-performance BSH device successfully.[244] The procedure applied $NiCo_2O_4$ (NCO) as the chemical storage material, whereas Ketjenblack (KB) was employed as the physical storage compound. These materials were then dispersed in an electrolyte of Ni^{2+} ions. Therefore, it was possible to ascribe a positive surface charge on the electrode materials that enabled a similar EPD rate of both NCO and KB materials on nickel foam (NF) substrates. This ensured a good manipulation strategy to be applied to the KB to NCO proportion in the composite electrode and optimize its operation. In this electrode architecture, the KB chains functioned as a rapid electron route enabling decent conductivity for the NCO electroactive compound (Figure 17).[244] In particular, the KB chains maintained effective contact with NCO despite mechanical wear and tear throughout the electrochemical reaction. Hence, the robust hybrid electrode exhibited decent specific capacity (460 C g^{-1} at 1 A g^{-1}) and enhanced cycling operation (82.5% retention despite undergoing 15 000 galvanostatic charge/discharge or GCD cycles). When the NF/NCO-KB electrode was used as the positive in combination with AC as negative electrodes, the BSH displayed an excellent cycling performance of 88.6% capacitance retention upon undergoing 10 000 cycles along with a high energy density of 53.0 W-h kg^{-1} at a power density of 746 W kg^{-1} (Figure 17).[244]

7 | DEVELOPING RESEARCH AREAS ON THE APPLICATIONS OF EPD FOR ELECTROCHEMICAL ENERGY STORAGE

7.1 | Background

Carbon-based composites and carbon-containing materials have recently been successfully applied in a range of industrially relevant activities, which include energy storage devices, fuel cells and membranes. To augment the properties and operation of carbon comprising EES devices, polymeric electrodes may be appropriately altered by carbon-containing compounds and metal oxides by means of EPD to assemble a composite that supports the charge accumulation and gathering processes owing to enhanced electrode surface areas. The carbon-polymer nanocomposite architectures help circumvent issues associated with the maintenance of high-performance polymeric materials that consequently can be assembled into exceptional composites for application in outstanding EES devices.[261] This section briefly reviews some of the challenges still faced by conventional EPD techniques and also assesses some new methods being reported in the literature, such as the incorporation of advanced nanomaterials to prepare exceptional electrode materials.[262] For example, in Section 6.4, the decoration of carbon paper electrodes with nitrogen-doped graphene nanomaterials with EPD displayed the versatility of this automated process for enhancing hybrid flow cell performance.[25,263] In addition, EPD set-up is relatively facile and is able to deposit films that meet industrial standards for EES electrode thicknesses and mass loadings by regulating a range of practical factors of operation.[264]

The electrolyte/electrode interaction in EES systems is an extremely important factor governing their performance. Although it is well known that EPD is used for producing superhydrophobic surfaces[265] for applications in aqueous-based electrolyte EES systems, it needs to be ensured that both the substrate on which deposition occurs as well as the colloidal particles embedded onto the substrate are hydrophilic in nature. This may be easily ensured by EPD because it is an in-situ means for preparing either hydrophilic or hydrophobic surface coatings with effective control over film porosity and tap density, which are direct functions of the deposition voltage (in contrast to slurry casting procedures that are dependent upon a secondary step like electrode calendaring to ensure effective tap densities). A very good example of the effective application of hydrophilic surface coatings involves the EPD of rGO on carbon paper electrodes for providing excellent electrochemical performance for applications in RFBs as discussed above.[203] Other EES devices use organic electrolytes, which are not so reliant on hydrophilic electrodes for generating decent performance, and thus it is not essential to be concerned about the wettability of the EPD electrodes. A reasonable example may be the application of LiB electrodes, which interact with the standard organic-based electrolyte consisting of a mixture of ethyl carbonate and dimethyl carbonate, containing 1 M $LiPF_6$ salt, to provide a reversible capacity of around 650 mAh g^{-1} at 0.5 A g^{-1} up to 150 cycles.[147]

Despite the fact that the widespread commercial adoption of EPD for manufacturing EES devices is rather scarce, there is yet a significant increase in the number of patents filed recently for industrial applications of EPD for the large-scale production of electrode materials for batteries (see Table 7 for a summary). Among several different companies and academicians that applied for such patents, some examples are discussed herein. For instance, Golodnitsky and co-workers used a sequential

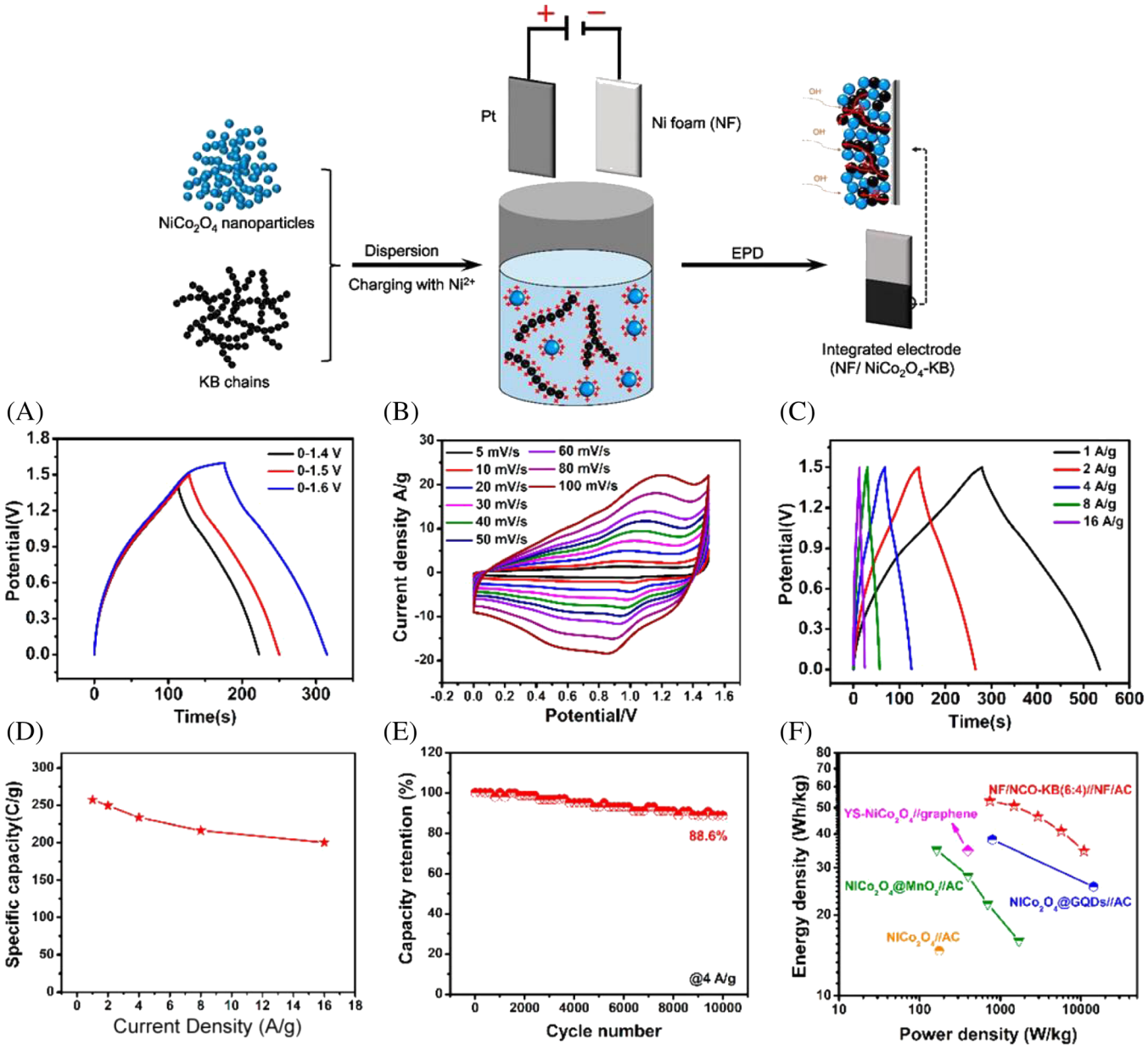

FIGURE 17 Top figure shows a schematic of KB and NCO nanoparticles on NF manufactured by means of EPD. Electrochemical performances are shown in the graphs as: (A) GCD graphs of NF/NCO-KB(6:4)//NF/AC BSH device at different potential windows. Electrochemical performance of NF/NCO-KB(6:4)//NF/AC BSH device: (B) CV and (C) GCD graphs. (D) Specific capacity and capacity retention (E) of NF/NCO-KB(6:4)//NF/AC BSH cycled at a relatively high current density of 4 A g^{-1}. (f) Ragone plot of the BSH device. Reproduced with permission from ACS[244]

EPD method on a single conductive substrate for developing three-layer lean-film battery (TFB) architectures.[266] In another patent application, bipolar electrochemical devices were made by means of electrophoresis.[267] Xiao patented a method that included EPD for the production of electrode materials for LiBs.[268] In this process, a potential was applied between a current collector and a counter-electrode submerged in a colloidal formulation consisting of GO, binding material and also other components to deposit the active materials such as rGO on the working electrode surface.[268]

SiO-based carbon nanofiber composite anode materials produced on a nickel/copper catalyst by means of EPD were also patented for particular applications in lithium-based EES devices.[269] Ruoff and co-workers used the EPD method for effective reduction of GO to make graphene film on an electrode surface such as aluminium foil, copper plate, nickel plate and Si wafer substrates.[272] In another application, GO was deposited on a titanium sheet electrode surface by means of EPD and it was reduced by thermal treatment for the production of anode materials for LiBs.[273] A potential production

TABLE 7 A summary on the latest patents related with the application of EPD for LiBs

Battery component made	EPD conditions	Performance	Ref.
Electrode; three-layer thin-film battery	LFP, PVDF, BP at 0.28 mg/L in acetone +0.4% v/v triton-X. 60 V for 1 minute on Ni disk. IED = 15 mm	1.5 to 2.3 mAh cm^{-1} reversible capacity in 100 cycles per battery footprint	266
Electrode	$LiCoO_2$, MCMB, Super P, ITO, LFP at 1 g/L in solvents like IPA, acetone, acetonitrile, etc. 10 V from seconds to minutes	Positive electrode capacity of 10.1 mAh with 4% capacity fade in 10 cycles	267
Electrode	Particles such as silicon, NMC or $LiCoO_2$ mixed with GO at 1:9 to 9:1 ratios in aqueous or non-aqueous solvents at 5 to 100 V from 10 s to 10 minutes	For Si:GO of 1:1 ratio LiB gives 1200 mAh g^{-1} for 14 cycles at C/3	268
Electrode; SiO_2/carbon nanofiber composite	Nickel (II) acetate and copper (II) acetate with tetraethyl orthosilicate, ammonia water and nitric acid in 64% ethanol used for depositing Ni and Cu catalysts on carbon fiber fabric-IED = 85 mm	Specific capacity drops from 2053 to 1295 in 30 cycles. Coulombic efficiency = 96%. However, C-rate is not given	269
Electrode; thin film	3 to 10 g/L of Li battery material suspended in water or ketone or alcohol, binding polymers like PVDF, 40 mV zeta potential, 10 V cm^{-1}	Decent lithium peak observed using cyclic voltammetry at 0.1 V s^{-1}, good adhesion of battery material	270
Electrode; composite material	2 g/L of LTO, 0.02 g/L of carbon powder, 0.3 g/L binder, few ppm citric acid in ethanol. EPD voltage = 80 V for 30 seconds	Battery or cell performance not described in detail	271

Abbreviations: BP, Black pearl carbon; IED, inter-electrode distance; ITO, indium tin oxide; LFP, lithium iron phosphate; MCMB, mesoporous microbeads; MWCNT, multi-walled carbon nanotube; NMC, lithium nickel manganese cobalt oxide; Super P, carbon black.

method of dense thin coatings by means of EPD for the use of electrode materials in batteries and in electronic devices was shown by Bouyer et al.[270] The use of EPD for the production of composite anode materials for LiBs was also patented.[271] Functionalized MWCNTs including active materials were electrophoretically deposited to form nanostructured composite electrodes for the use in batteries.[274] Gaben also applied for a patent for manufacturing all-solid-state batteries in a multi-coated architecture by means of a range of methodologies that comprised of EPD processes.[275] In short, the use of the EPD method played a key role for the production of anode materials for LiBs in many patent applications.[276,277]

Adaptation of the EPD method towards industrial applications is a critical issue. In particular, the development of systems that will allow mass production in comparison to standard slot-die casting processes is vital for the use of the electrophoresis method in electrode production methods for EES devices. With this key point in mind, Oakes and co-workers published a crucial work about the use of EPD in a roll-to-roll production process for high-quality electrode materials.[278] Since the parameters such as low cost, homogeneous coating, reproducibility and simplicity are important for the production of such electrode materials, the published method heralds a new perspective in this important area of research.[278] Figure 18 shows the basic structure of the system for benchtop roll-to-roll EPD coater and the subsequently processed materials obtained by use of this process.[278] The authors illustrated a methodology involving the EPD of the hybrid assortments of CNTs, MoS_2 nanosheets, silicon nanoparticles, carbon nanohorns and graphene nanoplatelets without applying any surfactants. Indeed, production of the positive and negative electrode

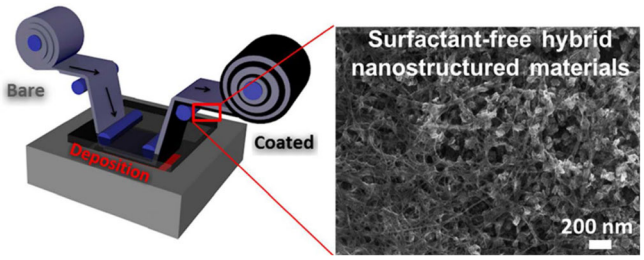

FIGURE 18 Basic structure of the system for benchtop roll-to-roll EPD coater and SEM picture of obtained electrode materials by means of this process. Reproduced with permission from ACS[278]

materials of LiBs was completed in less than 30 seconds.[278] Pascall and Kuntz also patented the use of a light-directed EPD system for the production of flexible electrode web substrates.[279]

Cathodic EPD was initially commercialized by PPG, which became an industrially relevant process for the corrosion protection of vehicle panels. Of late, PPG acquired financial support of $2.2-million from the US Department of Energy (DOE) for investigating the comparative application of EPD against standard slot-die casting for the preparation of LiB electrodes.[280] PPG's process concentrates on tackling engineering approaches of EPD to prepare sophisticated LiB materials and devices in collaboration with Oak Ridge National Laboratory in Tennessee.

The employment of EPD for EES devices has augmented in time and enhanced the operation of prevailing battery/supercapacitor electrodes considerably. More investigations are necessary to comprehensively study the properties and mechanism of the EPD method. An awareness of the effect of significant parameters such as deposition time, inter-electrode distance or applied voltage on colloidal properties during the EPD process is essential (discussed briefly in Section 3). This comprehension will facilitate improved manipulation of the structure and morphology of the nanomaterials and may result in the discovery of original functional composites. Furthermore, extensive EPD investigations may involve the effects of modulated electric fields, such as throbbing direct current[281] and alternating currents[282] to devise electrodes with diverse architectures for EES applications because EPD under modulated electric fields can convey enhanced traits in comparison to those acquired by traditional EPD,[283] in addition to well-orientated microstructures.[284] Furthermore, there is a tendency for decent reproducibility because automation of EPD operating with modulated fields is potentially facile.[281] Accordingly, attention should be paid to the design and manufacture of 2D and 3D architectures for the innovative application of progressive EES devices. Finally, potential future EPD investigations may focus on applying a range of unknown nanomaterials to design and develop electrodes for revolutionizing supercapacitors, batteries, and regenerative fuel cells[36] (or hybrid RFBs) such as the hydrogen/benzoquinone[5] and other similar RFCs as reported recently.[209]

In addition, EPD is already used in industry on large scale such as car painting. Yet, we expect that it will also penetrate other areas, where large area electrodes are required (e.g., in the field of water electrochemical treatment and electrolyzing). The significant advantage of EPD stems from the ability to predesign and characterize the nanoparticles that are deposited, which maintain their performance. Hence, for example, ZnO nanoparticles that are used for the photodegradation of organic dyes can be synthesized with optimal photonic properties. More specifically, for EES, we anticipate that EPD will slowly take a lead and will be used for the mass production of electrodes. Besides its low-cost advantage, EPD can be integrated into line production quite easily. Yet, to become a leading manufacturing technique in electrode production for EES, EPD still has to prove that it can be used to form relatively thick coatings with good adhesion and reproducibility. Furthermore, EPD can readily be used for producing graded materials, which still have not entered EES. The fact that EPD is a 'binder-free' approach is still not enough to make it an appealing process in the industry. Moreover, the rate of deposition will have to increase to compete with the current methods. To conclude, when EPD demonstrates some unique advantages that cannot be obtained easily and for the same costs by the current techniques, EPD will pave its way to the most advanced production lines.

7.2 | Hybrid technology

Niu et al produced flexible micro-supercapacitors by means of a combination of photolithography and EPD to develop graphene microelectrodes.[241,285] These graphene microelectrodes facilitated the electrolyte ions transportation, allowing more accessible surface area. Also, the reported specific capacitance of the as-prepared graphene-based micro-supercapacitor was 285 F g^{-1}, nearly three times more as compared with conventional graphene-based supercapacitors (86 F g^{-1}).

In other applications, a new type of 3D metal printing is known as laser-assisted EPD (Figure 19). This method is based on an optical trap of locally concentrated nanoparticles in a solvent to which an electric field is applied to obtain a compact morphology.[288] A firmly focused laser beam is directed onto an electrolyte consisting of negatively charged metallic nanoparticles that are then subjected to optical traps that agglomerate particles in the focal spot of the laser beam.[287] The focal spot is used to gather a large number of charged particles in the region of interest for further processing, which includes EPD.[286] EPD compels the particles to coagulate and deposit on the surface possessing positive charges.[289] Crucially, this association of laser with EPD should be further investigated to develop electrode materials with high mass loadings and film thicknesses of electrode materials that meet industrial standards for future studies. For example, the LiB electrodes developed in WMG could be further enhanced by combining laser concentration approach with EPD for application in practical EES devices.[2]

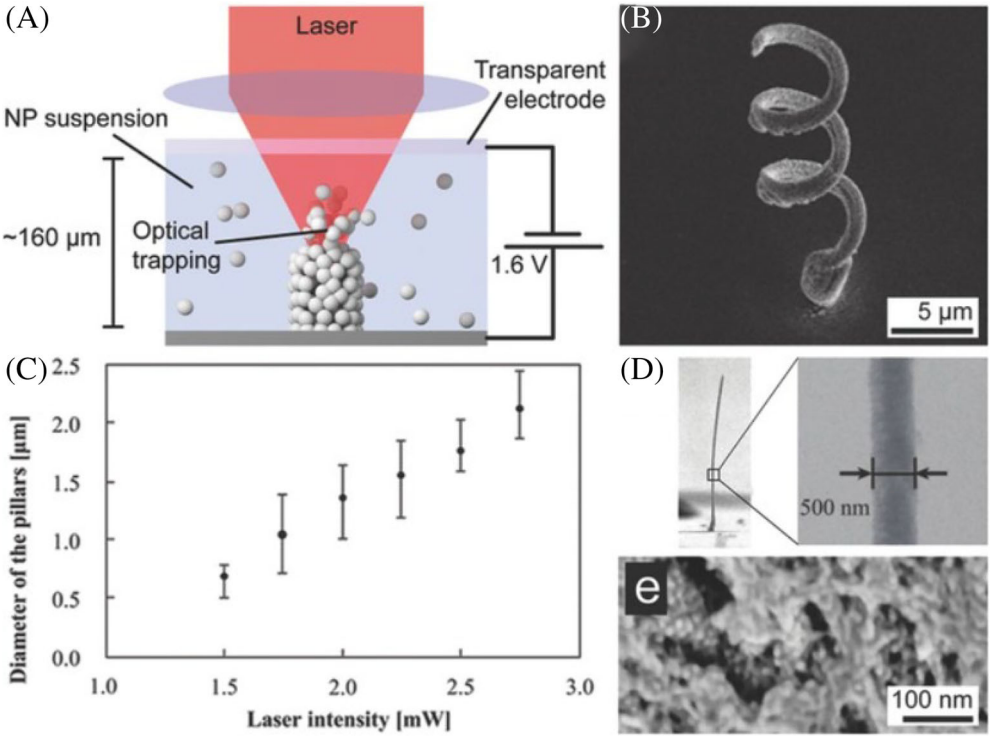

FIGURE 19 Laser-assisted EPD. (A) Cartoon showing how by the use of the focal spot a laser beam can constrict nanoparticles locally in a solution between a conductive substrate and a transparent electrode surface. The trapped particles can then be deposited on the substrate by means of EPD. (B) Example of a gold coil manufactured by means of laser-assisted EPD (SEM image shown). (C) Graph showing how laser intensity affects the feature magnitudes of the gold coil. (D) The laser-assisted EPD method has the ability to produce nanowires of 500 nm in diameter. (B-D) Reproduced with permission.[286] Copyright 2014, Optical Society of America. (E) FIB cross-section image of a perforated microstructure (although, crucially, the film thickness is not fully indicated). Permission to re-display this figure was obtained from Wiley[287]

7.3 | EPD of solid electrolytes and separators for batteries: a developing area of research

EPD has been employed for designing and manufacturing an innovative combination of electrodes and solid electrolytes with decent performances in EES devices when compared with those assemblies prepared by means of classical processes.[19] EPD of solid-state electrolytes is a relatively new topic for LiBs, and reports in the literature are rather scarce.[154,290]

However, this topic appears to be more well established for solid oxide fuel cells.[19] Although not the focus of this review, some of the solid oxide fuel cell materials that have similar composition as LiB solid-state electrolytes are mentioned briefly herein to present a platform for researchers for taking up this important topic in future investigations. There are no such investigations for supercapacitors at present and may be an interesting topic of fundamental and applied research.

Among the scarce publications on EPD for solid electrolyte LiBs,[291] one work reports on the EPD of a PVDF-HFP {Poly(vinylidene fluoride-co-hexafluoropropylene)} membrane deposited on the anode.[292] The resulting separator/anode (see Figure 20A) facilitates a decent ionic conductivity of 8.1×10^{-4} S cm^{-1}, and when used in a LiB, produces 370 mA-h g^{-1} discharge capacity (99.5% of the theoretical capacity) at 0.1 C, a capacity retention of ~100% in >300 charge/discharge cycles, and a rate capability of 270 mA-h g^{-1} at 1 C. Interestingly, the porosity of the polymer membrane is tuneable by choosing the appropriate solvent, resulting in an improvement of conductivity and durability of the separator/solid electrolyte film. In a separate investigation by Goodenough and coworkers an HFP separator is successfully impregnated by means of EPD with atomic interlamellar lithium-channel phyllosilicate clay.[293] This enhanced membrane architecture remarkably diminishes lithium dendrite formation resulting in an exceptional capacity of 152 mAh.g^{-1} at 0.5C as shown in Figure 20B.

Additionally, hybrid solid electrolytes combining ceramic and polymeric ionic conductors have been exhaustively investigated as benign electrolytes for employment in solvent-free rechargeable LiBs.[294] The

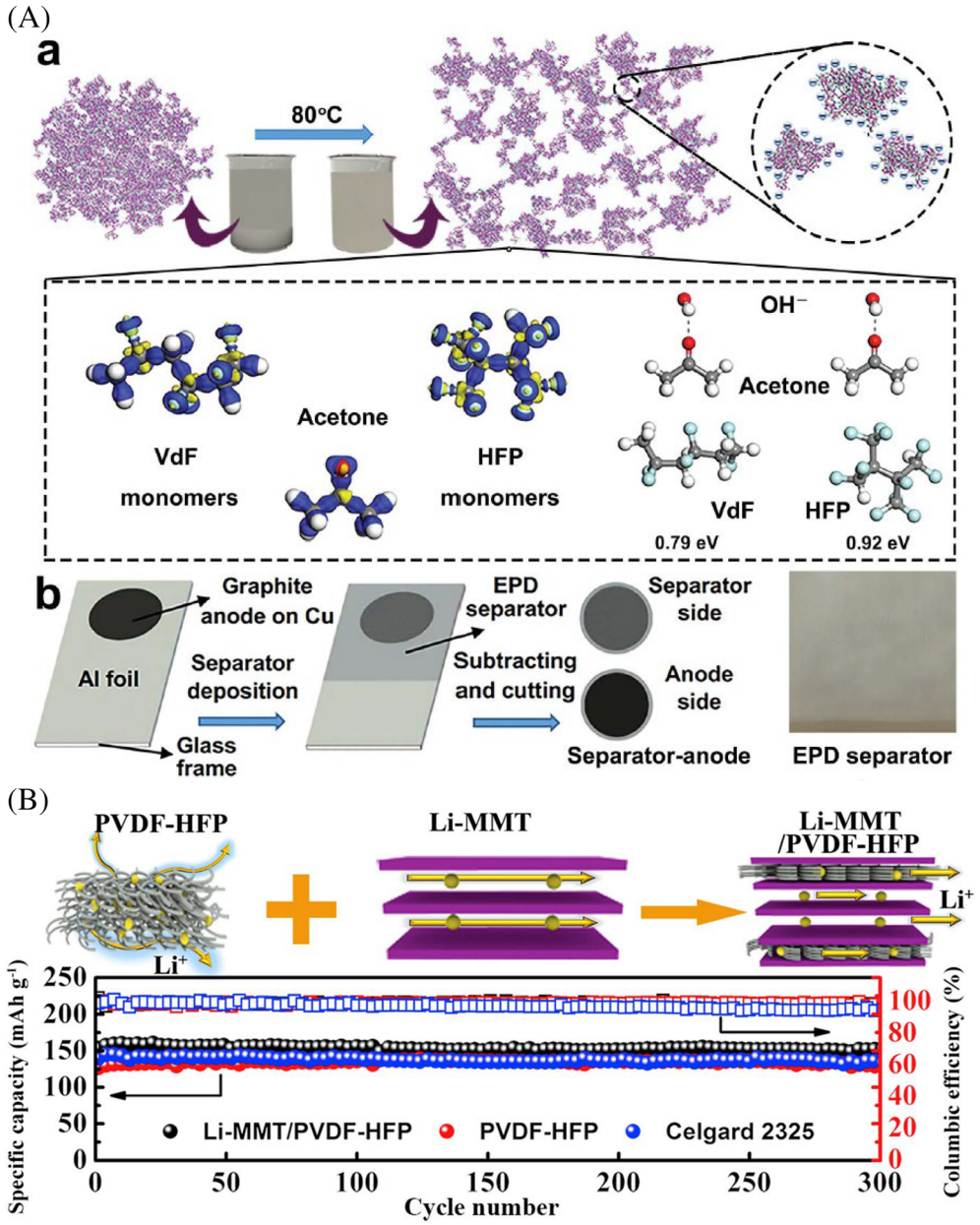

FIGURE 20
(A) (a) Cartoon showing how the interaction of molecules within the PVDF-HFP/acetone colloidal solution may be exploited for EPD. Grey, white, red and cyan spheres are associated with carbon, hydrogen, oxygen and fluorine atoms, respectively. Blue surfaces display a charge gain of 0.15 $eÅ^{-3}$ while yellow surfaces correspond to an equivalent charge loss. (b) EPD process used to fabricate the half LiB. The separator side and the anode side of the separator-anode structure and the EPD separator deposited on an Al substrate are shown, respectively. Reproduced with permission from RSC.[292] (B) A LiB coin cell assembled with Li-MMT/PVDF-HFP (PVDF-HFP/Li-montmorillonite) separator (prepared via EPD) delivers an excellent discharge capacity of 152 mAh g^{-1} with a capacity retention of 98.5% after 300 cycles at 0.5C, which is beyond those delivered by PVDF-HFP (145 mAh g^{-1}) and the common literature reported Celgard 2325 (138 mAh g^{-1}) separators. Reproduced with permission from Elsevier[293]

unique benefits of such a combination of solid electrolytes include flame resistance, flexibility, more stable anode/electrolyte interfacial resistance compared with conventional liquid electrolytes, and low-cost design owing to the highly versatile EPD process.[295] For instance, EPD was used to prepare an aggregated solid ceramic/polymerized electrolyte loaded with lithium iodide. Even though the coarseness of polyethylene oxide (PEO)-$LiAlO_2$ composite coatings was larger than that of PEO depleted compounds, the deposits were comprised of densely packed decently separated nanoparticles in contradiction to the highly visible aggregation in polymer depleted deposited electrolytes, in which salt/ceramic grain-peripheries perform a principal part in the conveyance of Li^+ ions. The solid $LiAlO_2$:LiI:$P(EO)_{3+x}$ electrolyte film was uniformly deposited on the substrate with controllable thickness in the range of tens of micrometres and was characterized by means of a high, temperature-independent conductivity of 0.5 mS cm^{-1}.[296]

It is imperative that ceramic particles are electrically charged to allow transport by EPD.[297] It should be noted that cathodic EPD is desirable to anodic EPD, owing to issues connected with anodic dissolution, corrosion of substrates and deposit adulteration. Therefore, as reported in a recent investigation on the EPD of NMC111 on 2D and 3D Al-based current collectors in WMG,[2] it is imperative to apply electrolyte additives like PDDA for ascribing positive charges on electrochemically active particles. Additionally, it is imperative for EPD to efficiently deposit uniform coatings of various battery-

related substances, incorporating cathode and anode composite substances, electrolytes and separators. Cathodic deposition is preferred by employing analogous bath compositions. Undeniably, varying the course of the electric field as well as altering the solvent or additives for deposition of specific materials may cause the delamination of the previously deposited material coatings.[297]

EPD of sub-micrometre powders enables compact assembly, reliable sinter-ability and uniform microstructure.[298] Despite that, since the sub-micrometre particles possess large surface areas, they have a compelling propensity to agglomerate. Decently scattered and steady suspensions of fine materials may be acquired by means of an appropriate choice of an efficacious dispersant.[299] A crucial issue to take into account involves the use of fine particles for EPD, which could render the coatings to become prone to cracking when being dried, and therefore the selection of the binding material becomes imperative to prevent this. The optimal quantity of binder is governed by particle size and surface area.[297]

To effectively exploit the benefits of the methodology established in the EPD of solid electrolyte materials,[300] a selection of processing factors needs to be ascertained. The effect that electrolyte additives have upon deposition morphology and EPD rate is important to clarify.[297] Advanced studies are needed for optimization of colloidal bath composition to diminish the number of additives and attain homogeneous and robust deposits of manipulative thickness, as well as to hinder pinholes, cracks and further imperfections.

7.4 | Sodium-ion batteries and capacitors

New trends in EES technologies can also be useful application areas for EPD technology. Na-ion batteries (SiBs) and Na-ion supercapacitors (SiCs) are two important examples of these EES technologies. While the main structure of LiBs and SiBs is the same, SiBs consist of sodium-based material as cathode instead of lithium.[301] Although Na^+ ions are larger than Li^+ ions, Na^+ transport properties in a battery are highly connected with the crystallographic morphology of the electrodes for long cycle applications.[302] Here, electrode materials hold a significant function in the operation of the SiBs. Whereas layered transition metal oxides, polyanionic compounds can be used as electrode materials in SiBs, carbon-based materials, transition metal oxides, alloying materials, phosphorous-based materials and insertion materials (ie, MXene, titanate) may be employed in anode materials of SiBs.[303] As can be seen from the structure of the anodic and cathodic materials, the EPD method can be useful for the production of high surface area electrode materials without binders for SiBs. Dashairya et al used the EPD technique to prepare anodic materials consisting of Sb/rGO on Cu foil for use in SiBs. They obtained 350 mAh g^{-1} specific capacity at 0.2 C current rate up to 100 cycles (Figure 7A).[138] SiCs are another important developing EES technology with its comparable properties such as high energy density, fast energy delivery and long cycle life, which have attracted attention to compete with LiCs.[304] In the classical anodic design of SiCs, battery-like anodic compounds, such as hard carbon materials, transition metal sulphides and selenides, Ti- and Nb-based compounds consisting of various types of reactions (insertion, alloying and conversion) have been studied.[304] On the other hand, capacitive cathodic materials such as AC, graphene and CNTs can be used to improve the performances of SiCs.[304] As can be seen from the used electrode materials in SiBs and SiCs, the EPD method has great potential for use in the production of high-performance electrodes with its inherent advantages. Similar advantages for EPD could be envisaged for magnesium ion batteries, as reported recently, but this is still a developing area of research.[305]

Finally, the potential for EPD to manufacture 2D MXene-based membranes with high sodium-ion selectivity could pave the way for highly effective means for sourcing sodium salts. For instance, in a recently published work, a rapid means for preparing a 2D membrane of two orders of magnitude larger area (575 cm^2) than those made via standard vacuum filtration was reported using EPD.[306] Around 99.5% recovery of sodium and other ions were reported and it is postulated that this technology could be extended to sourcing lithium ions for LiBs in future studies.

8 | CONCLUSIONS

Sustainable energy supply is getting more important day by day as a consequence of the increasing energy demand of today's knowledge-based societies. In this regard, the storage of energy obtained from different sources such as renewable and/or classical sources via EES devices plays a key role. In most EES devices such as LiB, supercapacitors and RFBs, electrode materials and their preparation have a critical influence on the cost and the performance of the devices. From this point of view, preparation of the electrodes in easy, economical, sustainable and industrially applicable ways is needed by the battery/supercapacitor manufacturers. Electrophoretic deposition is also increasingly being used to meet this demand since it has many advantages such as low cost, facile applicability, short formation time, simple apparatus requirement, homogeneous coatings preparation,

binder-free processing and selective modification as a function of thickness and mass loading. Although this technology has been used for numerous academic studies, it also has great potential for industrial applications, especially in the manufacture of battery materials, as demonstrated in a recent publication by WMG. So far, most of the EPD activity has focused on the preparation of LiBs and LiCs. One common drawback usually noticed from academic publications on energy storage electrode materials is the substantially thin-film coatings that do not conform to industrial standards for, say, supercapacitor applications. Many of the literature reports address the enhanced specific capacity and power density but hardly discuss the mass loading and film thickness that are necessary for wide-scale commercial adoption. Additionally, the challenges that EPD as a process faces in meeting these industrially relevant standards while maintaining sufficient porosity and tortuosity of the as-prepared films is of utmost importance that needs full attention to detail. Therefore, this review also attempts to highlight these key aspects of the development of the EPD process such that future research activities consider these practical aspects. Recently WMG reported the production of activated carbon-based supercapacitors meeting industrial standards for film thicknesses above 50 μm and mass loadings in excess of 8 mg cm^{-2}.

In addition to the above, there is a critical need to enhance the EPD technology for use in other emerging energy storage applications such as RFBs. Since this technology allows the production of electrode materials without the use of binders, it has the potential to reduce the cost of the battery materials by enabling the manufacturing of purer electrodes than conventional means. Hence, this review includes recently published studies, which emphasize the significant role of EPD in enhancing organic redox flow battery performance and discusses key processing information for researchers to follow up. It also opens a fresh perspective for the use of this technology in the electrode modification/production processes of highly economical and market-ready hybrid redox flow cells as reported in a recent study by WMG. Other potential uses of EPD electrodes may involve the recycling of valuable materials from lithium-ion processes for re-purposing as energy storage devices for efficient EV applications. Finally, this review shows early evidence in the evolution of EPD processes and manufacturing tools to produce technologically improved solid electrolytes and separators for LiBs, with future potential applications in both academic and industrial research. However, it is noted that almost no research outputs are reported on the application of EPD electrodes for aluminium and magnesium ion batteries, which could be a significant area of development in the near future. The facts and perspectives discussed herein are expected to raise more interest in this technology for more widespread industrial applications of EPD for EES devices over and above what is already known for solid oxide fuel cells.

Summarizing the EPD studies and the advantages that this technology offers leads to drawing some perspectives and predictions about future activities. It is evident that once thicker films are deposited on a routine base, the barrier towards commercialization will be lowered significantly, which will form strong feedback for further development and applications that are currently neglected. The good control of the EPD process will enable the formation of graded materials, and integration of the technology in flow systems, thus making it possible to form layered deposition very fast. Furthermore, as EPD takes place on electrically conducting surfaces, the selective deposition on conducting patterns and the build-up of high aspect ratio structures can also be foreseen. EPD can be combined in the future with micro- and nano-electrochemistry and with technologies such as scanning electrochemical microscopy, allowing high-resolution patterning of surfaces. The spectrum of materials, in particular, for EES systems will be expanded and also the size and complexity of the building blocks. The optimal size of the building blocks in EES devices is not necessarily in the nanometer range and EPD will have to cope with this. Finally, new approaches will have to be developed for controlling the orientation of the deposited non-spherical materials, such as nanorods. This will give EPD an even stronger advantage over gaseous-based deposition methods and will make EPD an indispensable approach for the construction of highly sophisticated and efficient EES devices.

ACKNOWLEDGEMENTS

This work has received financial support from Engineering and Physical Sciences Research Council First Grant: Energy Storage Electrode Manufacture (EP/P026818/1) and EPSRC Industrial Strategy Challenge Fund: 3D Electrodes from 2D Materials (EP/R023034/1). Funding has enabled Prof. Low to initiate a research group and establish programmes from electrode to cell testing and recycling of lithium-ion battery, both Assistant Professor (2013) and Associate Professor (2019) in WMG, University of Warwick, United Kingdom. World-class battery prototyping facility and resources of industrial relevance provided by the High Value Manufacturing Catapult at Warwick are fully acknowledged. D. Mandler acknowledges the support of Israel National Research Center for Electrochemical Propulsion (INREP).

DATA AVAILABILITY STATEMENT

Data sharing is not applicable to this article as no new data were created or analyzed in this study.

ORCID

Barun Kumar Chakrabarti https://orcid.org/0000-0002-0172-986X
Metin Gençten https://orcid.org/0000-0002-5552-0156
Chee Tong John Low https://orcid.org/0000-0003-4411-9890

REFERENCES

1. Bissett MA, Worrall SD, Kinloch IA, Dryfe RAW. Comparison of two-dimensional transition metal dichalcogenides for electrochemical supercapacitors. *Electrochim Acta*. 2016;201:30-37. doi:10.1016/j.electacta.2016.03.190
2. Lalau CC, Low CTJ. Electrophoretic deposition for lithium-ion battery electrode manufacture. *Batter Supercaps*. 2019;2:551-559. doi:10.1002/batt.201900017
3. Chakrabarti B, Yufit V, Kavei A, et al. Charge/discharge and cycling performance of flexible carbon paper electrodes in a regenerative hydrogen/vanadium fuel cell. *Int J Hydrog Energy*. 2019;44:30093-30107. doi:10.1016/j.ijhydene.2019.09.151
4. Bissett MA, Kinloch IA, Dryfe RAW. Characterization of MoS 2 –graphene composites for high-performance coin cell supercapacitors. *ACS Appl Mater Interfaces*. 2015;7:17388-17398. doi:10.1021/acsami.5b04672
5. Rubio-Garcia J, Kucernak A, Parra-Puerto A, Liu R, Chakrabarti B. Hydrogen/functionalized benzoquinone for a high-performance regenerative fuel cell as a potential large-scale energy storage platform. *J Mater Chem A*. 2020;8:3933-3941. doi:10.1039/C9TA12396B
6. Liu X, Ouyang M, Orzech MW, et al. In-situ fabrication of carbon-metal fabrics as freestanding electrodes for high-performance flexible energy storage devices. *Energy Storage Mater*. 2020;30:329-336. doi:10.1016/j.ensm.2020.04.001
7. Merla Y, Wu B, Yufit V, Brandon NP, Martinez-Botas RF, Offer GJ. Extending battery life: a low-cost practical diagnostic technique for lithium-ion batteries. *J Power Sources*. 2016;331:224-231. doi:10.1016/j.jpowsour.2016.09.008
8. Wu B, Offer GJ. Environmental impact of hybrid and electric vehicles. Environ Impacts Road Veh Past, Present Futur, 2017, p. 133–56. doi:10.1039/9781788010221-00133
9. Brandon NP, Edge JS, Aunedi M, et al. UK Research Needs in Grid Scale Energy Storage Technologies. Energy Storage Res Network 2015.
10. UNFCCC. Conference of the parties (COP). Paris Climate Change Conference-November 2015, COP 21. 2015.
11. Zhang W-J, Huang K-J. A review of recent progress in molybdenum disulfide-based supercapacitors and batteries. *Inorg Chem Front*. 2017;4:1602-1620. doi:10.1039/C7QI00515F
12. Pazhamalai P, Krishnamoorthy K, Manoharan S, Kim SJ. High energy symmetric supercapacitor based on mechanically delaminated few-layered MoS2 sheets in organic electrolyte. *J Alloys Compd*. 2019;771:803-809. doi:10.1016/j.jallcom.2018.08.203
13. Sun H, Zhu J, Baumann D, et al. Hierarchical 3D electrodes for electrochemical energy storage. *Nat Rev Mater*. 2019;4:45-60. doi:10.1038/s41578-018-0069-9
14. Gencten M, Sahin Y. A critical review on progress of the electrode materials of vanadium redox flow battery. *Int J Energy Res*. 2020;44:7903-7923. doi:10.1002/er.5487
15. Liu Z, Yuan X, Zhang S, et al. Three-dimensional ordered porous electrode materials for electrochemical energy storage. *NPG Asia Mater*. 2019;11:12. doi:10.1038/s41427-019-0112-3
16. Hooch Antink W, Choi Y, Seong K, Kim JM, Piao Y. Recent progress in porous graphene and reduced graphene oxide-based nanomaterials for electrochemical energy storage devices. *Adv Mater Interfaces*. 2018;5:1701212. doi:10.1002/admi.201701212
17. Han T, Han J-J, Ma H, Zhang N, Sun D-D. Synthesis of benzenesulfonated PANI/RGO as cathode material for rechargeable lithium-polymer batteries. *Ionics (Kiel)*. 2019;25:4739-4749. doi:10.1007/s11581-019-03040-2
18. Hosseini MG, Mousavihashemi S, Murcia-López S, Flox C, Andreu T, Morante JR. High-power positive electrode based on synergistic effect of N- and WO3 -decorated carbon felt for vanadium redox flow batteries. *Carbon*. 2018;136:444-453. doi:10.1016/j.carbon.2018.04.038
19. Ye L, Wen K, Zhang Z, et al. Highly efficient materials assembly via electrophoretic deposition for electrochemical energy conversion and storage devices. *Adv Energy Mater*. 2016;6:1502018. doi:10.1002/aenm.201502018
20. Atiq Ur Rehman M, Chen Q, Braem A, Shaffer MSP, Boccaccini AR. Electrophoretic deposition of carbon nanotubes: recent progress and remaining challenges. *Int Mater Rev*. 2020;66:533-562. doi:10.1080/09506608.2020.1831299
21. Obregón S, Amor G, Vázquez A. Electrophoretic deposition of photocatalytic materials. *Adv Colloid Interf Sci*. 2019;269:236-255. doi:10.1016/j.cis.2019.05.003
22. Corni I, Ryan MP, Boccaccini AR. Electrophoretic deposition: from traditional ceramics to nanotechnology. *J Eur Ceram Soc*. 2008;28:1353-1367. doi:10.1016/j.jeurceramsoc.2007.12.011
23. Hamaker HC. Formation of a deposit by electrophoresis. *Trans Faraday Soc*. 1940;35:279. doi:10.1039/tf9403500279
24. Sarkar P, Nicholson PS. Electrophoretic deposition (EPD): mechanisms, kinetics, and application to ceramics. *J Am Ceram Soc*. 1996;79:1987-2002. doi:10.1111/j.1151-2916.1996.tb08929.x
25. Besra L, Liu M. A review on fundamentals and applications of electrophoretic deposition (EPD). *Prog Mater Sci*. 2007;52:1-61. doi:10.1016/j.pmatsci.2006.07.001
26. Chávez-Valdez A, Herrmann M, Boccaccini AR. Alternating current electrophoretic deposition (EPD) of TiO_2 nanoparticles in aqueous suspensions. *J Colloid Interface Sci*. 2012;375:102-105. doi:10.1016/j.jcis.2012.02.054
27. Sarkar P, Haung X, Nicholson PS. Structural ceramic microlaminates by electrophoretic deposition. *J Am Ceram Soc*. 1992;75:2907-2909. doi:10.1111/j.1151-2916.1992.tb05531.x
28. Schäfer M, Vogt L, Raether F, Kurth DG. Towards local deposition of particles by electrophoresis in dc electric fields in polar and nonpolar media and mixtures thereof. *Ceram Int*. 2020;46:17857-17866. doi:10.1016/j.ceramint.2020.04.092

29. Nold A, Clasen R. Bubble-free electrophoretic shaping from aqueous suspension with micro point-electrode. *J Eur Ceram Soc*. 2010;30:2971-2975. doi:10.1016/j.jeurceramsoc.2010.03.005
30. Islam MA, Xia Y, Telesca DA, Steigerwald ML, Herman IP. Controlled electrophoretic deposition of smooth and robust films of CdSe nanocrystals. *Chem Mater*. 2004;16:49-54. doi:10.1021/cm0304243
31. An Q, Rider AN, Thostenson ET. Electrophoretic deposition of carbon nanotubes onto carbon-fiber fabric for production of carbon/epoxy composites with improved mechanical properties. *Carbon*. 2012;50:4130-4143. doi:10.1016/j.carbon.2012.04.061
32. Frajkorová F, Molero E, Montero P, Gomez-Guillen MC, Sanchez-Herencia AJ, Ferrari B. Biodegradable bi-layered coatings shaped by dipping of Ti films followed by the EPD of gelatin/hydroxyapatite composites. *J Eur Ceram Soc*. 2016;36:343-355. doi:10.1016/j.jeurceramsoc.2015.07.005
33. Kang Y, Deng C, Chen Y, et al. Binder-free electrodes and their application for Li-ion batteries. *Nanoscale Res Lett*. 2020;15:112. doi:10.1186/s11671-020-03325-w
34. Xu S, Wei G, Li J, et al. Binder-free $Ti_3C_2T_x$ MXene electrode film for supercapacitor produced by electrophoretic deposition method. *Chem Eng J*. 2017;317:1026-1036. doi:10.1016/j.cej.2017.02.144
35. Basu RN, Randall CA, Mayo MJ. Fabrication of dense zirconia electrolyte films for tubular solid oxide fuel cells by electrophoretic deposition. *J Am Ceram Soc*. 2001;84:33-40. doi:10.1111/j.1151-2916.2001.tb00604.x
36. Lee SH, Woo SP, Kakati N, Kim D-J, Yoon YS. A comprehensive review of nanomaterials developed using electrophoresis process for high-efficiency energy conversion and storage systems. *Energies*. 2018;11:3122. doi:10.3390/en11113122
37. Hiemenz PC, Rajagopalan R, eds. *Principles of Colloid and Surface Chemistry, Revised and Expanded*. Boca Raton: CRC Press; 2016. doi:10.1201/9781315274287
38. Palmer TR. Investigation of Electrophoretic Deposition as a Fabrication Technique for High Performance Composites. 2011.
39. Jayaraman AS, Klaseboer E, Chan DYC. The unusual fluid dynamics of particle electrophoresis. *J Colloid Interface Sci*. 2019;553:845-863. doi:10.1016/j.jcis.2019.06.029
40. Wiersema P, Loeb A, Overbeek JT. Calculation of the electrophoretic mobility of a spherical colloid particle. *J Colloid Interface Sci*. 1966;22:78-99. doi:10.1016/0021-9797(66)90069-5
41. Booth F. The cataphoresis of spherical, solid non-conducting particles in a symmetrical electrolyte. *Proc R Soc A: Math Phys Eng Sci*. 1950;203:514-533. doi:10.1098/rspa.1950.0154
42. Carrique F, Ruiz-Reina E, Arroyo FJ, Jiménez ML, Delgado ÁV. Dynamic electrophoretic mobility of spherical colloidal particles in salt-free concentrated suspensions. *Langmuir*. 2008;24:2395-2406. doi:10.1021/la7030544
43. Ohshima H. Approximate expression for the electrophoretic mobility of a spherical colloidal particle in a solution of general electrolytes. *Colloids Surf A Physicochem Eng Asp*. 2005;267:50-55. doi:10.1016/j.colsurfa.2005.06.036
44. O'Brien RW, White LR. Electrophoretic mobility of a spherical colloidal particle. *J Chem Soc Faraday Trans*. 1978;74:1607. doi:10.1039/f29787401607
45. Vandeperre L, Van Der Biest O, Bouyer F, Persello J, Foissy A. Electrophoretic forming of silicon carbide ceramics. *J Eur Ceram Soc*. 1997;17:373-376. doi:10.1016/S0955-2219(96)00106-9
46. Harbach F, Nienburg H. Homogeneous functional ceramic components through electrophoretic deposition from stable colloidal suspensions—I. Basic concepts and application to zirconia. *J Eur Ceram Soc*. 1998;18:675-683. doi:10.1016/S0955-2219(97)00197-0
47. Kanamura K. Innovation of novel functional material processing technique by using electrophoretic deposition process. *Solid State Ionics*. 2004;172:303-308. doi:10.1016/j.ssi.2004.01.039
48. Wu M-S, Huang C-Y, Lin K-H. Facile electrophoretic deposition of Ni-decorated carbon nanotube film for electrochemical capacitors. *Electrochem Solid-State Lett*. 2009;12:A129. doi:10.1149/1.3125283
49. Jeng K-T, Huang W-M, Hsu N-Y. Application of low-voltage electrophoretic deposition to fabrication of direct methanol fuel cell electrode composite catalyst layer. *Mater Chem Phys*. 2009;113:574-578. doi:10.1016/j.matchemphys.2008.08.018
50. Wang YH, Chen QZ, Cho J, Boccaccini AR. Electrophoretic co-deposition of diamond/borosilicate glass composite coatings. *Surf Coat Technol*. 2007;201:7645-7651. doi:10.1016/j.surfcoat.2007.02.037
51. Fotovvati B, Namdari N, Dehghanghadikolaei A. On coating techniques for surface protection: a review. *J Manuf Mater Process*. 2019;3:28. doi:10.3390/jmmp3010028
52. Tyona MD. Doped zinc oxide nanostructures for photovoltaic solar cells application. Zinc Oxide Based Nano Mater Devices, IntechOpen; 2019. doi:10.5772/intechopen.86254
53. Santos L, Neto JP, Crespo A, et al. Electrodeposition of WO3 nanoparticles for sensing applications. Electroplat Nanostructures, InTech. 2015. doi:10.5772/61216
54. Awasthi S, Pandey SK, Pandey CP, Balani K. Progress in electrochemical and electrophoretic deposition of nickel with carbonaceous allotropes: a review. *Adv Mater Interfaces*. 2020;7:1901096. doi:10.1002/admi.201901096
55. Awasthi S, Pal VK, Choudhury SK. Effect of surface modifications by abrasive water jet machining and electrophoretic deposition on tribological characterisation of Ti6Al4V alloy. *Int J Adv Manuf Technol*. 2018;96:1769-1777. doi:10.1007/s00170-017-1164-6
56. Wang QJ, Chung Y-W, eds. *Encyclopedia of Tribology*. Boston, MA: Springer US; 2013. doi:10.1007/978-0-387-92897-5
57. Simon P, Gogotsi Y. Materials for electrochemical capacitors. *Nat Mater*. 2008;7:845-854. doi:10.1038/nmat2297
58. Sangeetha S, Kalaignan GP. Studies on the electrodeposition and characterization of PTFE polymer inclusion in Ni–W–BN nanocomposite coatings for industrial applications. *RSC Adv*. 2015;5:74115-74125. doi:10.1039/C5RA11069F
59. Xiao XF, Liu RF, Tang XL. Electrophoretic deposition of silicon substituted hydroxyapatite coatings from n-butanol–chloroform mixture. *J Mater Sci Mater Med*. 2008;19:175-182. doi:10.1007/s10856-007-0161-y
60. Avcu E, Baştan FE, Abdullah HZ, Rehman MAU, Avcu YY, Boccaccini AR. Electrophoretic deposition of chitosan-based composite coatings for biomedical applications: a review. *Prog Mater Sci*. 2019;103:69-108. doi:10.1016/j.pmatsci.2019.01.001

61. Sun J, Zhu Y, Meng L, et al. Electrophoretic deposition of colloidal particles on mg with cytocompatibility, antibacterial performance, and corrosion resistance. *Acta Biomater*. 2016; 45:387-398. doi:10.1016/j.actbio.2016.09.007
62. Qi H, Heise S, Zhou J, et al. Electrophoretic deposition of bioadaptive drug delivery coatings on magnesium alloy for bone repair. *ACS Appl Mater Interfaces*. 2019;11:8625-8634. doi:10.1021/acsami.9b01227
63. Lei M, Qu X, Liu H, et al. Programmable electrofabrication of porous Janus films with tunable Janus balance for anisotropic cell guidance and tissue regeneration. *Adv Funct Mater*. 2019; 29:1900065. doi:10.1002/adfm.201900065
64. Cheng X, Deng D, Chen L, Jansen JA, Leeuwenburgh SGC, Yang F. Electrodeposited assembly of additive-free silk fibroin coating from pre-assembled nanospheres for drug delivery. *ACS Appl Mater Interfaces*. 2020;12:12018-12029. doi:10.1021/acsami.9b21808
65. Chen J, Peng K, Tu W. Novel waterborne UV-curable coatings based on hyperbranched polymers via electrophoretic deposition. *RSC Adv*. 2019;9:11013-11025. doi:10.1039/C9RA01500K
66. Wu M-S, Lin K-H. One-step electrophoretic deposition of Ni-decorated activated-carbon film as an electrode material for supercapacitors. *J Phys Chem C*. 2010;114:6190-6196. doi:10.1021/jp9109145
67. Mora J, Dudoff JK, Moran BD, et al. Projection based light-directed electrophoretic deposition for additive manufacturing. *Addit Manuf*. 2018;22:330-333. doi:10.1016/j.addma.2018.05.020
68. Boccaccini AR, Keim S, Ma R, Li Y, Zhitomirsky I. Electrophoretic deposition of biomaterials. *J R Soc Interface*. 2010;7: S581-S613. doi:10.1098/rsif.2010.0156.focus
69. Wang Y, Shi Z, Fang J, Xu H, Ma X, Yin J. Direct exfoliation of graphene in methanesulfonic acid and facile synthesis of graphene/polybenzimidazole nanocomposites. *J Mater Chem*. 2011;21:505-512. doi:10.1039/C0JM02376K
70. Shou W, Pan H. Direct printing of microstructures by femtosecond laser excitation of nanocrystals in solution. *Appl Phys Lett*. 2016;108:214101. doi:10.1063/1.4952615
71. Boccaccini AR, Kaya C, Chawla KK. Use of electrophoretic deposition in the processing of fibre reinforced ceramic and glass matrix composites: a review. *Compos Part A Appl Sci Manuf*. 2001;32:997-1006. doi:10.1016/S1359-835X(00)00168-8
72. Novak S, Ivekovič A, Hattori Y. Production of bulk SiC parts by electrophoretic deposition from concentrated aqueous suspension. *Adv Appl Ceram*. 2014;113:14-21. doi:10.1179/1743676113Y.0000000113
73. Kitabatake T, Uchikoshi T, Munakata F, Sakka Y, Hirosaki N. Emission color tuning of laminated and mixed SiAlON phosphor films by electrophoretic deposition. *J Ceram Soc Jpn*. 2010;118:1-4. doi:10.2109/jcersj2.118.1
74. Sullivan KT, Zhu C, Duoss EB, et al. Controlling material reactivity using architecture. *Adv Mater*. 2016;28:1934-1939. doi:10.1002/adma.201504286
75. Benehkohal NP, Sussman MJ, Chiu H, Uceda M, Gauvin R, Demopoulos GP. Enabling green fabrication of Li-ion battery electrodes by electrophoretic deposition: growth of thick binder-free mesoporous TiO 2 -carbon anode films. *J Electrochem Soc*. 2015;162:D3013-D3018. doi:10.1149/2.0111511jes
76. Huang W-C, Hu S-H, Liu K-H, Chen S-Y, Liu D-M. A flexible drug delivery chip for the magnetically-controlled release of anti-epileptic drugs. *J Control Release*. 2009;139:221-228. doi:10.1016/j.jconrel.2009.07.002
77. Lee SH, Jung CK, Bae JS, Jung SL, Choi YJ, Kang CS. Liquid-based cytology improves preoperative diagnostic accuracy of the tall cell variant of papillary thyroid carcinoma. *Diagn Cytopathol*. 2014;42:11-17. doi:10.1002/dc.23007
78. Cannio M, Boccaccini DN, Ponzoni C, Leonelli C. Electrophoretic deposition: an effective technique to obtain functionalized nanocoatings. *Handbook of Modern Coating Technologies*. Amsterdam: Elsevier; 2021:209-230. doi:10.1016/B978-0-444-63240-1.00008-5
79. Cordero-Arias L, Cabanas-Polo S, Gilabert J, et al. Electrophoretic deposition of nanostructured TiO_2/alginate and TiO_2 -bioactive glass/alginate composite coatings on stainless steel. *Adv Appl Ceram*. 2014;113:42-49. doi:10.1179/1743676113Y.0000000096
80. Mao H, Wang K, Wang C, Wu M. An improvement of color electrophoretic paint via ultrafine modified pigment paste. *J Adhes Sci Technol*. 2014;28:186-200. doi:10.1080/01694243.2013.833403
81. Verma K, Oder J, Wille R. Simulating industrial electrophoretic deposition on distributed memory architectures. 2019 27th Euromicro Int. Conf. Parallel, Distrib. Network-based process. IEEE; 2019, p. 414–21. doi:10.1109/EMPDP.2019.8671570
82. Zhang Q, Huang C, Wang H, Hu M, Li H, Liu X. UV-curable coating crosslinked by a novel hyperbranched polyurethane acrylate with excellent mechanical properties and hardness. *RSC Adv*. 2016;6:107942-107950. doi:10.1039/C6RA21081C
83. Fieberg A, Reis O. UV curable electrodeposition systems. *Prog Org Coat*. 2002;45:239-247. doi:10.1016/S0300-9440(02)00065-6
84. Ruffo R, Wessells C, Huggins RA, Cui Y. Electrochemical behavior of $LiCoO_2$ as aqueous lithium-ion battery electrodes. *Electrochem Commun*. 2009;11:247-249. doi:10.1016/j.elecom.2008.11.015
85. Anné G, Vanmeensel K, Vleugels J, van der Biest O. Electrophoretic deposition as a novel near net shaping technique for functionally graded biomaterials. *Key Eng Mater*. 2006;314: 213-218. doi:10.4028/0-87849-998-9.213
86. Nold A, Zeiner J, Assion T, Clasen R. Electrophoretic deposition as rapid prototyping method. *J Eur Ceram Soc*. 2010;30: 1163-1170. doi:10.1016/j.jeurceramsoc.2009.03.021
87. Pascall AJ, Qian F, Wang G, Worsley MA, Li Y, Kuntz JD. Light-directed electrophoretic deposition: a new additive manufacturing technique for arbitrarily patterned 3D composites. *Adv Mater*. 2014;26:2252-2256. doi:10.1002/adma.201304953
88. Pascall AJ, Mora J, Jackson JA, Kuntz JD. Light directed electrophoretic deposition for additive manufacturing: spatially localized deposition control with photoconductive counter electrodes. *Key Eng Mater*. 2015;654:261-267.
89. Thellaputta GR, Chandra PS, Rao CSP. Machinability of nickel based superalloys: a review. *Mater Today Proc*. 2017;4: 3712-3721. doi:10.1016/j.matpr.2017.02.266
90. Rui B, Yang M, Zhang L, et al. Reduced graphene oxide-modified biochar electrodes via electrophoretic deposition

with high rate capability for supercapacitors. *J Appl Electrochem*. 2020;50:407-420. doi:10.1007/s10800-020-01397-1

91. Wang C, Li J, Sun S, et al. Electrophoretic deposition of graphene oxide on continuous carbon fibers for reinforcement of both tensile and interfacial strength. *Compos Sci Technol*. 2016;135:46-53. doi:10.1016/j.compscitech.2016.07.009
92. Lu T, Pan L, Li H, Nie C, Zhu M, Sun Z. Reduced graphene oxide–carbon nanotubes composite films by electrophoretic deposition method for supercapacitors. *J Electroanal Chem*. 2011;661:270-273. doi:10.1016/j.jelechem.2011.07.042
93. Zhang F, Wei M, Viswanathan VV, et al. 3D printing technologies for electrochemical energy storage. *Nano Energy*. 2017;40:418-431. doi:10.1016/j.nanoen.2017.08.037
94. An SJ, Zhu Y, Lee SH, et al. Thin film fabrication and simultaneous anodic reduction of deposited graphene oxide platelets by electrophoretic deposition. *J Phys Chem Lett*. 2010;1:1259-1263. doi:10.1021/jz100080c
95. Bazzarella, R, Carter WC, Chiang Y-M, Cross J, Ota N. Semi-solid electrode cell having a porous current collector and methods of manufacture. WO2013036801A1, 2017.
96. Zhan Y, Edison E, Manalastas W, et al. Electrochemical deposition of highly porous reduced graphene oxide electrodes for Li-ion capacitors. *Electrochim Acta*. 2020;337:135861. doi:10.1016/j.electacta.2020.135861
97. Le Fevre LW. 2D Materials for Energy Storage. The University of Manchester. 2018.
98. Liu Z, Mukherjee PP. Microstructure evolution in lithium-ion battery electrode processing. *J Electrochem Soc*. 2014;161:E3248-E3258. doi:10.1149/2.026408jes
99. Gürsu H, Güner Y, Dermenci KB, et al. A novel green and one-step electrochemical method for production of sulfur-doped graphene powders and their performance as an anode in Li-ion battery. *Ionics (Kiel)*. 2020;26:4909-4919. doi:10.1007/s11581-020-03671-w
100. Gürsu H, Güner Y, Dermenci KB, et al. Preparation of N-doped graphene powders by cyclic voltammetry and a potential application of them: anode materials of Li-ion batteries. *Int J Energy Res*. 2019;43:5346-5354. doi:10.1002/er.4618
101. Bitsch B, Dittmann J, Schmitt M, Scharfer P, Schabel W, Willenbacher N. A novel slurry concept for the fabrication of lithium-ion battery electrodes with beneficial properties. *J Power Sources*. 2014;265:81-90. doi:10.1016/j.jpowsour.2014.04.115
102. Doberdò I, Löffler N, Laszczynski N, et al. Enabling aqueous binders for lithium battery cathodes – carbon coating of aluminum current collector. *J Power Sources*. 2014;248:1000-1006. doi:10.1016/j.jpowsour.2013.10.039
103. Ludwig B, Zheng Z, Shou W, Wang Y, Pan H. Solvent-free manufacturing of electrodes for Lithium-ion batteries. *Sci Rep*. 2016;6:23150. doi:10.1038/srep23150
104. Tiwari P, Ferson ND, Andrew JS. Elucidating the role of electrophoretic mobility for increasing yield in the electrophoretic deposition of nanomaterials. *J Colloid Interface Sci*. 2020;570:109-115. doi:10.1016/j.jcis.2020.02.103
105. Van der Biest OO, Vandeperre LJ. Electrophoretic deposition of materials. *Annu Rev Mater Sci*. 1999;29:327-352. doi:10.1146/annurev.matsci.29.1.327
106. van der Biest O, Put S, Anné G, Vleugels J. Electrophoretic deposition for coatings and free standing objects. *J Mater Sci*. 2004;39:779-785. doi:10.1023/B:JMSC.0000012905.62256.39
107. Vleugels J, Anné G, Put S, Van Der Biest O. Thick plate-shaped Al_2O_3/ZrO_2 composites with continuous gradient processed by electrophoretic deposition. *Mater Sci Forum*. 2003;423–425:171-176.
108. Anné G, Neirinck B, Vanmeensel K, Van der Biest O, Vleugels J. Influence of electrostatic interactions in the deposit on the electrical field strength during electrophoretic deposition. *Key Eng Mater*. 2006;314:181-186.
109. Stappers L, Zhang L, Van der Biest O, Fransaer J. Study of the deposit resistance during electrophoretic deposition. *Key Eng Mater*. 2009;412:9-14.
110. Huang C, Zhang J, Young NP, Snaith HJ, Grant PS. Solid-state supercapacitors with rationally designed heterogeneous electrodes fabricated by large area spray processing for wearable energy storage applications. *Sci Rep*. 2016;6:25684. doi:10.1038/srep25684
111. Kim K, Kim M-S, Cha P-R, Kang SH, Kim J-H. Structural modification of self-organized Nanoporous niobium oxide via hydrogen treatment. *Chem Mater*. 2016;28:1453-1461. doi:10.1021/acs.chemmater.5b04845
112. Ma Y, Han J, Wang M, Chen X, Jia S. Electrophoretic deposition of graphene-based materials: a review of materials and their applications. *J Mater*. 2018;4:108-120. doi:10.1016/j.jmat.2018.02.004
113. Chakrabarti B, Rubio-Garcia J, Kalamaras E, et al. Evaluation of a non-aqueous vanadium redox flow battery using a deep eutectic solvent and graphene-modified carbon electrodes via electrophoretic deposition. *Batteries*. 2020;6:38. doi:10.3390/batteries6030038
114. Sridhar TM, Eliaz N, Mudali UK, Raj B. Electrophoretic deposition of hydroxyapatite coatings and corrosion aspects of metallic implants. *Corros Rev*. 2002;20:255-294. doi:10.1515/CORRREV.2002.20.4-5.255
115. Islam MS, Fisher CAJ. Lithium and sodium battery cathode materials: computational insights into voltage, diffusion and nanostructural properties. *Chem Soc Rev*. 2014;43:185-204. doi:10.1039/C3CS60199D
116. Yang Y, Li J, Chen D, Zhao J. A facile electrophoretic deposition route to the Fe_3O_4/CNTs/rGO composite electrode as a binder-free anode for lithium ion battery. *ACS Appl Mater Interfaces*. 2016;8:26730-26739. doi:10.1021/acsami.6b07990
117. Xia X, Tu J, Mai Y, et al. Graphene sheet/porous NiO hybrid film for supercapacitor applications. *Chem - A Eur J*. 2011;17:10898-10905. doi:10.1002/chem.201100727
118. Hu S, Li W, Finklea H, Liu X. A review of electrophoretic deposition of metal oxides and its application in solid oxide fuel cells. *Adv Colloid Interf Sci*. 2020;276:102102. doi:10.1016/j.cis.2020.102102
119. Dunn JB, Gaines L, Kelly JC, James C, Gallagher KG. The significance of Li-ion batteries in electric vehicle life-cycle energy and emissions and recycling's role in its reduction. *Energy Environ Sci*. 2015;8:158-168. doi:10.1039/C4EE03029J
120. Yilmaz M, Raina S, Hsu S-H, Kang WP. Micropatterned arrays of vertically-aligned CNTs grown on aluminum as a new cathode platform for LiFePO4 integration in lithium-ion batteries. *Ionics (Kiel)*. 2019;25:421-427. doi:10.1007/s11581-018-2651-y
121. Golubkov AW, Fuchs D, Wagner J, et al. Thermal-runaway experiments on consumer Li-ion batteries with metal-oxide and olivin-type cathodes. *RSC Adv*. 2014;4:3633-3642. doi:10.1039/C3RA45748F

122. Yang Y, Huang J, Zeng J, Xiong J, Zhao J. Direct electrophoretic deposition of binder-free Co_3O_4/graphene Sandwich-like hybrid electrode as remarkable lithium ion battery anode. *ACS Appl Mater Interfaces*. 2017;9:32801-32811. doi:10.1021/acsami.7b10683
123. Hu Y, Sun X. Flexible rechargeable lithium ion batteries: advances and challenges in materials and process technologies. *J Mater Chem A*. 2014;2:10712-10738. doi:10.1039/C4TA00716F
124. Cohen E, Lifshitz M, Gladkikh A, Kamir Y, Ben-Barak I, Golodnitsky D. Novel one-step electrophoretic deposition of the membrane-electrode assembly for flexible-battery applications. *J Mater Chem A*. 2020;8:11391-11398. doi:10.1039/D0TA02328K
125. Kyerematen NA, Dinh TM, Pech D. Electrophoretic deposition of $Li_4Ti_5O^{12}$ nanoparticles with a novel additive for Li-ion microbatteries. *RSC Adv*. 2015;5:61502-61507. doi:10.1039/C5RA11039D
126. Kyerematen NA, Lebouin C, Knauth P, Djenizian T. The electrochemical behaviour of TiO_2 nanotubes with Co_3O_4 or NiO submicron particles: composite anode materials for Li-ion micro batteries. *Electrochim Acta*. 2013;88:814-820. doi:10.1016/j.electacta.2012.09.120
127. Li J, Liang X, Liou F, Park J. Macro−/micro-controlled 3D lithium-ion batteries via additive manufacturing and electric field processing. *Sci Rep*. 2018;8:1846. doi:10.1038/s41598-018-20329-w
128. Huang C, Dontigny M, Zaghib K, Grant PS. Low-tortuosity and graded lithium ion battery cathodes by ice templating. *J Mater Chem A*. 2019;7:21421-21431. doi:10.1039/C9TA07269A
129. Seo S-D, Hwang I-S, Lee S-H, Shim H-W, Kim D-W. 1D/2D carbon nanotube/graphene nanosheet composite anodes fabricated using electrophoretic assembly. *Ceram Int*. 2012;38:3017-3021. doi:10.1016/j.ceramint.2011.11.083
130. Uceda M, Zhou J, Wang J, Gauvin R, Zaghib K, Demopoulos GP. Highly conductive NMP-free carbon-coated nano-lithium titanate/carbon composite electrodes via SBR-assisted electrophoretic deposition. *Electrochim Acta*. 2019;299:107-115. doi:10.1016/j.electacta.2018.12.166
131. Parsi Benehkohal N, Gomez MA, Gauvin R, Demopoulos GP. Enabling aqueous electrophoretic growth of adherent nanotitania mesoporous films via intrafilm cathodic deposition of hydrous zinc oxide. *Electrochim Acta*. 2013;87:169-179. doi:10.1016/j.electacta.2012.10.005
132. Cohen E, Menkin S, Lifshits M, et al. Novel rechargeable 3D-microbatteries on 3D-printed-polymer substrates: feasibility study. *Electrochim Acta*. 2018;265:690-701. doi:10.1016/j.electacta.2018.01.197
133. Hagberg J, Maples HA, Alvim KSP, et al. Lithium iron phosphate coated carbon fiber electrodes for structural lithium ion batteries. *Compos Sci Technol*. 2018;162:235-243. doi:10.1016/j.compscitech.2018.04.041
134. Michaud X, Shi K, Zhitomirsky I. Electrophoretic deposition of $LiFePO_4$ for Li-ion batteries. *Mater Lett*. 2019;241:10-13. doi:10.1016/j.matlet.2019.01.032
135. Liu Y, Luo D, Zhang T, et al. Film deposition mechanisms and properties of optically active chelating polymer and composites. *Colloids Surf A Physicochem Eng Asp*. 2015;487:17-25. doi:10.1016/j.colsurfa.2015.09.057
136. Shi Y, Kong Y, Song L, Zhang J, Ji Z, Ge Z. Synthesis and characterization of polyelectrolytes based on benzotriazole backbone. *Colloid Polym Sci*. 2018;296:1-9. doi:10.1007/s00396-017-4214-6
137. Huang Y, Liu H, Lu Y-C, Hou Y, Li Q. Electrophoretic lithium iron phosphate/reduced graphene oxide composite for lithium ion battery cathode application. *J Power Sources*. 2015;284:236-244. doi:10.1016/j.jpowsour.2015.03.037
138. Dashairya L, Das D, Saha P. Binder-free electrophoretic deposition of Sb/rGO on cu foil for superior electrochemical performance in Li-ion and Na-ion batteries. *Electrochim Acta*. 2020;358:136948. doi:10.1016/j.electacta.2020.136948
139. Moyer K, Carter R, Hanken T, Douglas A, Oakes L, Pint CL. Electrophoretic deposition of $LiFePO_4$ onto 3-D current collectors for high areal loading battery cathodes. *Mater Sci Eng B*. 2019;241:42-47. doi:10.1016/j.mseb.2019.02.003
140. Oltean G, Valvo M, Nyholm L, Edström K. On the electrophoretic and sol–gel deposition of active materials on aluminium rod current collectors for three-dimensional Li-ion micro-batteries. *Thin Solid Films*. 2014;562:63-69. doi:10.1016/j.tsf.2014.03.069
141. Zhang H, Yu X, Braun PV. Three-dimensional bicontinuous ultrafast-charge and -discharge bulk battery electrodes. *Nat Nanotechnol*. 2011;6:277-281. doi:10.1038/nnano.2011.38
142. Dashairya L, Das D, Saha P. Electrophoretic deposition of antimony/reduced graphite oxide hybrid nanostructure: a stable anode for lithium-ion batteries. *Mater Today Commun*. 2020;24:101189. doi:10.1016/j.mtcomm.2020.101189
143. Dewan M, Majumder T, Majumder SB. Electrophoretically deposited bismuth iron oxide as dual role anode material for both lithium and sodium-ion batteries. *Mater Today Commun*. 2021;27:102358. doi:10.1016/j.mtcomm.2021.102358
144. Sanchez JS, Xu J, Xia Z, Sun J, Asp LE, Palermo V. Electrophoretic coating of $LiFePO_4$/graphene oxide on carbon fibers as cathode electrodes for structural lithium ion batteries. *Compos Sci Technol*. 2021;208:108768. doi:10.1016/j.compscitech.2021.108768
145. Uceda M, Chiu H-C, Gauvin R, Zaghib K, Demopoulos GP. Electrophoretically co-deposited $Li_4Ti_5O_{12}$/reduced graphene oxide nanolayered composites for high-performance battery application. *Energy Storage Mater*. 2020;26:560-569. doi:10.1016/j.ensm.2019.11.029
146. Wang Y, Zhang W, Qi Y, et al. Uniform titanium nitride decorated cu foams by electrophoretic deposition for stable lithium metal anodes. *J Alloys Compd*. 2021;874:159916. doi:10.1016/j.jallcom.2021.159916
147. Das S, Das D, Jena S, Mitra A, Bhattacharya A, Majumder SB. Electrophoretic deposition of nickel ferrite anode for lithium-ion half cell with superior rate performance. *Surf Coat Technol*. 2021;421:127365. doi:10.1016/j.surfcoat.2021.127365
148. Du G, Xi Y, Tian X, et al. One-step hydrothermal synthesis of 3D porous microspherical $LiFePO_4$/graphene aerogel composite for lithium-ion batteries. *Ceram Int*. 2019;45:18247-18254. doi:10.1016/j.ceramint.2019.06.035
149. Huang C-Y, Kuo T-R, Yougbaré S, Lin L-Y. Design of $LiFePO_4$ and porous carbon composites with excellent high-rate charging performance for lithium-ion secondary battery. *J Colloid Interface Sci*. 2022;607:1457-1465. doi:10.1016/j.jcis.2021.09.118
150. Acharya T, Chaupatnaik A, Pathak A, Roy A, Pati S. Effect of calendering on rate performance of $Li_4Ti_5O_{12}$ anodes for

lithium-ion batteries. *J Electroceram*. 2020;45:85-92. doi:10.1007/s10832-020-00227-2
151. Lithium Titanate (LTO) Tapes | NEI Corporation n.d.
152. Lithium Iron Phosphate (LFP) Tapes | NEI Corporation n.d.
153. Li Z, Qiao N, Nie J, et al. $NiO/NiFe_2O_4$ nanocubes derived from Prussian blue as anode materials for Li-ion batteries. *Mater Lett*. 2020;275:128077. doi:10.1016/j.matlet.2020.128077
154. Hajizadeh A, Shahalizade T, Riahifar R, et al. Electrophoretic deposition as a fabrication method for Li-ion battery electrodes and separators – a review. *J Power Sources*. 2022;535:231448. doi:10.1016/j.jpowsour.2022.231448
155. Lu X, Zhou X, Yang Q, et al. An in-situ electrodeposited cobalt selenide promotor for polysulfide management targeted stable lithium–sulfur batteries. *J Colloid Interface Sci*. 2021;600:278-287. doi:10.1016/j.jcis.2021.05.036
156. Carter R, Oakes L, Muralidharan N, Cohn AP, Douglas A, Pint CL. Polysulfide anchoring mechanism revealed by atomic layer deposition of V_2O_5 and sulfur-filled carbon nanotubes for lithium–sulfur batteries. *ACS Appl Mater Interfaces*. 2017;9:7185-7192. doi:10.1021/acsami.6b16155
157. Boles MA, Ling D, Hyeon T, Talapin DV. The surface science of nanocrystals. *Nat Mater*. 2016;15:141-153. doi:10.1038/nmat4526
158. Rui X, Tan H, Yan Q. Nanostructured metal sulfides for energy storage. *Nanoscale*. 2014;6:9889-9924. doi:10.1039/C4NR03057E
159. Mahmood N, Tang T, Hou Y. Nanostructured anode materials for lithium ion batteries: progress, challenge and perspective. *Adv Energy Mater*. 2016;6:1600374. doi:10.1002/aenm.201600374
160. Boccaccini AR, Cho J, Roether JA, Thomas BJC, Jane Minay E, Shaffer MSP. Electrophoretic deposition of carbon nanotubes. *Carbon*. 2006;44:3149-3160. doi:10.1016/j.carbon.2006.06.021
161. Otelaja OO, Ha D-H, Ly T, Zhang H, Robinson RD. Highly conductive $Cu_{2-x}S$ nanoparticle films through room-temperature processing and an order of magnitude enhancement of conductivity via electrophoretic deposition. *ACS Appl Mater Interfaces*. 2014;6:18911-18920. doi:10.1021/am504785f
162. Boccaccini JHDAR. *Electrophoretic Deposition of Nanomaterials*. New York: Springer; 2010.
163. Jia S, Banerjee S, Herman IP. Mechanism of the electrophoretic deposition of CdSe nanocrystal films: influence of the nanocrystal surface and charge. *J Phys Chem C*. 2008;112:162-171. doi:10.1021/jp0733320
164. Zillner E, Kavalakkatt J, Eckhardt B, Dittrich T, Ennaoui A, Lux-Steiner M. Formation of a heterojunction by electrophoretic deposition of CdTe/CdSe nanoparticles from an exhaustible source. *Thin Solid Films*. 2012;520:5500-5503. doi:10.1016/j.tsf.2012.05.002
165. Zhao P, LeSergent LJ, Farnese J, Wen JZ, Ren CL. Electrophoretic deposition of carbon nanotubes on semi-conducting and non-conducting substrates. *Electrochem Commun*. 2019;108:106558. doi:10.1016/j.elecom.2019.106558
166. Ha D-H, Ly T, Caron JM, Zhang H, Fritz KE, Robinson RD. A general method for high-performance Li-ion battery electrodes from colloidal nanoparticles without the Introduction of binders or conductive-carbon additives: the cases of MnS, $Cu_{2-x}S$, and Ge. *ACS Appl Mater Interfaces*. 2015;7:25053-25060. doi:10.1021/acsami.5b03398
167. Ha D-H, Islam MA, Robinson RD. Binder-free and carbon-free nanoparticle batteries: a method for nanoparticle electrodes without polymeric binders or carbon black. *Nano Lett*. 2012;12:5122-5130. doi:10.1021/nl3019559
168. Singh A, English NJ, Ryan KM. Highly ordered nanorod assemblies extending over device scale areas and in controlled multilayers by electrophoretic deposition. *J Phys Chem B*. 2013;117:1608-1615. doi:10.1021/jp305184n
169. Krahne R, Morello G, Figuerola A, George C, Deka S, Manna L. Physical properties of elongated inorganic nanoparticles. *Phys Rep*. 2011;501:75-221. doi:10.1016/j.physrep.2011.01.001
170. Liu P, Singh S, Bree G, Ryan KM. Complete assembly of Cu_2ZnSnS_4 (CZTS) nanorods at substrate interfaces using a combination of self and directed organisation. *Chem Commun*. 2016;52:11587-11590. doi:10.1039/C6CC06417E
171. Bree G, Geaney H, Ryan KM. Electrophoretic deposition of tin sulfide nanocubes as high-performance lithium-ion battery anodes. *ChemElectroChem*. 2019;6:3049-3056. doi:10.1002/celc.201900524
172. Rosenthal S, Mcbride J, Pennycook S, Feldman L. Synthesis, surface studies, composition and structural characterization of CdSe, core/shell and biologically active nanocrystals. *Surf Sci Rep*. 2007;62:111-157. doi:10.1016/j.surfrep.2007.02.001
173. Ma Z, Kyotani T, Liu Z, Terasaki O, Tomita A. Very high surface area microporous carbon with a three-dimensional nanoarray structure: synthesis and its molecular structure. *Chem Mater*. 2001;13:4413-4415. doi:10.1021/cm010730l
174. Huang P, Pech D, Lin R, et al. On-chip micro-supercapacitors for operation in a wide temperature range. *Electrochem Commun*. 2013;36:53-56. doi:10.1016/j.elecom.2013.09.003
175. Cherng JS, Ho MY, Yeh TH, Chen WH. Anode-supported micro-tubular SOFCs made by aqueous electrophoretic deposition. *Ceram Int*. 2012;38:S477-S480. doi:10.1016/j.ceramint.2011.05.057
176. Mazor H, Golodnitsky D, Burstein L, Gladkich A, Peled E. Electrophoretic deposition of lithium iron phosphate cathode for thin-film 3D-microbatteries. *J Power Sources*. 2012;198:264-272. doi:10.1016/j.jpowsour.2011.09.108
177. Hadar R, Golodnitsky D, Mazor H, et al. Development and characterization of composite YSZ–PEI electrophoretically deposited membrane for Li-ion battery. *J Phys Chem B*. 2013;117:1577-1584. doi:10.1021/jp305087h
178. Aravindan V, Sundaramurthy J, Jain A, et al. Unveiling $TiNb_2O_7$ as an insertion anode for lithium ion capacitors with high energy and power density. *ChemSusChem*. 2014;7:1858-1863. doi:10.1002/cssc.201400157
179. Yang M, Zhong Y, Ren J, Zhou X, Wei J, Zhou Z. Fabrication of high-power Li-ion hybrid supercapacitors by enhancing the exterior surface charge storage. *Adv Energy Mater*. 2015;5:1500550. doi:10.1002/aenm.201500550
180. Wu M-S, Wang C, Jow J-J. Self-assembly of one-dimensional nitrogen-doped hollow carbon nanoparticle chains derived from zinc hexacyanoferrate coordination polymer for lithium-ion capacitors. *Electrochim Acta*. 2016;222:856-861. doi:10.1016/j.electacta.2016.11.047
181. Ghashghaie S, Cheng SH-S, Fang J, Shahzad HK, Ma RL-W, Chung C-Y. Electrophoretically deposited binder-free 3-D carbon/sulfur nanocomposite cathode for high-performance Li–S batteries. *J Energy Chem*. 2020;48:92-101. doi:10.1016/j.jechem.2019.12.015

182. Huang Y, Lin L, Zhang C, et al. Recent advances and strategies toward polysulfides shuttle inhibition for high-performance Li–S batteries. *Adv Sci*. 2022;9:2106004. doi:10.1002/advs.202106004
183. Blanga R, Goor M, Burstein L, et al. The search for a solid electrolyte, as a polysulfide barrier, for lithium/sulfur batteries. *J Solid State Electrochem*. 2016;20:3393-3404. doi:10.1007/s10008-016-3303-7
184. Zhang L, Jin Q, Zhao K, Zhang X, Wu L. Lithiophilic $Ti_3C_2T_x$ -modified cu foam by electrophoretic deposition for dendrite-free lithium metal anodes. *ACS Appl Energy Mater*. 2022;5:2514-2521. doi:10.1021/acsaem.1c04035
185. Wang Y, Sang H-Q, Zhang W, et al. Electrophoretic deposited black phosphorus on 3D porous current collectors to regulate Li nucleation for dendrite-free lithium metal anodes. *ACS Appl Mater Interfaces*. 2020;12:51563-51572. doi:10.1021/acsami.0c16430
186. Fernandez-Marchante CM, Millán M, Medina-Santos JI, Lobato J. Environmental and preliminary cost assessments of redox flow batteries for renewable energy storage. *Energ Technol*. 2020;8:1900914. doi:10.1002/ente.201900914
187. Thaller LH. Electrochemical cell for rebalancing redox flow system. U S Pat Appl 1978.
188. Rychcik M, Skyllas-Kazacos M. Characteristics of a new all-vanadium redox flow battery. *J Power Sources*. 1988;22:59-67. doi:10.1016/0378-7753(88)80005-3
189. Gencten M, Gursu H, Sahin Y. Anti-precipitation effects of TiO_2 and $TiOSO_4$ on positive electrolyte of vanadium redox battery. *Int J Hydrog Energy*. 2017;42:25608-25618. doi:10.1016/j.ijhydene.2017.05.111
190. Gencten M, Gursu H, Sahin Y. Effect of A- and Γ-alumina on the precipitation of positive electrolyte in vanadium redox battery. *Int J Hydrog Energy*. 2017;42:25598-25607. doi:10.1016/j.ijhydene.2017.05.049
191. Parasuraman A, Lim TM, Menictas C, Skyllas-Kazacos M. Review of material research and development for vanadium redox flow battery applications. *Electrochim Acta*. 2013;101:27-40. doi:10.1016/j.electacta.2012.09.067
192. Kocyigit N, Gencten M, Sahin M, Sahin Y. A novel electrolytes for redox flow batteries: cerium and chromium couples in aqueous system. *Int J Energy Res*. 2021;45:16176-16188. doi:10.1002/er.6850
193. Kocyigit N, Gencten M, Sahin M, Sahin Y. Chrome and cobalt-based novel electrolyte systems for redox flow batteries. *Int J Energy Res*. 2020;44:8014-8023. doi:10.1002/er.5546
194. Kocyigit N, Gencten M, Sahin M, Sahin Y. A novel vanadium/cobalt redox couple in aqueous acidic solution for redox flow batteries. *Int J Energy Res*. 2020;44:411-424. doi:10.1002/er.4938
195. Gençten M, Gürsu H, Şahin Y. Electrochemical investigation of the effects of V(V) and sulfuric acid concentrations on positive electrolyte for vanadium redox flow battery. *Int J Hydrog Energy*. 2016;41:9868-9875. doi:10.1016/j.ijhydene.2016.03.200
196. Gürsu H, Gençten M, Şahin Y. Cyclic voltammetric preparation of graphene-coated electrodes for positive electrode materials of vanadium redox flow battery. *Ionics (Kiel)*. 2018;24:3641-3654. doi:10.1007/s11581-018-2547-x
197. Gürsu H, Gençten M, Şahin Y. Preparation of N-doped graphene-based electrode via electrochemical method and its application in vanadium redox flow battery. *Int J Energy Res*. 2018;42:3851-3860. doi:10.1002/er.4117
198. Gursu H, Gencten M, Sahin Y. Synthesis of phosphorus doped graphenes via the Yucel's method as the positive electrode of a vanadium redox flow battery. *J Electrochem Soc*. 2021;168:60504. doi:10.1149/1945-7111/ac0457
199. Gursu H, Gencten M, Sahin Y. Preparation of Sulphur-doped graphene-based electrodes by cyclic voltammetry: a potential application for vanadium redox flow battery. *Int J Electrochem Sci*. 2018;13:875-885. doi:10.20964/2018.01.71
200. Chakrabarti B, Nir D, Vladimir Yufit PV, Aravind NB. Enhanced performance of an all-vanadium redox flow battery employing graphene modified carbon paper electrodes. *Int J Chem Mol Eng*. 2017;11:607-611.
201. Gursu H, Gençten M, Sahin Y. Novel chlorine doped graphene electrodes for positive electrodes of a vanadium redox flow battery. *Int J Energy Res*. 2018;42:3303-3314. doi:10.1002/er.4083
202. Ersozoglu MG, Gursu H, Gencten M, Sarac AS, Sahin Y. A green approach to fabricate binder-free S-doped graphene oxide electrodes for vanadium redox battery. *Int J Energy Res*. 2021;45:2126-2137. doi:10.1002/er.5906
203. Chakrabarti B, Nir D, Yufit V, et al. Performance enhancement of reduced graphene oxide-modified carbon electrodes for vanadium redox-flow systems. *ChemElectroChem*. 2017;4:194-200. doi:10.1002/celc.201600402
204. González Z, Flox C, Blanco C, et al. Outstanding electrochemical performance of a graphene-modified graphite felt for vanadium redox flow battery application. *J Power Sources*. 2017;338:155-162. doi:10.1016/j.jpowsour.2016.10.069
205. Wu Y, Holze R. Electrocatalysis at electrodes for VanadiumRedox flow batteries. *Batteries*. 2018;4:47. doi:10.3390/batteries4030047
206. Wang H, Ling W, Chen J, et al. A three-dimensional conducting network of rGO-in-graphite-felt as electrode for vanadium redox flow batteries. *Electrochem Energy Technol*. 2018;4:60-65. doi:10.1515/eetech-2018-0008
207. Shabani Shayeh J, Ehsani A, Ganjali MR, Norouzi P, Jaleh B. Conductive polymer/reduced graphene oxide/Au nano particles as efficient composite materials in electrochemical supercapacitors. *Appl Surf Sci*. 2015;353:594-599. doi:10.1016/j.apsusc.2015.06.066
208. Sheng K, Sun Y, Li C, Yuan W, Shi G. Ultrahigh-rate supercapacitors based on eletrochemically reduced graphene oxide for AC line-filtering. *Sci Rep*. 2012;2:247. doi:10.1038/srep00247
209. Chakrabarti BK, Feng J, Kalamaras E, et al. Hybrid redox flow cells with enhanced electrochemical performance via binderless and electrophoretically deposited nitrogen-doped graphene on carbon paper electrodes. *ACS Appl Mater Interfaces*. 2020;12:53869-53878. doi:10.1021/acsami.0c17616
210. García-Alcalde L, González Z, Barreda D, Rocha VG, Blanco C, Santamaría R. Unraveling the relevance of carbon felts surface modification during electrophoretic deposition of nanocarbons on their performance as electrodes for the VO_2+/VO_2+ redox couple. *Appl Surf Sci*. 2021;569:151095. doi:10.1016/j.apsusc.2021.151095
211. Ma D, Hu B, Wu W, et al. Highly active nanostructured CoS2/CoS heterojunction electrocatalysts for aqueous polysulfide/iodide redox flow batteries. *Nat Commun*. 2019;10:3367. doi:10.1038/s41467-019-11176-y
212. Gorduk O, Gencten M, Gorduk S, Sahin M, Sahin Y. Electrochemical fabrication and supercapacitor performances of metallo phthalocyanine/functionalized-multiwalled carbon

nanotube/polyaniline modified hybrid electrode materials. *J Energy Storage*. 2021;33:102049. doi:10.1016/j.est.2020.102049

213. Flox C, Skoumal M, Rubio-Garcia J, Andreu T, Morante JR. Strategies for enhancing electrochemical activity of carbon-based electrodes for all-vanadium redox flow batteries. *Appl Energy*. 2013;109:344-351. doi:10.1016/j.apenergy.2013.02.001
214. Sankar A, Michos I, Dutta I, Dong J, Angelopoulos AP. Enhanced vanadium redox flow battery performance using graphene nanoplatelets to decorate carbon electrodes. *J Power Sources*. 2018;387:91-100. doi:10.1016/j.jpowsour.2018.03.045
215. Jiang HR, Shyy W, Wu MC, Zhang RH, Zhao TS. A bi-porous graphite felt electrode with enhanced surface area and catalytic activity for vanadium redox flow batteries. *Appl Energy*. 2019;233–234:105-113. doi:10.1016/j.apenergy.2018.10.033
216. Nia PM, Abouzari-Lotf E, Woi PM, et al. Electrodeposited reduced graphene oxide as a highly efficient and low-cost electrocatalyst for vanadium redox flow batteries. *Electrochim Acta*. 2019;297:31-39. doi:10.1016/j.electacta.2018.11.109
217. Yang D-S, Lee JY, Jo S-W, Yoon SJ, Kim T-H, Hong YT. Electrocatalytic activity of nitrogen-doped CNT graphite felt hybrid for all-vanadium redox flow batteries. *Int J Hydrog Energy*. 2018;43:1516-1522. doi:10.1016/j.ijhydene.2017.11.145
218. Chakrabarti BK, Kalamaras E, Ouyang M, et al. Trichome-like carbon-metal fabrics made of carbon microfibers, carbon nanotubes, and Fe-based nanoparticles as electrodes for regenerative hydrogen/vanadium flow cells. *ACS Appl Nano Mater*. 2021;4:10754-10763. doi:10.1021/acsanm.1c02195
219. Gürsu H, Gençten M, Şahin Y. One-step electrochemical preparation of graphene-coated pencil graphite electrodes by cyclic voltammetry and their application in vanadium redox batteries. *Electrochim Acta*. 2017;243:239-249. doi:10.1016/j.electacta.2017.05.065
220. Prifti H, Parasuraman A, Winardi S, Lim TM, Skyllas-Kazacos M. Membranes for redox flow battery applications. *Membranes*. 2012;2:275-306. doi:10.3390/membranes2020275
221. Zhang LL, Zhao XS. Carbon-based materials as supercapacitor electrodes. *Chem Soc Rev*. 2009;38:2520. doi:10.1039/b813846j
222. Zhang LL, Zhao X, Stoller MD, et al. Highly conductive and porous activated reduced graphene oxide films for high-power supercapacitors. *Nano Lett*. 2012;12:1806-1812. doi:10.1021/nl203903z
223. Arvas MB, Gençten M, Sahin Y. A two-dimensional material for high capacity supercapacitors: S-doped graphene. *Int J Energy Res*. 2020;44:1624-1635. doi:10.1002/er.4973
224. Gorduk O, Gorduk S, Gencten M, Sahin M, Sahin Y. One-step electrochemical preparation of ternary phthalocyanine/acid-activated multiwalled carbon nanotube/polypyrrole-based electrodes and their supercapacitor applications. *Int J Energy Res*. 2020;44:9093-9111. doi:10.1002/er.5634
225. Arvas MB, Gürsu H, Gencten M, Sahin Y. Preparation of different heteroatom doped graphene oxide based electrodes by electrochemical method and their supercapacitor applications. *J Energy Storage*. 2021;35:102328. doi:10.1016/j.est.2021.102328
226. Arvas MB, Karatepe N, Gencten M, Sahin Y. Fabrication of high-performance symmetrical coin cell supercapacitors by using one step and green synthesis sulfur doped graphene powders. *New J Chem*. 2021;45:6928-6939. doi:10.1039/D0NJ06061E
227. Yildirim Kalyon H, Gencten M, Gorduk S, Sahin Y. Novel composite materials consisting of polypyrrole and metal organic frameworks for supercapacitor applications. *J Energy Storage*. 2021;48:103699. doi:10.1016/j.est.2021.103699
228. Wang M, Duong LD, Mai NT, et al. All-solid-state reduced graphene oxide supercapacitor with large volumetric capacitance and ultralong stability prepared by electrophoretic deposition method. *ACS Appl Mater Interfaces*. 2015;7:1348-1354. doi:10.1021/am507656q
229. Dubal DP, Ayyad O, Ruiz V, Gómez-Romero P. Hybrid energy storage: the merging of battery and supercapacitor chemistries. *Chem Soc Rev*. 2015;44:1777-1790. doi:10.1039/C4CS00266K
230. Chang L, Hu YH. Breakthroughs in designing commercial-level mass-loading graphene electrodes for electrochemical double-layer capacitors. *Matter*. 2019;1:596-620. doi:10.1016/j.matt.2019.06.016
231. Pope MA, Korkut S, Punckt C, Aksay IA. Supercapacitor electrodes produced through evaporative consolidation of graphene oxide-water-ionic liquid gels. *J Electrochem Soc*. 2013;160:A1653-A1660. doi:10.1149/2.017310jes
232. Gogotsi Y, Simon P. True performance metrics in electrochemical energy storage. *Science*. 2011;334:917-918. doi:10.1126/science.1213003
233. Rashti A, Wang B, Hassani E, Feyzbar-Khalkhali-Nejad F, Zhang X, Oh T-S. Electrophoretic deposition of nickel cobaltite/polyaniline/rGO composite electrode for high-performance all-solid-state asymmetric supercapacitors. *Energy Fuel*. 2020;34:6448-6461. doi:10.1021/acs.energyfuels.0c00408
234. Yang L, Zheng W, Zhang P, et al. MXene/CNTs films prepared by electrophoretic deposition for supercapacitor electrodes. *J Electroanal Chem*. 2018;830–831:1-6. doi:10.1016/j.jelechem.2018.10.024
235. Lee K, Lee H, Shin Y, Yoon Y, Kim D, Lee H. Highly transparent and flexible supercapacitors using graphene-graphene quantum dots chelate. *Nano Energy*. 2016;26:746-754. doi:10.1016/j.nanoen.2016.06.030
236. Liu W-W, Feng Y-Q, Yan X-B, Chen J-T, Xue Q-J. Superior micro-supercapacitors based on graphene quantum dots. *Adv Funct Mater*. 2013;23:4111-4122. doi:10.1002/adfm.201203771
237. Tjandra R, Liu W, Zhang M, Yu A. All-carbon flexible supercapacitors based on electrophoretic deposition of graphene quantum dots on carbon cloth. *J Power Sources*. 2019;438:227009. doi:10.1016/j.jpowsour.2019.227009
238. Pech D, Brunet M, Durou H, et al. Ultrahigh-power micrometre-sized supercapacitors based on onion-like carbon. *Nat Nanotechnol*. 2010;5:651-654. doi:10.1038/nnano.2010.162
239. Zhu C, Liu T, Qian F, et al. 3D printed functional nanomaterials for electrochemical energy storage. *Nano Today*. 2017;15:107-120. doi:10.1016/j.nantod.2017.06.007
240. Du C, Pan N. High power density supercapacitor electrodes of carbon nanotube films by electrophoretic deposition. *Nanotechnology*. 2006;17:5314-5318. doi:10.1088/0957-4484/17/21/005
241. Niu Z, Zhang L, Liu L, Zhu B, Dong H, Chen X. All-solid-state flexible ultrathin micro-supercapacitors based on graphene. *Adv Mater*. 2013;25:4035-4042. doi:10.1002/adma.201301332
242. Argüello JA, Rojo JM, Moreno R. Electrophoretic deposition of manganese oxide and graphene nanoplatelets on graphite paper for the manufacture of supercapacitor electrodes.

Electrochim Acta. 2019;294:102-109. doi:10.1016/j.electacta.2018.10.091

243. Nguyen DK, Schepisi IM, Amir FZ. Extraordinary cycling stability of $Ni_3(HITP)_2$ supercapacitors fabricated by electrophoretic deposition: cycling at 100,000 cycles. *Chem Eng J*. 2019;378:122150. doi:10.1016/j.cej.2019.122150
244. Ouyang Y, Geuli O, Hao Q, Mandler D. Controllable assembly of hybrid electrodes by electrophoretic deposition for high-performance battery–supercapacitor hybrid devices. *ACS Appl Energy Mater*. 2020;3:1784-1793. doi:10.1021/acsaem.9b02242
245. Amir FZ, Pham VH, Mullinax DW, Dickerson JH. Enhanced performance of HRGO-RuO_2 solid state flexible supercapacitors fabricated by electrophoretic deposition. *Carbon*. 2016;107:338-343. doi:10.1016/j.carbon.2016.06.013
246. Chakrabarti BK, Kalamaras E, John Low CT. Practical aspect of electrophoretic deposition to produce commercially viable activated carbon Supercapacitor electrode. ECS Meet Abstr 2020;MA2020-02:3783. doi:10.1149/MA2020-02453783mtgabs
247. Shrestha M, Amatya I, Wang K, Zheng B, Gu Z, Fan QH. Electrophoretic deposition of activated carbon YP-50 with ethyl cellulose binders for supercapacitor electrodes. *J Energy Storage*. 2017;13:206-210. doi:10.1016/j.est.2017.07.015
248. Chakrabarti BK, John Low CT. Practical aspects of electrophoretic deposition to produce commercially viable supercapacitor energy storage electrodes. *RSC Adv*. 2021;11:20641-20650. doi:10.1039/D0RA09197A
249. Zhao W, Zhu Y, Zhang L, Xie Y, Ye X. Facile synthesis of three-dimensional porous carbon for high-performance supercapacitors. *J Alloys Compd*. 2019;787:1-8. doi:10.1016/j.jallcom.2019.02.025
250. Gurten Inal II, Aktas Z. Enhancing the performance of activated carbon based scalable supercapacitors by heat treatment. *Appl Surf Sci*. 2020;514:145895. doi:10.1016/j.apsusc.2020.145895
251. Liu Y, Wang Y, Zhang G, Liu W, Wang D, Dong Y. Preparation of activated carbon from willow leaves and evaluation in electric double-layer capacitors. *Mater Lett*. 2016;176:60-63. doi:10.1016/j.matlet.2016.04.065
252. Vijayakumar M, Rohita DS, Rao TN, Karthik M. Electrode mass ratio impact on electrochemical capacitor performance. *Electrochim Acta*. 2019;298:347-359. doi:10.1016/j.electacta.2018.12.034
253. Kim T, Yi S-H, Chun S-E. Electrophoretic deposition of a supercapacitor electrode of activated carbon onto an indium-tin-oxide substrate using ethyl cellulose as a binder. *J Mater Sci Technol*. 2020;58:188-196. doi:10.1016/j.jmst.2020.03.072
254. Kyerematen NA, Gukte D, Ferch M, Buk J, Hrebicek T, Hahn R. Preparation of a self-supported SiO_2 membrane as a separator for lithium-ion batteries. *Batter Supercaps*. 2020;3:456-462. doi:10.1002/batt.201900169
255. Su Y, Zhitomirsky I. Electrophoretic assembly of organic molecules and composites for electrochemical supercapacitors. *J Colloid Interface Sci*. 2013;392:247-255. doi:10.1016/j.jcis.2012.09.083
256. Kumar N, Yu Y-C, Lu YH, Tseng TY. Fabrication of carbon nanotube/cobalt oxide nanocomposites via electrophoretic deposition for supercapacitor electrodes. *J Mater Sci*. 2016;51:2320-2329. doi:10.1007/s10853-015-9540-9
257. Jang JH, Machida K, Kim Y, Naoi K. Electrophoretic deposition (EPD) of hydrous ruthenium oxides with PTFE and their supercapacitor performances. *Electrochim Acta*. 2006;52:1733-1741. doi:10.1016/j.electacta.2006.01.075
258. Jang JH, Kato A, Machida K, Naoi K. Supercapacitor performance of hydrous ruthenium oxide electrodes prepared by electrophoretic deposition. *J Electrochem Soc*. 2006;153:A321. doi:10.1149/1.2138672
259. Ghasemi S, Hosseinzadeh R, Jafari M. MnO_2 nanoparticles decorated on electrophoretically deposited graphene nanosheets for high performance supercapacitor. *Int J Hydrog Energy*. 2015;40:1037-1046. doi:10.1016/j.ijhydene.2014.11.072
260. Gonzalez Z, Yus J, Moratalla R, Ferrari B. Electrophoretic deposition of binder-free TiN nanoparticles to design 3D microstructures. the role of sintering in the microstructural robustness of supercapacitor electrodes. *Electrochim Acta*. 2021;369:137654. doi:10.1016/j.electacta.2020.137654
261. Siwal SS, Zhang Q, Devi N, Thakur VK. Carbon-based polymer nanocomposite for high-performance energy storage applications. *Polymers*. 2020;12:505. doi:10.3390/polym12030505
262. Santhanagopalan S, Balram A, Meng DD. Scalable high-power redox capacitors with aligned nanoforests of crystalline MnO_2 nanorods by high voltage electrophoretic deposition. *ACS Nano*. 2013;7:2114-2125. doi:10.1021/nn3044462
263. Zhitomirsky I. Cathodic electrodeposition of ceramic and organoceramic materials. Fundamental aspects. *Adv Colloid Interf Sci*. 2002;97:279-317. doi:10.1016/S0001-8686(01)00068-9
264. Kaya C, Boccaccini AR, Chawla KK. Electrophoretic deposition forming of nickel-coated-carbon-fiber-reinforced borosilicate-glass-matrix composites. *J Am Ceram Soc*. 2004;83:1885-1888. doi:10.1111/j.1151-2916.2000.tb01486.x
265. Saji VS. Electrophoretic-deposited superhydrophobic coatings. *Chem Asian J*. 2021;16:474-491. doi:10.1002/asia.202001425
266. Golodnitsky D, Peled E, Nathan M, et al. Electrophoretic deposition of thin film batteries. WO2012076950A1. 2012.
267. Chiang Y-M, Hellweg B, Holman RK, Tobias SM, Kim D, Wartena RC. Electrophoretic assembly of electrochemical devices. US7662265B2, 2010.
268. Xiao X. Electrophoretic deposition of an electrode for a lithium-based battery. US20170222210A1, 2017.
269. Lee KMN, Seop HK, Park C. Method for manufacturing SiO-based carbon nanofiber composite on basis of nickel-copper catalyst using electrophoretic deposition, and method for manufacturing secondary battery using same. US10014516B2, 2016.
270. Bouyer F, Vuillemin B, Gaben F. Method for producing dense thin films by electrophoresis. US20140339085A1, 2014.
271. Zhang H, Yao M, Liu X. Composite anode of Lithium-ion batteries. US20140186701A1, 2014.
272. Ruoff RS, An SJ, Stoller M, Emilsson T, Agnihotri D. Electrophoretic deposition and reduction of graphene oxide to make graphene film coatings and electrode structures. US20110227000A1, 2011.
273. Oguni T, Osada T, Takeuchi T, Nomoto K. Single-layer and multilayer graphene, method of manufacturing the same, object including the same, and electric device including the same. US20200259179A1, 2020.
274. Data RUSA, Examiner P, Williams JL. Method for preparing a nanostructured composite electrode through electrophoretic deposition and a product prepared thereby, 2010.

275. Gaben F, Bouyer F, Vuillemin B. Method for manufacturing all-solid-state batteries in a multilayer structure. US20150333376A1, 2015.
276. Rust HJ, Lahiri A, Ramasubramanian M, Spotnitz R. Three-dimensional batteries and methods of manufacturing the same, 2014.
277. Mukherjee R, Koratkar N, Singh E. Porous graphene network electrodes and an all-carbon lithium ion battery containing the same. CA2937765A1, n.d.
278. Oakes L, Hanken T, Carter R, Yates W, Pint CL. Roll-to-roll nanomanufacturing of hybrid nanostructures for energy storage device design. *ACS Appl Mater Interfaces*. 2015;7:14201-14210. doi:10.1021/acsami.5b01315
279. Pascall AJ, Kuntz J. Roll-to-roll light directed electrophoretic deposition system and method. US20160222538A1, 2016.
280. PPG receives $ 2. 2M from DOE to study coatings applications in automotive lithium-ion batteries 2020. https://www.greencarcongress.com/2020/09/20200917-ppg.html.
281. Neirinck B, Van der Biest O, Vleugels J. A current opinion on electrophoretic deposition in pulsed and alternating fields. *J Phys Chem B*. 2013;117:1516-1526. doi:10.1021/jp306777q
282. Yoshioka T, Chávez-Valdez A, Roether JA, Schubert DW, Boccaccini AR. AC electrophoretic deposition of organic–inorganic composite coatings. *J Colloid Interface Sci*. 2013;392:167-171. doi:10.1016/j.jcis.2012.09.087
283. Keshmarzi MK, Daryakenari AA, Omidvar H, et al. Pulsed electrophoretic deposition of nanographitic flake-nanostructured Co_3O_4 layers for efficient lithium-ion-battery anode. *J Alloys Compd*. 2019;805:924-933. doi:10.1016/j.jallcom.2019.07.078
284. Ammam M. Electrophoretic deposition under modulated electric fields: a review. *RSC Adv*. 2012;2:7633. doi:10.1039/c2ra01342h
285. Shao Y, El-Kady MF, Wang LJ, et al. Graphene-based materials for flexible supercapacitors. *Chem Soc Rev*. 2015;44:3639-3665. doi:10.1039/C4CS00316K
286. Takai T, Nakao H, Iwata F. Three-dimensional microfabrication using local electrophoresis deposition and a laser trapping technique. *Opt Express*. 2014;22:28109-28117. doi:10.1364/OE.22.028109
287. Hirt L, Reiser A, Spolenak R, Zambelli T. Additive manufacturing of metal structures at the micrometer scale. *Adv Mater*. 2017;29:1604211. doi:10.1002/adma.201604211
288. Hong J, Murphy AB, Ashford B, Cullen PJ, Belmonte T, Ostrikov K. Plasma-digital nexus: plasma nanotechnology for the digital manufacturing age. *Rev Mod Plasma Phys*. 2020;4:1. doi:10.1007/s41614-019-0039-8
289. Iwata F, Kaji M, Suzuki A, Ito S, Nakao H. Local electrophoresis deposition of nanomaterials assisted by a laser trapping technique. *Nanotechnology*. 2009;20:235303. doi:10.1088/0957-4484/20/23/235303
290. Matsuda A, Azuma S, Yamada H, Kawamura G, Muto H, Uchikoshi T. EPD for composite cathode layer in all-solid-Atate lithium ion battery based on sulfide electrolyte. Electrophor Depos ViI Fundam Appl. n.d.
291. He T, Zeng G, Feng C, et al. A solid-electrolyte-reinforced separator through single-step electrophoretic assembly for safe high-capacity lithium ion batteries. *J Power Sources*. 2020;448:227469. doi:10.1016/j.jpowsour.2019.227469
292. Han Y, Ye L, Boateng B, et al. Direct electrophoretic deposition of an ultra-strong separator on an anode in a surfactant-free colloidal system for lithium ion batteries. *J Mater Chem A*. 2019;7:1410-1417. doi:10.1039/C8TA09092K
293. Zhao J, Chen D, Boateng B, et al. Atomic interlamellar ion path in polymeric separator enables long-life and dendrite-free anode in lithium ion batteries. *J Power Sources*. 2020;451:227773. doi:10.1016/j.jpowsour.2020.227773
294. Fergus JW. Ceramic and polymeric solid electrolytes for lithium-ion batteries. *J Power Sources*. 2010;195:4554-4569. doi:10.1016/j.jpowsour.2010.01.076
295. Blanga R, Burstein L, Berman M, Greenbaum SG, Golodnitsky D. Solid polymer-in-ceramic electrolyte formed by electrophoretic deposition. *J Electrochem Soc*. 2015;162:D3084-D3089. doi:10.1149/2.0221511jes
296. Golodnitsky D, Strauss E, Peled E, Greenbaum S. Review—on order and disorder in polymer electrolytes. *J Electrochem Soc*. 2015;162:A2551-A2566. doi:10.1149/2.0161514jes
297. Zhitomirsky I, Petric A. Electrophoretic deposition of electrolyte materials for solid oxide fuel cells. *J Mater Sci*. 2004;39:825-831. doi:10.1023/B:JMSC.0000012910.70526.61
298. Zhitomirsky I, Gal-Or L. Electrophoretic deposition of hydroxyapatite. *J Mater Sci Mater Med*. 1997;8:213-219. doi:10.1023/a:1018587623231
299. Winslow WM. Induced fibration of suspensions. *J Appl Phys*. 1949;20:1137-1140. doi:10.1063/1.1698285
300. Zhitomirsky I, Petric A. Electrophoretic deposition of ceramic materials for fuel cell applications. *J Eur Ceram Soc*. 2000;20:2055-2061. doi:10.1016/S0955-2219(00)00098-4
301. Slater MD, Kim D, Lee E, Johnson CS. Sodium-Ion Batteries. *Adv Funct Mater*. 2013;23:947-958. doi:10.1002/adfm.201200691
302. Karuppasamy K, Jothi VR, Nichelson A, et al. Nanostructured transition metal sulfide/selenide anodes for high-performance sodium-ion batteries. *Nanostructured, Functional, and Flexible Materials for Energy Conversion and Storage Systems*. Amsterdam: Elsevier; 2020:437-464.
303. Chen L, Fiore M, Wang JE, Ruffo R, Kim D-K, Longoni G. Readiness level of sodium-ion battery technology: a materials review. *Adv Sustain Syst*. 2018;2:1700153. doi:10.1002/adsu.201700153
304. Zhang Y, Jiang J, An Y, et al. Sodium-ion capacitors: materials, mechanism, and challenges. *ChemSusChem*. 2020;13:2522-2539. doi:10.1002/cssc.201903440
305. Prabakar SJR, Park C, Ikhe AB, Sohn K-S, Pyo M. Simultaneous suppression of metal corrosion and electrolyte decomposition by graphene oxide protective coating in magnesium-ion batteries: toward a 4-V-wide potential window. *ACS Appl Mater Interfaces*. 2017;9:43767-43773. doi:10.1021/acsami.7b16103
306. Deng J, Lu Z, Ding L, et al. Fast electrophoretic preparation of large-area two-dimensional titanium carbide membranes for ion sieving. *Chem Eng J*. 2021;408:127806. doi:10.1016/j.cej.2020.127806

How to cite this article: Chakrabarti BK, Gençten M, Bree G, Dao AH, Mandler D, Low CTJ. Modern practices in electrophoretic deposition to manufacture energy storage electrodes. *Int J Energy Res*. 2022;46(10):13205-13250. doi:10.1002/er.8103